ERDC/GSL TR-14-13

US Army Corps
of Engineers®
Engineer Research and
Development Center

ERDC
INNOVATIVE SOLUTIONS
for a safer, better world

Evaluation of Faun MLC-70 Trackway Mat System Under Simulated F-15 Traffic

Timothy W. Rushing, Lyan Garcia, and Quint S. Mason

May 2014

Geotechnical and Structures Laboratory

The US Army Engineer Research and Development Center (ERDC) solves the nation's toughest engineering and environmental challenges. ERDC develops innovative solutions in civil and military engineering, geospatial sciences, water resources, and environmental sciences for the Army, the Department of Defense, civilian agencies, and our nation's public good. Find out more at www.erdc.usace.army.mil.

To search for other technical reports published by ERDC, visit the ERDC online library at http://acwc.sdp.sirsi.net/client/default.

ERDC/GSL TR-14-13
May 2014

Evaluation of Faun MLC-70 Trackway Mat System Under Simulated F-15 Traffic

Timothy W. Rushing, Lyan Garcia, and Quint S. Mason

Geotechnical and Structures Laboratory
US Army Engineer Research and Development Center
3909 Halls Ferry Road
Vicksburg, MS 39180-6199

Final report

Prepared for Headquarters, Air Force Civil Engineer Support Agency
Tyndall Air Force Base, FL 32403-5319

Under Airfield Damage Repair Modernization Program

Abstract

Faun Trackway's airfield matting products have been encountered by US military personnel during joint operations with coalition partners. The MLC-70 Trackway matting system was previously evaluated under F-15E and C-17 simulated traffic over a subgrade with a California Bearing Ratio (CBR) of 6 and was found to be inadequate. However, substantially stronger materials are often found around existing airfields. Therefore, the US Air Force Civil Engineer Center tasked the US Army Engineer Research and Development Center to evaluate the MLC-70 system under simulated F-15E aircraft traffic to determine the number of allowable aircraft passes the system can sustain over stronger soils. Results of traffic tests presented herein include individual mat panel properties, pretest and posttest subgrade soil conditions, subgrade earth pressure cell instrumentation results, physical damage descriptions of the mat system, and system passes-to-failure under simulated F-15E aircraft traffic for specified failure criteria. Results from these evaluations showed that the MLC-70 Trackway system was capable of supporting more than 1,000 F-15E operations when placed over a subgrade with a CBR of 25 or greater. Operations over weaker soils should be limited to emergency or expedient operations for heavy fighter aircraft.

Contents

Figures and Tables

Figures

Tables

Preface

This study was conducted for the US Air Force Civil Engineer Center (AFCEC) to evaluate Faun Trackway's MLC-70 airfield matting systems under simulated F-15E aircraft traffic over subgrade materials with California Bearing Ratios ranging from 25 to 100. Technical oversight was provided by Jeb Tingle (ERDC) and program management was provided by the AFCEC, Tyndall Air Force Base, Florida.

This work was performed by the Airfields and Pavements Branch (GM-A) of the Engineering Systems and Materials Division (GM), US Army Engineer Research and Development Center, Geotechnical and Structures Laboratory (ERDC-GSL). At the time of this publication, Dr. Gary L. Anderton, was Chief, CEERD-GM-A, and Dr. Larry N. Lynch was Chief, CEERD-GM. The Deputy Director of ERDC-GSL was Dr. William P. Grogan, and the Director was Dr. David W. Pittman.

COL Jeffrey R. Eckstein was Commander of the ERDC, and Dr. Jeffery P. Holland was the Director.

Unit Conversion Factors

Multiply	By	To Obtain
cubic feet	0.02831685	cubic meters
feet	0.3048	meters
inches	0.0254	meters
kip-inches	112.948	newton-meters
pounds (force)	4.448222	newtons
pounds (force) per square foot	47.88026	pascals
pounds (force) per square inch	6.894757	kilopascals
pounds (mass)	0.45359237	kilograms
square feet	0.09290304	square meters
square inches	6.4516 E-04	square meters

Definitions

California Bearing Ratio (CBR) – A measure of the bearing capacity of the soil based upon its shearing resistance. The CBR value is calculated by dividing the unit load required to force a standard piston into the soil by the unit load required to force the same piston the same depth into a standard sample of crushed stone and multiplying by 100%. Throughout this report, the CBR is expressed as a value with no units (e.g., 6 CBR).

Elastic Deflection – Temporary vertical deformation of mat panels and/or subgrade soil under the static load from the test wheel. Elastic deflection values measured on the mat surfaces in this report are the sum of the elastic deflections of the mat and the subgrade.

Load Cart – A specially constructed vehicle used in engineering tests for simulating aircraft taxiing and braking operations.

Pass – One traverse of a load wheel across a given length of runway, taxiway, or test section surface.

Pattern – The completion by the test load cart of one simulated normal distribution of traffic on a test item.

Plastic/Permanent Deformation – The permanent change in elevation of the subgrade soil or bending of the mat panel resulting from individual load applications.

Subgrade – An area of soil processed under controlled conditions to provide a desired bearing capacity upon which the airfield matting is placed. Typically, it is the bottom layer of a foundation or pavement structure.

Test Section – A subgrade soil surfaced with airfield matting.

Test Wheel – The main load-bearing wheel on the load cart. In this test, the test wheel is an actual F-15E aircraft wheel mounted on a load cart.

Traffic Lane – That portion of the test section that is subjected to the moving wheel load of the load cart.

1 Introduction

1.1 Background

Since the beginning of World War II, expedient surfacing has been used to rapidly expand existing airfield facilities to support increased numbers of aircraft. Currently, the primary expeditionary airfield surfacing for the US military is AM2 mat, which has been used for temporary runway, taxiway, and parking apron surfaces since the 1960s. Recent NATO operations in the Middle East and Afghanistan have introduced the US military to expedient surfaces used by our allied nations. Many of these systems have not been independently evaluated under modern aircraft by the US military; therefore, commanders operating in joint coalition environments place US aircraft at risk if they decide to operate on untested matting systems. Since many nations use Faun Trackway's Military Load Class (MLC) 70 matting system for aircraft operations, the US Air Force (USAF) sponsored its evaluation under simulated aircraft loads to determine its capabilities and limitations for carrying modern US military aircraft. A literature review found that the MLC-70 system (formerly Class 60) was evaluated by Burgmann and Ingebretson (1969) under tank traffic and by Rollings (1975) as a bomb damage repair option for F-4 fighter aircraft. Although the information was considered useful, if failed to address current operational needs; therefore, a new evaluation under modern aircraft loadings was required.

1.2 Objective and scope of investigation

The primary objective of the evaluations described in this report was to determine the ability of Faun Trackway's MLC-70 matting system to carry US military fighter aircraft loads. The objective was accomplished by constructing full-scale foundation subgrades to specified strengths, installing the mat system directly on top of the prepared subgrade, and trafficking the mat system with simulated F-15E aircraft traffic until predefined failure criteria were achieved. Results of the evaluations were then analyzed to determine the load-carrying capability of the MLC-70 mat system.

In this report, Chapter 2 includes the descriptions of the MLC-70 matting system; construction of the full-scale test sections; traffic application; data

collection; and failure criteria. The results and analyses of the individual traffic tests are presented in Chapters 3 through 5. A comparison of all the test section data is included in Chapter 6. Pertinent conclusions and recommendations are noted in Chapter 7.

2 Experimental Program

Traffic tests were conducted on full-scale test sections constructed and trafficked at the ERDC Hangar 4 pavement test facility and an outdoor test site in Vicksburg, Mississippi. Mat panels were placed directly on top of three different subgrade materials constructed to California Bearing Ratios (CBRs) of 25 to 100. This chapter describes the MLC-70 matting system; construction of the full-scale test section subgrade; installation of the matting system; traffic application; data collection; and failure criteria. A summary of the testing program for the MLC-70 mat system is presented in Table 1.

Table 1. Experimental subgrade materials tested.

Test Location	Subgrade USCS Classification	Subgrade CBR	Simulated Aircraft
Outdoor Site	CL (cement stabilized)	25-50	F-15E
Hangar 4	CH	25	F-15E
Hangar 4	GW	100	F-15E

2.1 General description of the test sections

2.1.1 25-50 CBR cement-stabilized low-plasticity clay (CL)

The cement-stabilized low-plasticity clay (CL) subgrade for the 25-50 CBR test section was constructed to a thickness of 8 in. Mat panels were placed directly over the subgrade and trafficked until failure. The MLC-70 test section consisted of a 30-ft-wide by 40.17-ft-long section of matting. The center of the item had a 3.75-ft-wide traffic area designated for simulated F-15E traffic. The mat was trafficked according to a normally distributed wander pattern associated with the F-15E aircraft. A plan view showing the trafficked configuration is in Figure 1. Throughout the report, this test section is referred to as the 25-50 CBR test section.

2.1.2 25 CBR high-plasticity clay (CH)

The high-plasticity clay (CH) subgrade for the 25 CBR test section was constructed to a thickness of 24 in. The mat panels were placed directly over the subgrade and trafficked until failure. The MLC-70 test section consisted of a 22.5-ft-wide by 27.75-ft-long section of matting. A 3.75-ft-wide traffic

Figure 1. 25-50 CBR test section mat panel layout.

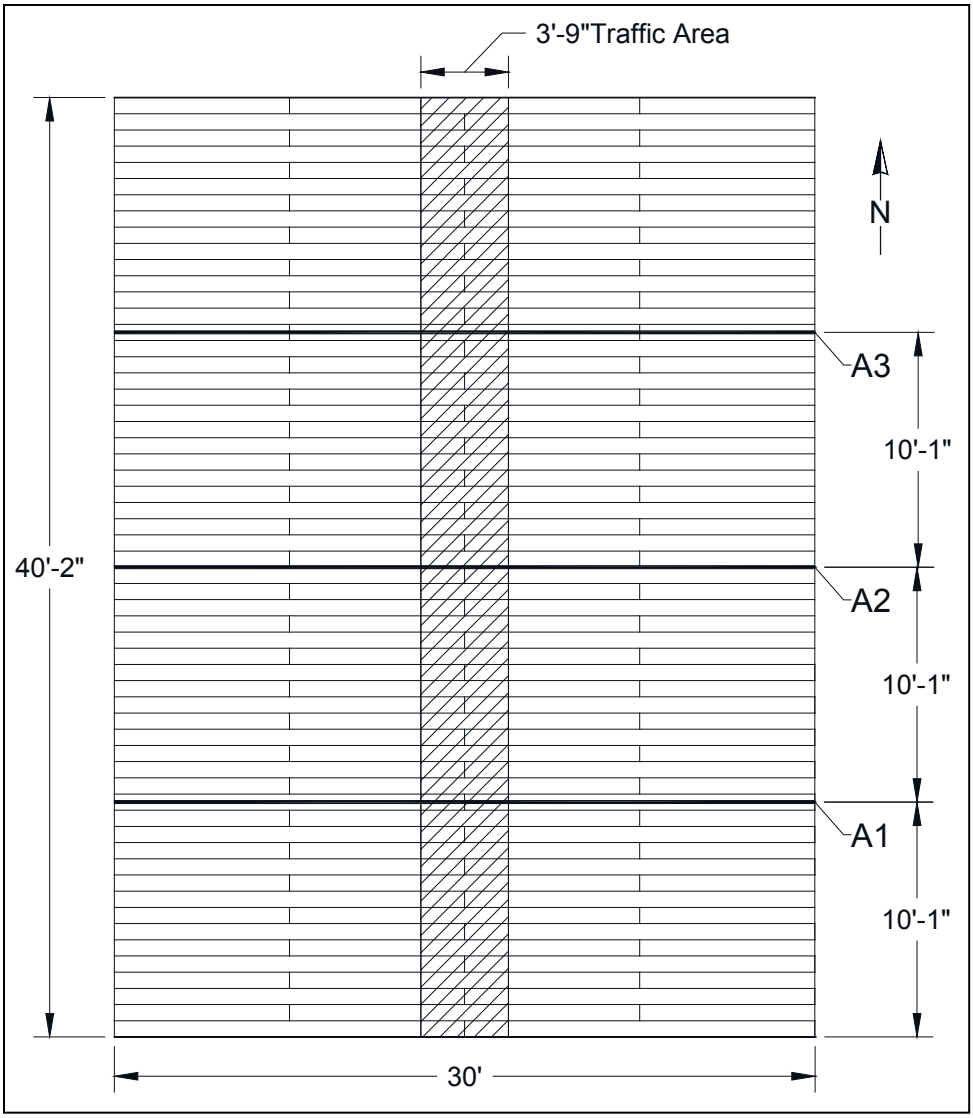

area was designated for simulated F-15E traffic in the center of the experimental mat section. The mat was trafficked according to a normally distributed wander pattern associated with the F-15E aircraft. A plan view showing the trafficked configuration is in Figure 2. Throughout the report, this test section is referred to as the 25 CBR test section.

2.1.3 100 CBR poorly-graded gravel with sand and silt

The poorly-graded gravel with sand and silt (GP-GM) subgrade for the 100 CBR test section was constructed to a thickness of 24 in. The mat panels were placed directly over the subgrade and trafficked until failure. The MLC-70 test section consisted of a 22.5-ft-wide by 21.5-ft-long section

Figure 2. 25 CBR test section mat panel layout.

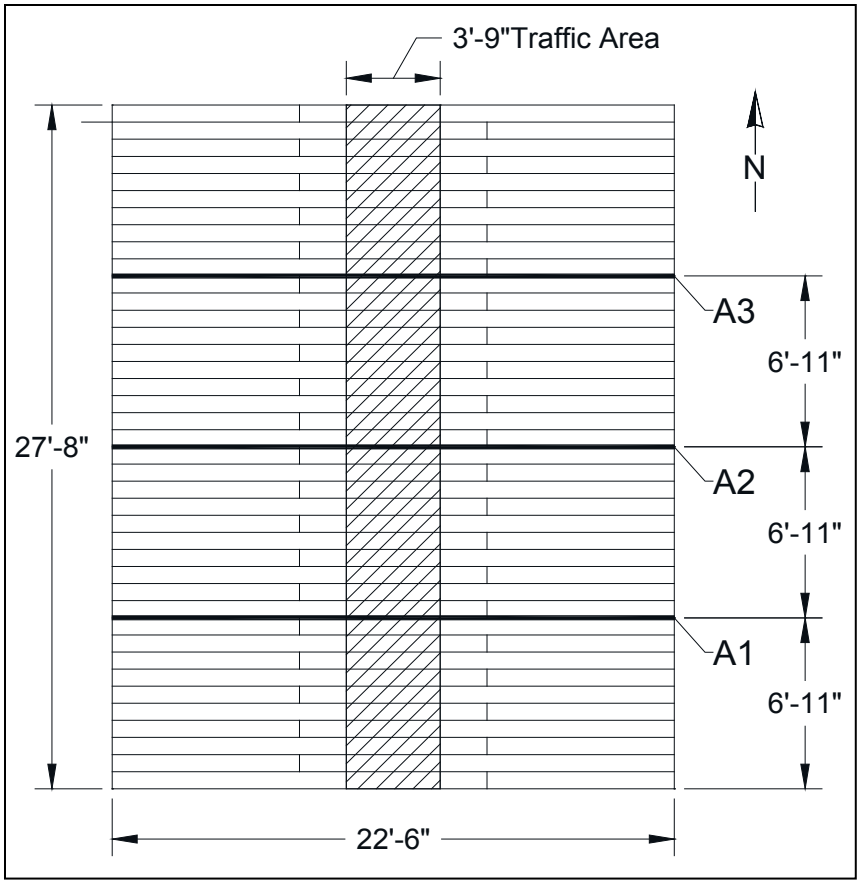

of matting without end joints along the center (Item A) followed by a 30-ft-wide by 13.17-ft-long section of matting with end joints along the center (Item B). A 3.75-ft-wide traffic area was designated for simulated F-15E traffic in the center of the mat section. The mat was trafficked according to a normally distributed wander pattern associated with the F-15E aircraft. A plan view showing the trafficked configuration is in Figure 3. Throughout the report, this test section is referred to as the 100 CBR test section.

2.2 Materials

The following sections describe the MLC-70 mat system and the subgrade materials used for construction. All panels were visually inspected upon receipt to ensure that the material had not been damaged prior to testing. The MLC-70 system is currently in production, and new panels were delivered for evaluation. The dimensions and weights of the matting system are provided in Table 2.

Figure 3. 100 CBR test section mat panel layout.

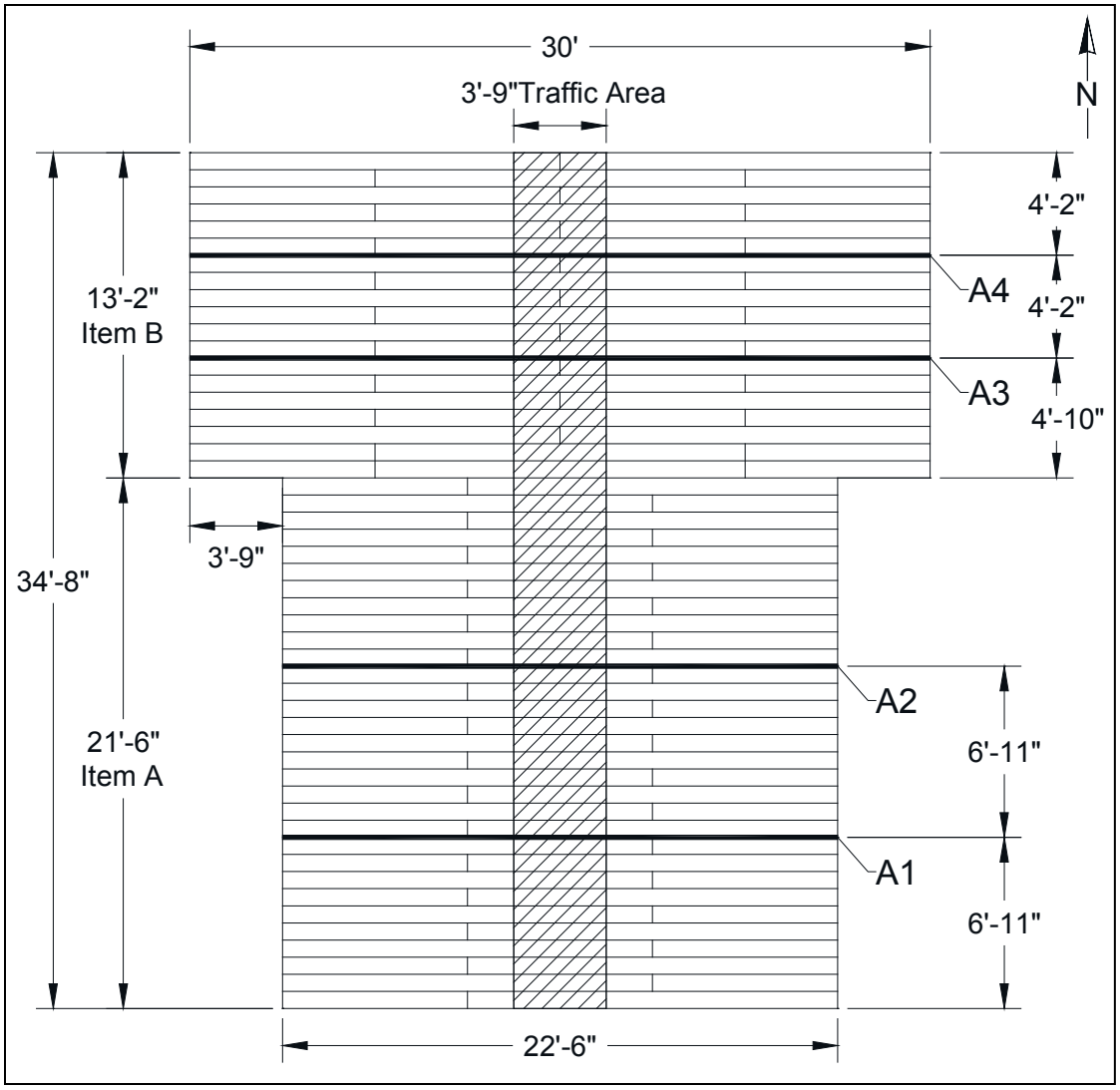

Table 2. Mat properties.

Mat	Length in.	Width in.	Thickness in.	Total Panel Weight lbf	Unit Weight lbf/ft²
MLC-70 Full-Panel	180	9	1.25	73.7	6.55
MLC-70 Half-Panel	90	9	1.25	36.9	6.55

2.2.1 MLC-70

The MLC-70 Trackway matting system was developed in the 1960s to create temporary roadways for heavy military vehicles used by the United Kingdom Ministry of Defence. MLC-70 panels, shown in Figures 4 and 5, are made from a single aluminum extrusion. When the panels are assembled in an array, they can be rolled up for storage and transportation.

Figure 4. MLC-70 Trackway panels.

Figure 5. Profile of MLC-70 Trackway joints.

Each full-panel measures 9 in. by 180 in. by 1.25 in. and weighs an average of 73.7 lbf, or 6.55 lbf/ft^2. The connection system along the 180-in. side was a male/female T-slot. To join the panels, the male "T" edge was slid into the

female C-shaped edge of the adjoining panel. Once the panel was in the desired position, shoot bolts were inserted into slots in the male edge of the panel to prevent lateral movement of the panels along each row. Panels were assembled in a brickwork configuration with half-panels used on the ends of every other row. No connection system was included along the 9-in. edges. Faun Trackway supplied full-panels and half-panels for testing. The panels used in the 25-50 CBR test and the 25 CBR test did not appear to be new; however, no panel damage was found during inspection or assembly. New panels were delivered for the 100 CBR test. Properties of MLC-70 are shown in Table 2.

2.2.2 Cement-stabilized CL material

The CL material used for construction was in situ soil at an outdoor test site on the ERDC campus in Vicksburg. The CL soil is a native loess silt deposit, commonly referred to as Vicksburg Silt, that has a low affinity for water, dries quickly, and is easily erodible. In situ CBR tests, conducted according to US Army Corps of Engineers Standard CRD-C 654-95, indicated the natural soil had CBRs ranging from 4 to 12. The intent was to create a subgrade with a 20 to 40 CBR; therefore, cement was blended into the CL material in an attempt to increase the CBR to the desired strength. Details of the cement mixing are shown in the test section construction section. Classification data for the subgrade soil are shown in Figure 6.

2.2.3 CH material

The CH material used for construction was procured from a local source in Vicksburg. The CH soil is a native deposit along the Mississippi River commonly called “Buckshot Clay.” Classification data for the soil are shown in Figure 6. CBR-moisture content relationships are shown in Figure 7. These data indicated that a moisture content of approximately 25% was required to obtain the target 25-CBR soil strength.

2.2.4 GP-GM material

The GP-GM material used for construction was a standard limestone material stockpiled at a local facility. Classification data for the GP-GM material are shown in Figure 6.

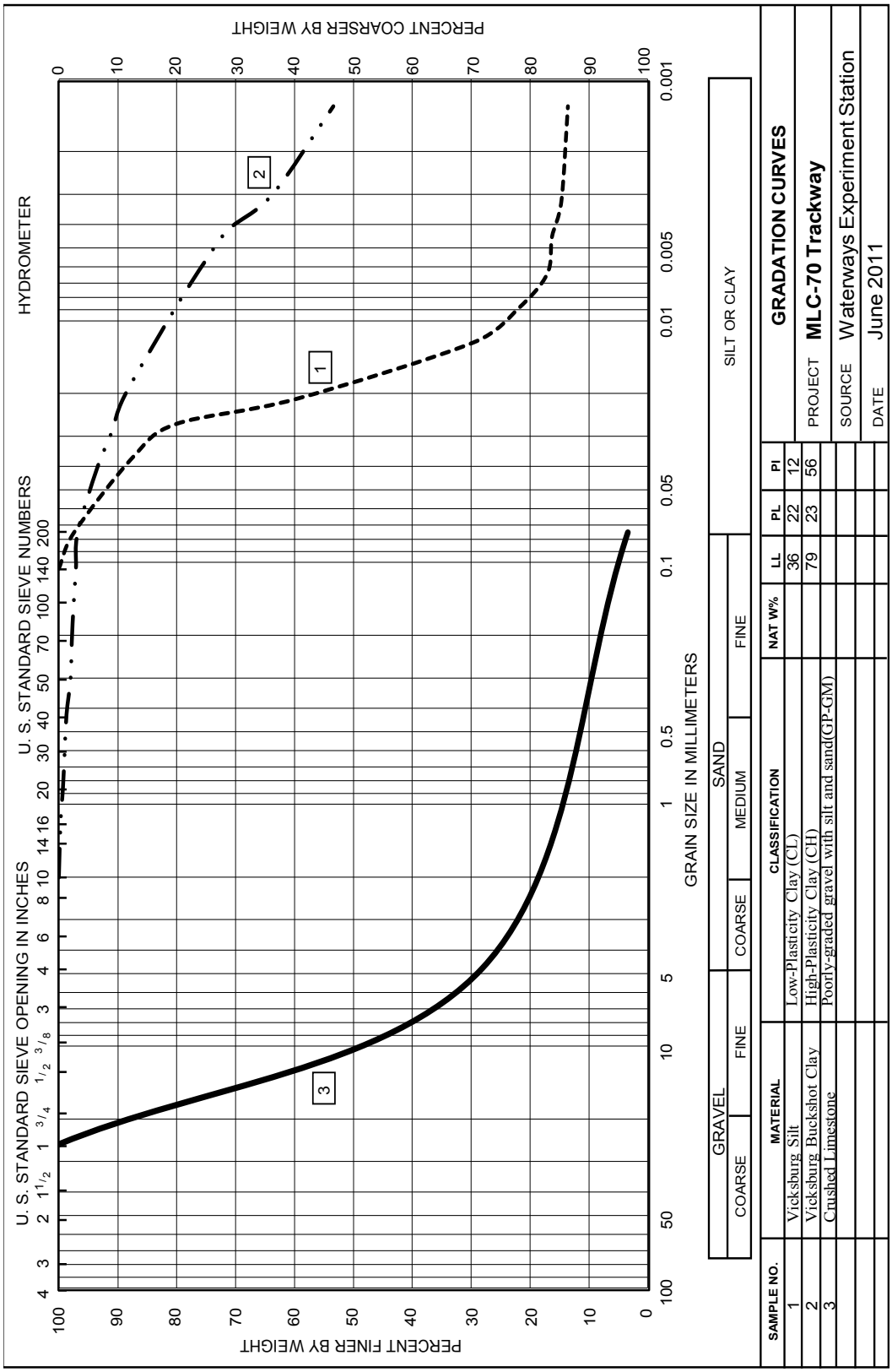

Figure 6. Gradation curves for test section materials.

Figure 7. CBR vs. moisture content for CH subgrade material.

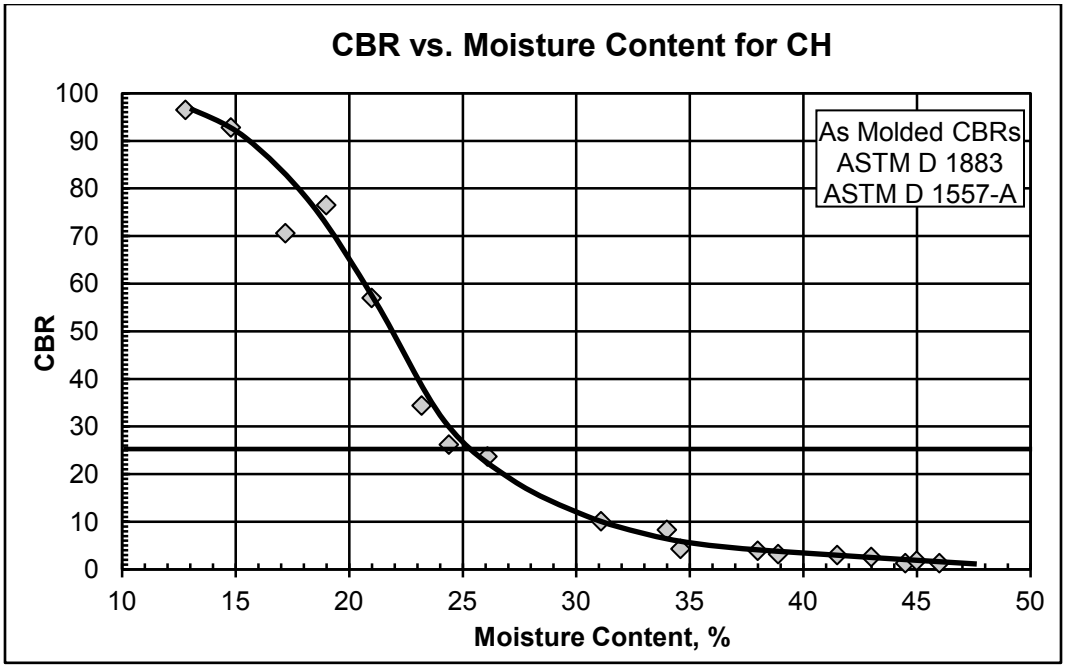

2.3 Test section construction

The following sections describe the methods used to construct the foundation subgrades for the MLC-70 test sections and the installation of the mat system. Field and laboratory soil testing data used to determine the bearing capacity in terms of CBR of each test item are also included.

2.3.1 25-50 CBR

2.3.1.1 Subgrade construction

In situ field CBR tests conducted on the existing CL soil at the outdoor test site chosen for test section construction found strengths on the soil surface ranging from 4 to 12 CBR. To achieve the desired 20 to 40 CBR strength, cement stabilization of the upper 8 in. of the existing soil was required. To determine the cement content needed to achieve the desired strength, a stabilized soil mix design was performed using 3%, 5%, and 7% cement, by volume, added to the CL material with 12% optimum water content. Samples were prepared by mixing the soil and cement in a portable concrete mixer and compacting the samples in 6-in.-diam by 12-in.-deep concrete cylinder molds. Field CBR tests were conducted after a 24-hr cure time in the cylinders, as shown in Figure 8, to determine their representative strengths. Based on the test results, 5% cement was adequate to obtain a 20-40 CBR subgrade. The 30-ft-wide by 40-ft-long test section was

Figure 8. Conducting field CBR test in 6-in. cylinder molds.

stabilized by mixing 80 bags of type III cement into the top 8 in. of existing soil with a Terex reclaimer/stabilizer. The test section area was divided into a grid based on the soil volumetric measurements such that one 80-lbf bag of cement spread over the area inside a grid square and mixed 8 in. deep would result in 5% cement. After the bags were placed, as shown in Figure 9 and spread inside each grid, additional cement was added along the approach lane of the stabilizer to ensure the cement inside the test area was consistent and not dragged outside the test area. Then the cement was thoroughly mixed with the soil, as shown in Figure 10, and the test section was compacted with three coverages of a vibratory steel wheel compactor, as shown in Figure 11.

After 24 hr of cure time, field CBR, as shown in Figure 12, and dynamic cone penetrometer (DCP) tests were conducted, according to ASTM D6951, on the test section at three quarter-point locations (10, 20, and 30 ft from the leading edge) along the length of the test section. The DCP tests were conducted to compare values to the field CBRs and to determine the strength profile and approximate thickness of the stabilized layer. The field CBR method could measure only bearing capacity of the surface without disturbing the stabilized material below. Perpendicular lines labeled A1, A2, and A3 were painted on the subgrade to mark the prescribed data collection locations as shown in Figure 1. Along A1, the

Figure 9. Cement bags placed in grid area prior to spreading.

Figure 10. Mixing cement into the soil with a reclaimer/mixer.

Figure 11. Compacting stabilized subgrade with vibratory steel wheel roller.

Figure 12. Field CBR test.

field CBR tests yielded values of 23, 26, and 25 CBR, and a single DCP reading showed approximately 50 CBR for the upper 5-in. soil layer. Along A2, field CBR values were 31, 35, and 33 CBR, and the DCP showed a

strength of approximately 60 CBR in the upper 5-in. layer. Along A3, field CBR values were 32, 31, and 30 CBR, and the DCP indicated approximately 35 CBR in the upper 5-in. layer. Based on these values, researchers determined that the CBR of the section generally fell within the desired 25-50 CBR range near the surface, although there was significant variability.

After the mat testing had been completed, in situ CBR and DCP measurements were conducted to determine if the strength of the subgrade had changed during the evaluation. The average pretest and posttest CBR measurements for each item are shown in Table 3. Significant reductions in the surface CBR values were found using both the field CBR and DCP measurement methods. The bearing capacity at the surface appeared to have been reduced to approximately a 15 CBR. The large reduction was probably caused by pulverization of the upper surface of the cement-stabilized layer from the dynamic loading and unloading of the matting surface. The profile on the bottom surface of the mat system was not flat and, therefore, allowed the matting to penetrate and grind into the surface during trafficking. The reduction in the surface CBR allowed for an increased rate of deformation in the subgrade and likely led to premature failure of the test section.

Table 3. Average properties for the 25-50 CBR test section.

Test Location	In situ Field CBR	In situ DCP CBR Upper 5 in.	Change in Field CBR from Pretest	Change in DCP CBR from Pretest
Pretest				
A1	25.2	50		
A2	33.3	60		
A3	30.9	35		
Posttest				
A1	12.5	10	-12.7	-40
A2	18.5	15	-14.8	-45
A3	12.8	30	-18.1	-5

2.3.1.2 Mat installation

The MLC-70 Trackway matting system was pre-assembled before carrying it to the test site. Mat bundles were placed along the side of the assembly area with a forklift, and the individual panels were carried into position and installed by two men. Panels were assembled in a brickwork configuration

with half-panels inserted on each end of every other row. First, a full MLC-70 panel was placed along the baseline in the southwest corner of the assembly area. Subsequent rows were attached by inserting the male edge of the mat into the female edge of an existing mat and then sliding the panels together along their entire length while flat on the ground surface. No connection system was required on the short ends of the panels, so the system could be assembled from both sides of the installation area concurrently. Panels had to be "slid" across a maximum of only 15 ft of the area to complete assembly. Once panels were in position, shoot bolts were inserted into supplied notches in the male connector edges to prevent lateral movement of panels in each row. Figures 13 and 14 illustrate how the matting system was assembled. Once assembly was complete, the finished matting system was rolled (Figure 15) and loaded on a truck (Figure 16) that carried it to the test site.

Once the matting system arrived at the test site, it was unloaded and installed on the subgrade. The 30-ft-wide by 40-ft-long section was pushed by six men and was unrolled in approximately 5 sec. Figures 17 and 18 show how the mat was pushed and unrolled. Once unrolled, the mat was stretched to ensure all the slack had been removed from the joints and lead weights were placed along the edges to limit movement of the system. AM2 matting was placed at each end of the test section to create stable platforms for the load cart for entering and exiting the test area. The completed test section prior to trafficking is shown in Figure 19.

Figure 13. MLC-70 panel assembly.

Figure 14. MLC-70 shoot bolt insertion.

Figure 15. Rolling assembled mat expanse for transportation to the test section.

Figure 16. Loading mat expanse onto a flatbed trailer.

Figure 17. Unrolling MLC-70 matting on prepared test section.

Figure 18. Unrolling MLC-70 matting on prepared test section.

Figure 19. Final assembled F-15E traffic area with AM2 ramps.

2.3.2 25 CBR

2.3.2.1 Subgrade construction

Prior to construction of the MLC-70 test section, an AM2 mat test with an area approximately 60-ft-wide by 40-ft-long had been constructed over a 25 CBR in Hangar 4. To save time and resources, the subgrade for the MLC-70 test section was prepared by removing the upper 12 in. of CH in the existing test section. Field CBR tests indicated that the existing material at depths of 12 in. to 36 in. retained a CBR of approximately 25; therefore, reconstruction of the entire depth was unnecessary. Details of the original test section construction are discussed in Garcia and Rushing, 2014.

The upper 12 in. of CH material in a 25-ft-wide by 40-ft-long area was removed from the test section with a motor grader and was smoothed prior to mat placement. In situ field CBR tests were conducted on the north and south ends of the prepared area. Typically, if the average CBR of a lift differed from the target value by more than 0.5 CBR, the lift was reconstituted. However, since the strength of the CH is more susceptible to changes in moisture when the moisture content is less than 30% (Figure 7), the margin of variability was increased to 5 CBR for the target value. The measured values were averaged, and a CBR of 27.6 was determined; therefore, researchers concluded the target 25 CBR value had been reasonably achieved.

After the mat testing had been completed, in situ CBR measurements were conducted to determine the extent the subgrade had undergone gradual drying and densification under traffic. The average after construction (pretest) and after trafficking (posttest) CBR data for the test item are reported in Table 4. Some increase in bearing capacity was expected; however, significant changes in strength could have caused the number of passes allowed by the mat system prior to failure to increase. Typical increases based on historic data were 4 to 5 CBR on the surface, 2 to 3 CBR 6 in. deep, and 0 to 1 CBR 12 in. deep.

For the 25 CBR test item, the posttest CBR measurements at the surface showed an increase from 27.6 to 31.6 CBR during the trafficking. Since the increase fell within the expected ranges, no additional data were collected, and the test was determined to adequately represent a 25 CBR.

Table 4. Average soil properties for the 25 CBR test section.

Test Depth	Wet Density (lbf/ft³)[a]	Dry Density (lbf/ft³)[a]	Moisture (%)[a]	Oven Moisture (%)[b]	In situ CBR	Δ CBR Posttest
F-15E Item Pretest						
Surface	114.8	93.6	22.6	20.4	27.6	
F-15E Item Posttest						
Surface	113.1	93.6	20.9	19.0	31.6	4.0

[a] Readings are from nuclear density gauge. (ASTM D6938-10)

[b] ASTM D2216-10

2.3.2.2 *Mat installation*

The MLC-70 panels were installed in the same way as described for the 25-50 CBR test section above. AM2 ramps were installed at the north and south ends of the MLC-70 matting to facilitate the F-15E load cart movements. Steel weights were placed along the edges of the matting to limit movement of the test item and to mimic the effect of a larger expanse of matting. The final assembled test section is shown in Figure 20.

Figure 20. Final assembled 25 CBR test section.

2.3.3 100 CBR

2.3.3.1 Subgrade construction

Prior to construction of the MLC-70 test section, an AM2 mat test with an area approximately 30-ft-wide by 40-ft-long had been constructed over a 100 CBR in Hangar 4. To save time and resources, the subgrade for the MLC-70 test section was prepared by adding a thin layer of crushed limestone over the existing section and compacting it until smooth with a vibratory steel wheel roller. During all attempted in situ field CBR tests, the capacity of the proving ring was exceeded; therefore, an actual CBR number was not reported. We know only that the CBR exceeded 100. Since the material's bearing capacity was greater than our measuring abilities, researchers determined that reconstruction of the test section was unnecessary. Details of the original test section construction will be discussed in the upcoming 100 CBR AM2 Report being published by Garcia and Rushing (2014).

After the mat testing had been completed, in situ CBR measurements were conducted to determine if any measurable changes had occurred to the bearing capacity of the test material. The average after construction (pretest) and after trafficking (posttest) CBR data for the test item are reported in Table 5. The posttest CBR measurements at the surface showed no measurable increase during the trafficking; therefore, test pits were unnecessary.

Table 5. Average soil properties for the 100 CBR test section.

Test Depth	Wet Density (lbf/ft^3)[a]	Dry Density (lbf/ft^3)[a]	Moisture (%)[a]	Oven Moisture (%)[b]	In situ CBR	Δ CBR Posttest
Pretest						
Surface	136.7	134.0	2.7	2.2	100+	
Posttest						
Surface	141.9	139.2	2.7	1.1	100+	0

[a] Readings are from nuclear density gauge (ASTM D6938-10).

[b] ASTM D2216-10

2.3.3.2 Mat installation

The MLC-70 panels were installed in the same way as described for the 25-50 CBR test section above. The panels were configured as shown in Figure 3, with the purpose of evaluating two different panel joint

arrangements simultaneously. AM2 ramps were installed at the north and south ends of the MLC-70 matting to facilitate the F-15 load cart movements. Steel weights were placed along the edges of the matting to limit movement of the test item and to mimic the effect of a larger expanse of matting. The final assembled test section is shown in Figure 21.

Figure 21. Final assembled 100 CBR section.

2.3.3.3 Subgrade instrumentation

The 100 CBR subgrade was instrumented with 9-in.-diameter Geokon® earth pressure cells (EPCs) installed in the soil at eight locations under the matting to monitor the stress distribution provided by the mat system. EPCs were installed at depths of 6 in., 12 in., and 24 in. below the surface of the subgrade at two locations underneath the traffic centerline of the mat panels. Two EPCs were installed 6-ft offset from the traffic centerline at depths of 12 in. and 24 in. Pressure ranges for the cells at the 6 in., 12 in., and 24 in. depths were 300, 200, and 100 lbf/in.^{2}, respectively. The EPCs were installed during subgrade construction for the 100 CBR AM2 traffic test and remained in place for re-use during the MLC-70 Trackway mat evaluation. A photo of typical EPC installation is shown in Figure 22. A layout of the EPC positions is shown in Figure 23.

Figure 22. Typical EPC installation.

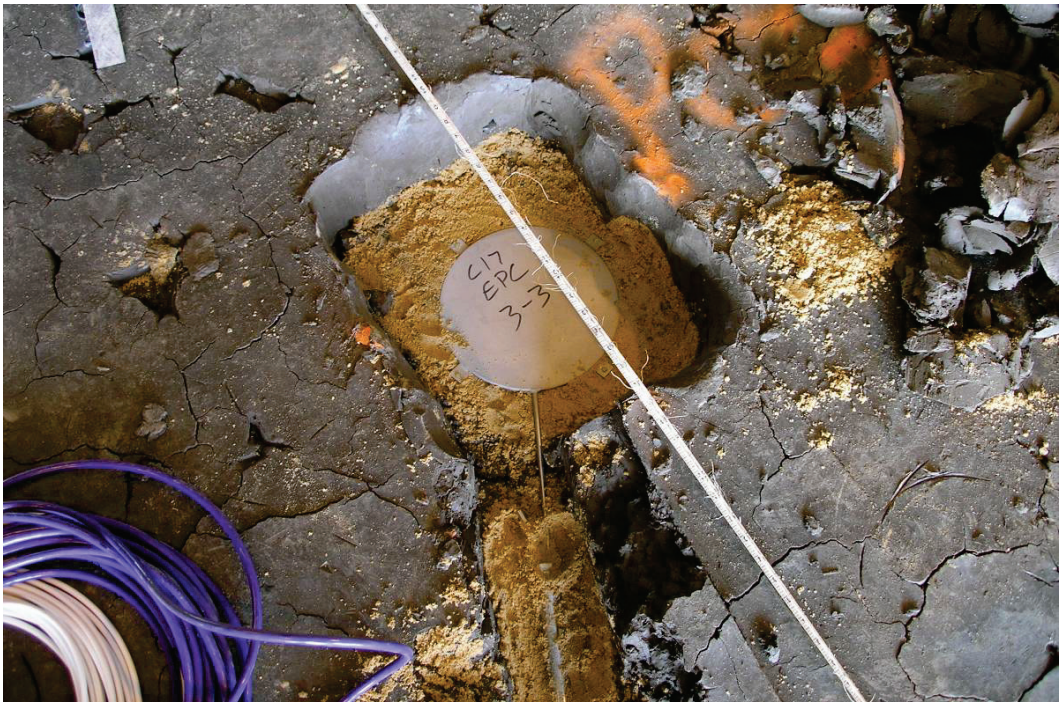

2.4 Traffic application

A specially designed single-wheel load cart was used to simulate F-15E aircraft traffic. The load cart was equipped with a 36 in.-by-11 in., 30-ply tire inflated to 325 lbf/in.^{2} and loaded such that the test wheel was supporting 35,235 lb. The F-15E load cart was equipped with an outrigger wheel to prevent overturning and was powered by a steel wheel compactor engine as shown in Figure 24.

A simulated, normally distributed traffic pattern was applied in a 3.75-ft-wide traffic area for the F-15E test items, as shown in Figure 25. Lanes were designed to simulate the traffic distribution pattern, or wander width, of the main landing gear wheels on a mat surface when taxiing to and from an active runway. The width of each lane corresponded to the contact width, 9 in., of the F-15E tire when fully loaded and not to the overall published tire width of 11 in. The normally distributed traffic pattern was simplified for ease of use by the load cart operator. Traffic was applied by driving the load cart forward and then backward over the length of the test item and then shifting the path of the load cart laterally approximately one tire width on each forward path. This procedure was continued until one pattern of traffic was completed. For the F-15E test area, one pattern resulted in 16 passes and 4 coverages. Traffic was continued in this manner until failure of either

Figure 23. Earth pressure cell layout for 100 CBR test section.

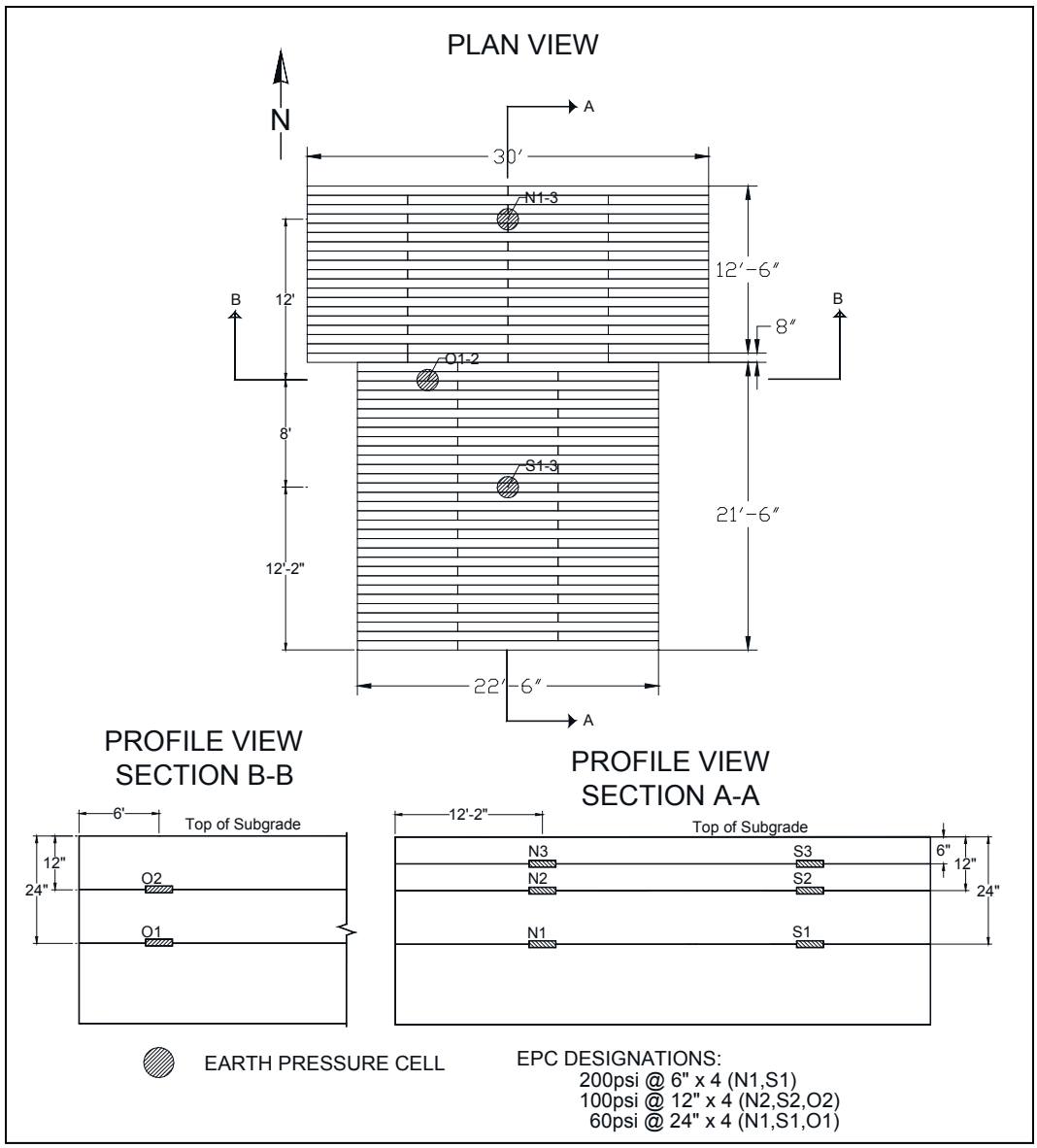

the mat or the subgrade occurred. Performance data, both static and dynamic, were collected periodically during trafficking, and the mat surface was inspected for damage during all trafficking breaks.

2.5 Data collection

The following sections describe data collection procedures used to characterize the response of each matting system to applied simulated aircraft traffic. Data collection intervals for the tests are shown in Table 6 for the F-15E.

Figure 24. F-15 test load cart.

Figure 25. Plan view showing F-15E normally distributed traffic lanes.

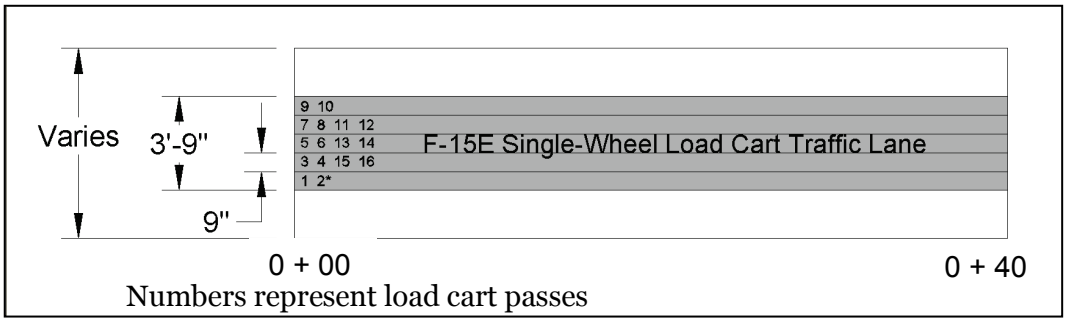

Table 6. Data collection intervals for the F-15E load cart.

Total Passes	Profile	Unloaded Cross Sections	Unloaded Rut Depth	Loaded Cross Sections	Loaded Rut Depth	Elastic Deflections	EPC[a]
Subgrade	X	X	X				
0	X	X	X	X	X	X	X
16	X	X	X	X	X	X	X
48	X	X	X	X	X	X	X
112	X	X	X	X	X	X	X
240	X	X	X	X	X	X	X
496	X	X	X	X	X	X	X
1008	X	X	X	X	X	X	X
2032	X	X	X	X	X	X	X
3056	X	X	X	X	X	X	X
3700	X	X	X	X	X	X	X
Subgrade	X	X	X				

[a] Only collected for the 100 CBR test section.

Typical data collection activities for each test section are shown in Figures 26 through 28. Data collection during trafficking of the three MLC-70 test sections included robotic total-station recordings along cross sections and centerlines, rut depth measurements, and elastic deflection measurements. Dynamic recordings of subgrade instrumentation response were included for the 100 CBR section.

The data collected prior to, at scheduled pass levels during, and after trafficking of the test sections were collected along the centerline and at the locations labeled A1, A2, and A3 (and A4 for the 100 CBR section), as shown in Figures 1 through 3. The locations of perpendicular lines A1, A2, and A3 for the 25-50 CBR and 25 CBR test sections were selected at the approximate quarter-points of the test items to characterize the average performance while avoiding potential end effects associated with boundary conditions at the ends of the test items. The 100 CBR section included two different panel arrangements, so an additional data collection line, A4, was added so that two locations on each arrangement were evaluated.

Figure 26. Typical centerline profile data collection.

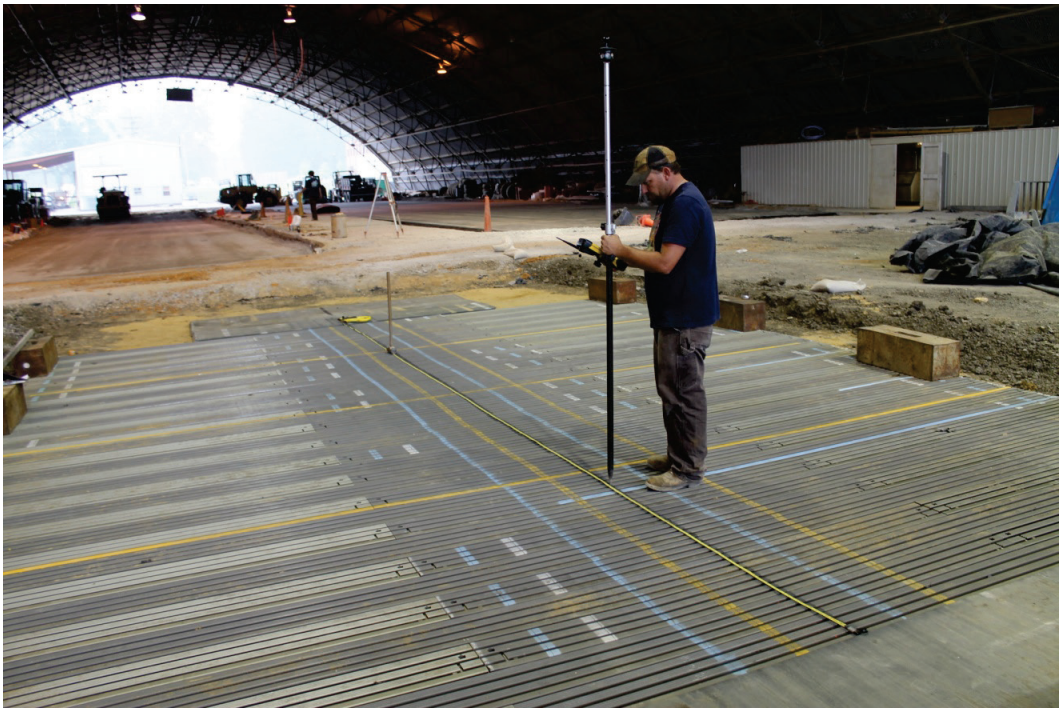

Figure 27. Typical loaded cross-section data collection.

Figure 28. Typical unloaded rut depth measurements.

Robotic total-station profile data collected at 1-ft intervals along these lines are called “cross sections” in this report. Robotic total-station profile data collected at 1-ft intervals along the traffic centerline are called

"centerline profiles" in this report. Rut depths were measured on each data collection line with an aluminum straightedge and a ruler. Measurements were taken at the centerline and at one foot east and west of the centerline. Elastic deflection measurements were recorded along the centerline by mounting a prism on the load cart above the test wheel and continuously recording the change in elevation while trafficking. The amount of mat damage and the mode of failure were recorded during the traffic phase.

2.6 Failure criteria

The failure criteria for the mat systems were defined as (1) 10% mat breakage or (2) the development of 1.25 in. of permanent surface deformation for the F-15E. These failure criteria were developed based upon previous testing of airfield matting and USAF requirements. Failure criteria values were recorded and monitored for compliance.

2.6.1 Mat breakage

Mat breakage percentages were calculated by dividing the area of the failed panel (or half-panel) by the area of the assembled test section. Individual panels were considered failed if damage posed a significant tire hazard or caused instability to the load cart. Tire hazards were defined as damage that could not be reasonably maintained by simple field maintenance procedures.

2.6.2 Permanent deformation

The permanent surface deformation limit of 1.25 in. is based on roughness limitations for the F-15E aircraft. An abrupt change in elevation or the development of a rut in the wheel path greater than the allowable value may exceed the roughness limit. The rut depth limit is required, since many connecting taxiways and aprons intersect at 90 deg, and crossing perpendicular to a pre-formed rut may cause an abrupt change in elevation exceeding aircraft limits. Failure by permanent surface deformation was determined from robotic total-station cross sections, profiles, and manual rut depth measurements. Each of the following data collection categories was analyzed for compliance with the failure criterion:

1. centerline profile deformation,
2. loaded surface deformation, and
3. unloaded surface deformation.

2.6.2.1 Centerline profile deformation

Centerline profile deformation was measured by a robotic total station and prism along the traffic centerline. The difference in elevation one or two stations apart was analyzed from plots of the data to determine if an abrupt change in elevation reached failure limits for each interval during trafficking.

2.6.2.2 Loaded surface deformation

An attempt was made to measure the permanent deformation of the subgrade underneath the mat surface by parking a forklift carrying lead weights adjacent to the data collection locations shown in Figures 1 through 3 and recording cross sections and rut depths along the lines. The wheel load applied was approximately 6,000 lb. The goal of the load application was to bend the mat enough to contact the subgrade, but not so much as to induce elastic deflections in the subgrade; however, since the panels' surfaces contained no holes, the extent of bending and the location of the subgrade surface were unknown. The maximum deformation at each location was determined as the difference in elevation from the average height of the elevated material on each side of the trough to the deepest point in the bottom of the trough. Measurements were averaged to obtain a single value for comparison to the failure criterion. The deformation measurements determined by this method are noted as "loaded cross sections" and "loaded rut depths" in this report.

2.6.2.3 Unloaded surface deformation

Unloaded surface deformation values were determined from cross sections and rut depths measured at the primary data collection locations on the mat surface shown in Figures 1 through 3. Measurements were averaged to obtain a single value for comparison to the failure criterion. The deformation measurements determined by this method are noted as "unloaded cross sections" and "unloaded rut depths" in this report.

3 25-50 CBR Results and Analysis

The 25-50 CBR test section was constructed in June of 2011 at an outdoor pavement test facility at the ERDC. The following sections describe the observations during trafficking by simulated F-15E aircraft loads; results of data collection; and analysis of the results.

3.1 25-50 CBR trafficking results

3.1.1 Behavior of mat under traffic: Visual observations

Trafficking began June 27, 2011, on the 25-50 CBR test section. After 16 passes, deformation was noted along the centerline of the panels near data collection line A1. Deformation continued to increase with each pass of the F-15E load cart. After 112 passes, a small section of matting between the shoot bolt and the end of a mat panel in the 20th panel row broke free as shown in Figure 29. The loaded deformation along A1 and A2 had reached 1.92 in. and 1.59 in., respectively, and therefore exceeded the failure limit. Also, slight corner curls were noted along centerline panel joints from rows 1 through 30. Once 240 passes had been completed, another piece of matting between the shoot bolt and panel end broke free from a mat on row 14, and the deformation along the first 15 ft of the test section was nearly 3 in. This large deformation caused a significant bow wave to form that resulted in instability in the load cart, as shown in Figure 30. The loaded deformation along A3 had reached 1.38 in., which also exceeded the failure limit. The subgrade material had worked its way through the mat joints and covered the mat section in the wheel path, as shown in Figure 31. Because of the instability and threat of a tire hazard by pinching the tire between the panel joints, traffic was stopped over the first 15 ft of the test section.

Traffic was resumed on the remaining section. After 496 passes, trafficking was stopped after tire damage was noted on the F-15E test wheel, as shown in Figure 32. At this time, the permanent deformation along lines A1, A2, and A3 ranged from 1.5 to 3.0 in., and therefore exceeded the 1.25 in. deformation limit over the entire length of the test section. No further traffic was applied. A summary of the panel damage and deformation is presented in Table 7.

Figure 29. Broken mat panel after 112 passes on the 25-50 CBR section.

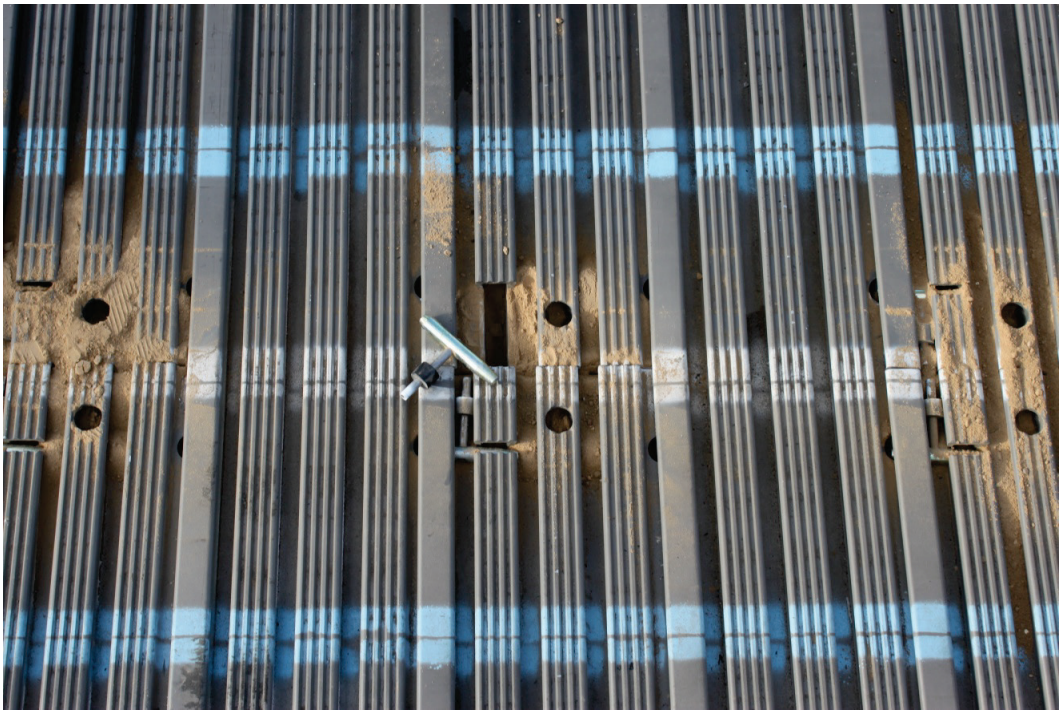

Figure 30. Excessive rutting and bow-wave formation after 240 passes near A1 on the 25-50 CBR section.

Figure 31. Deformation of MLC-70 panels after 240 passes on 25-50 CBR section.

Figure 32. Tire damage after trafficking 25-50 CBR test section.

Table 7. 25-50 CBR mat damage summary.

Number of Passes	Failure Type	Damage Description	Loaded Deformation (in.)		
			A1	A2	A3
112	Permanent Deformation	Loaded deformation >1.25 in. for A1 and A2	1.92	1.59	0.90
240	Permanent Deformation	Loaded deformation >1.25 in. for A3	2.98	2.10	1.38
496			NA	2.29	1.52

3.1.2 Permanent deformation

Permanent deformation was measured on the subgrade before and after the test and on the mat surface before trafficking; at intervals during trafficking, as shown in Table 6; and after trafficking was concluded. The pre-traffic data were subtracted from all subsequent data in attempt to normalize the data, or to show only the changes that occurred because of trafficking. The discussions that follow are based on normalized data.

Plots of the centerline profile data, as determined from robotic total-station measurements, are shown in Figures 33 and 34. Maximum abrupt changes in elevation were determined by observing the difference in elevation of data points within two stations of each other and choosing the maximum value for each plot. Each maximum value was then used for comparison to the roughness criterion. Beginning and ending stations for both test items were ignored because of changing boundary conditions at the interface of the test items and AM2 ramps. Since the two mats were not physically connected, and the AM2 panels are much stiffer, the movement of the AM2 panels under traffic loads was insignificant compared to that of the test item. As ruts began to form under the ends of the test item, an elevation difference was apparent at the interface of the ramps. The abrupt change in elevation caused the load cart to dynamically impact the ends of the test item and increase the rate of deformation of the subgrade in these areas. Therefore, the impact areas displayed behavior significantly different from that of the interior portions of the test item. Since these end effects are not representative of normal field conditions, they are largely ignored for data analysis. An example of this behavior can be seen in Figure 33 from Stations 0 to 4 and from Stations 36 to 40.

Figure 33. 25-50 CBR centerline profile on the subgrade.

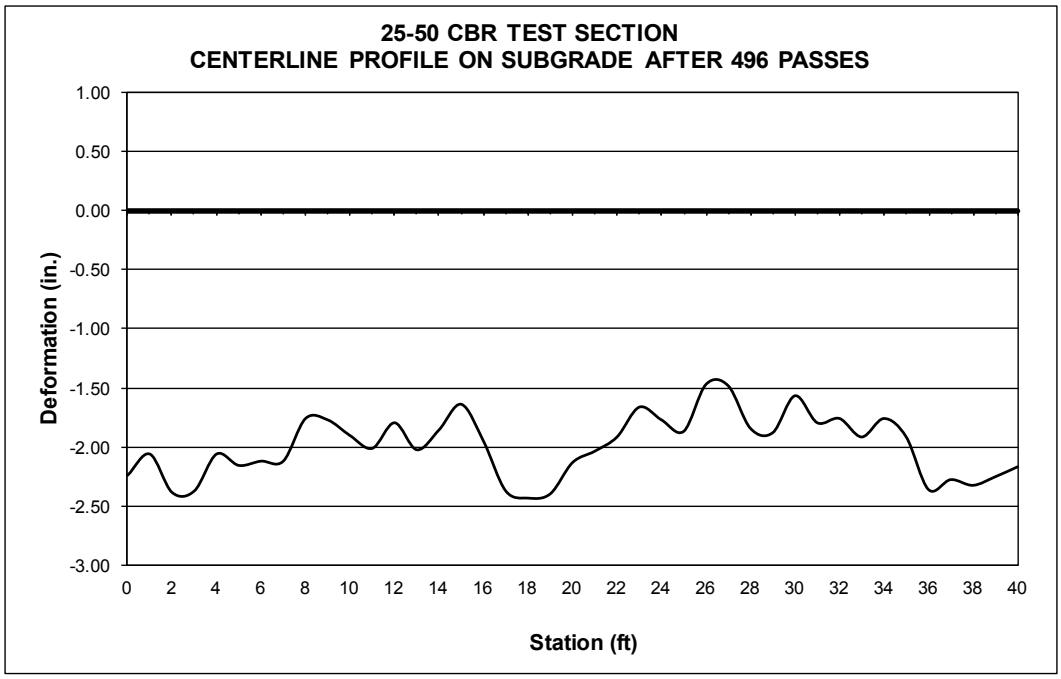

Figure 34. 25-50 CBR centerline profiles on the mat surface.

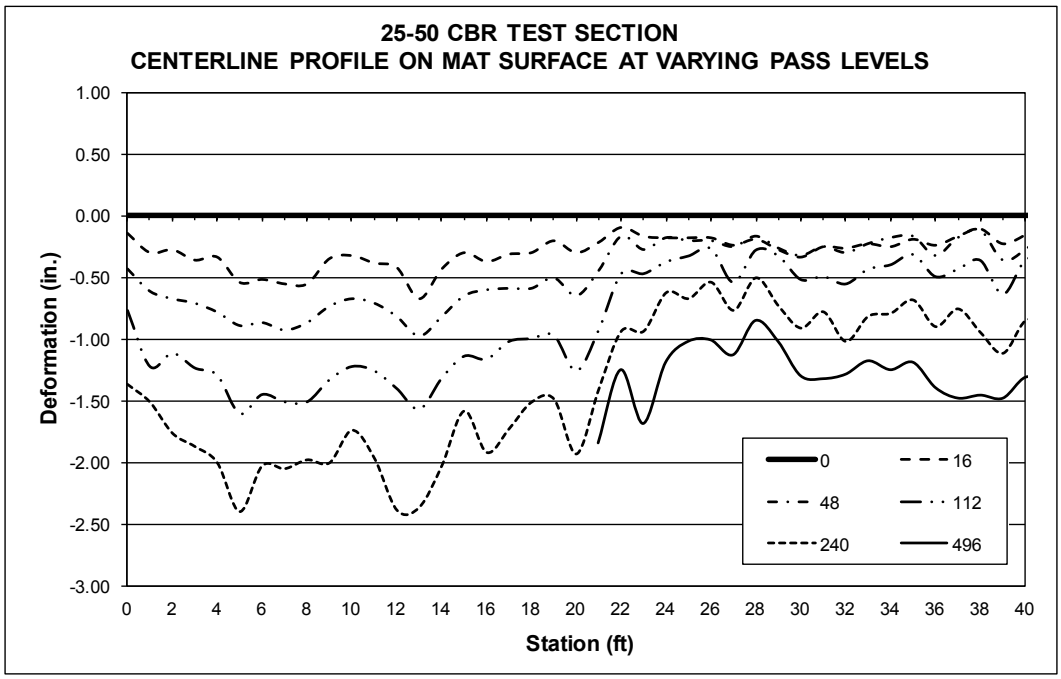

Plots of the cross-section data collected along lines A1, A2, and A3 are shown in Figures 35 through 40. Maximum deformation values for the loaded and unloaded cross sections were determined as the difference in elevation from the average height of the elevated material on each side of the trough to the deepest point in the bottom of the trough.

Figure 35. 25-50 CBR deformation on the loaded mat surface along A1.

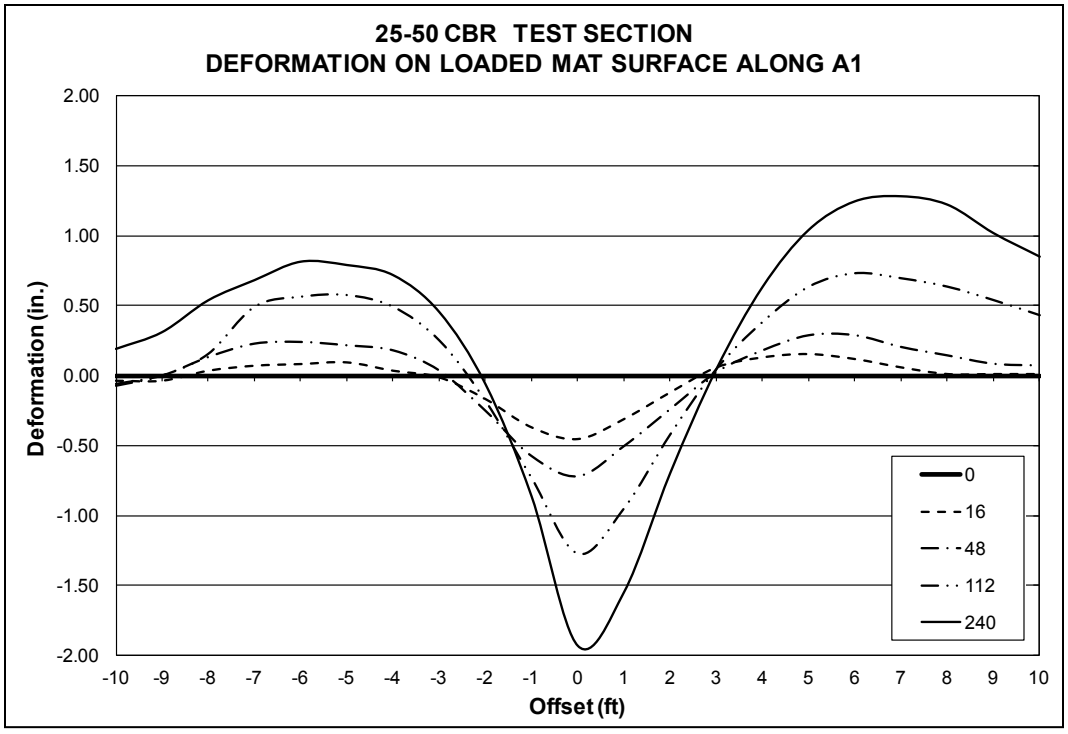

Figure 36. 25-50 CBR deformation on the loaded mat surface along A2.

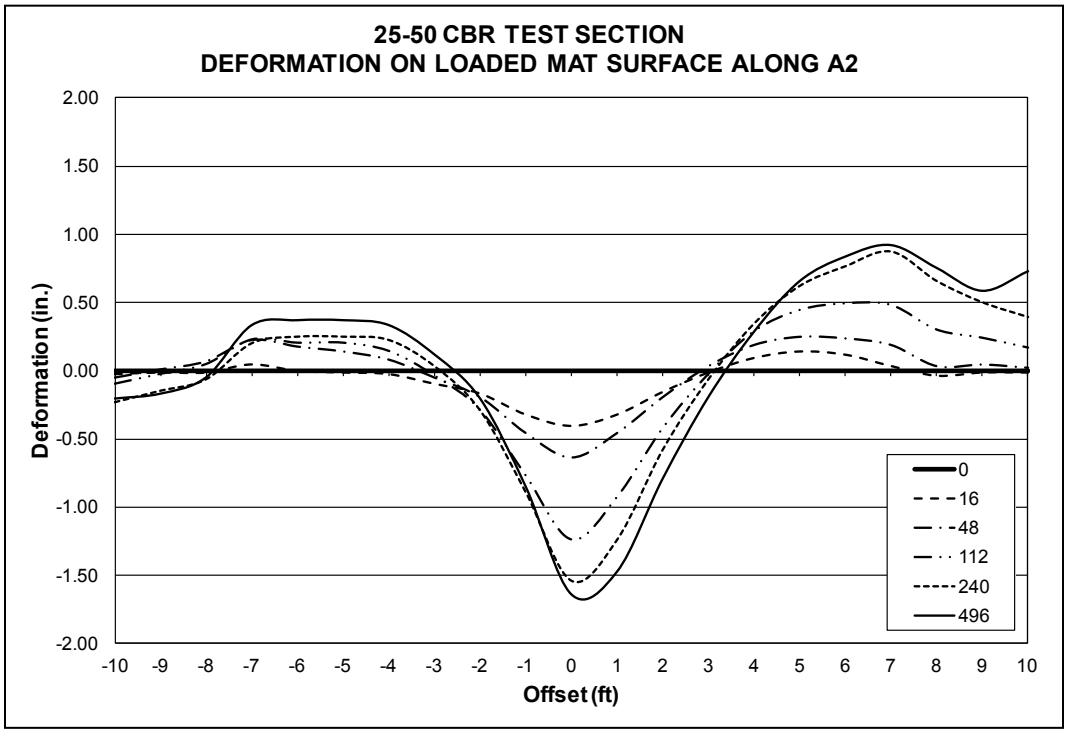

Figure 37. 25-50 CBR deformation on the loaded mat surface along A3.

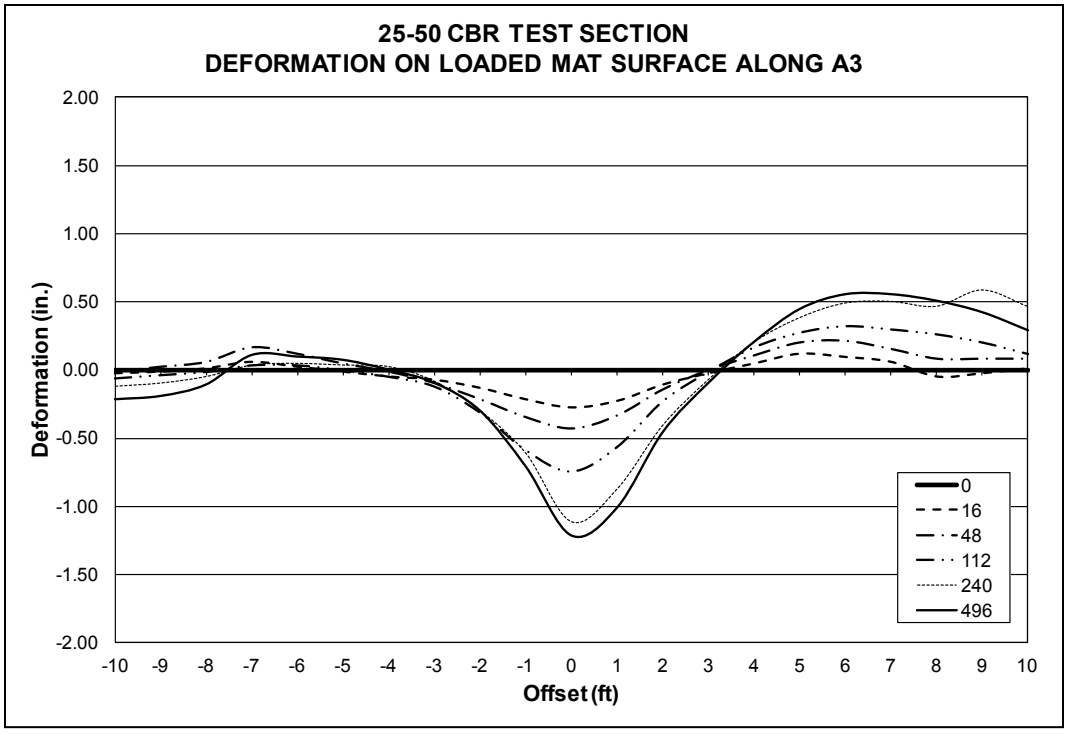

Figure 38. 25-50 CBR deformation on the unloaded mat surface along A1.

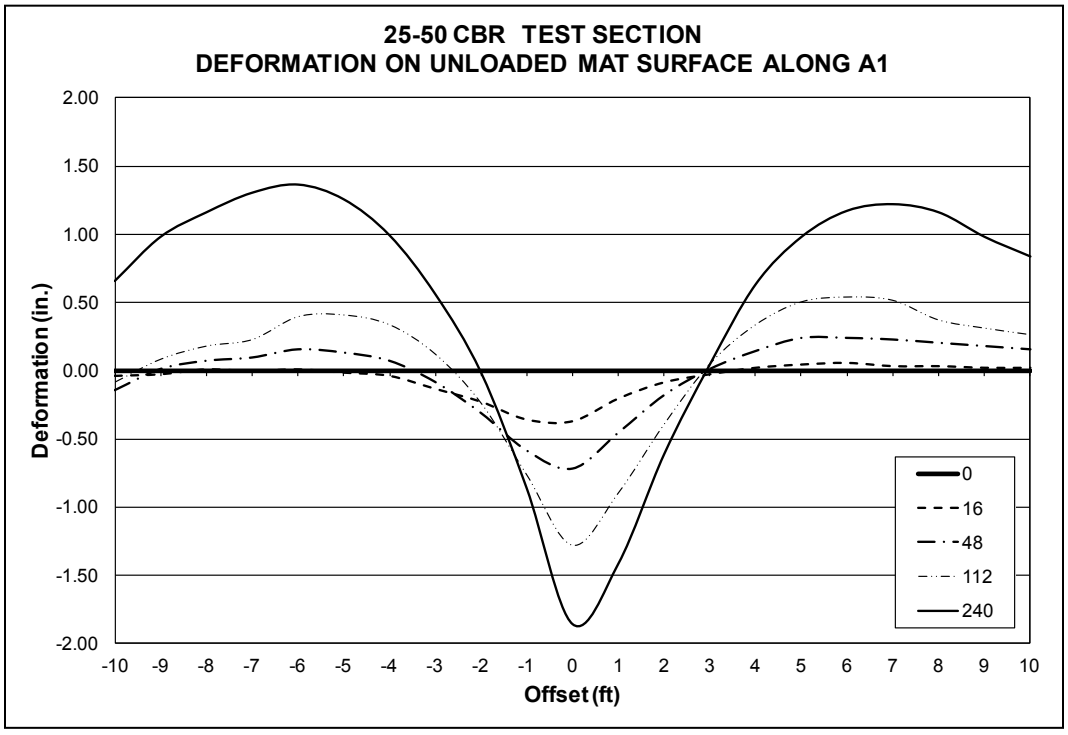

Figure 39. 25-50 CBR deformation on the unloaded mat surface along A2.

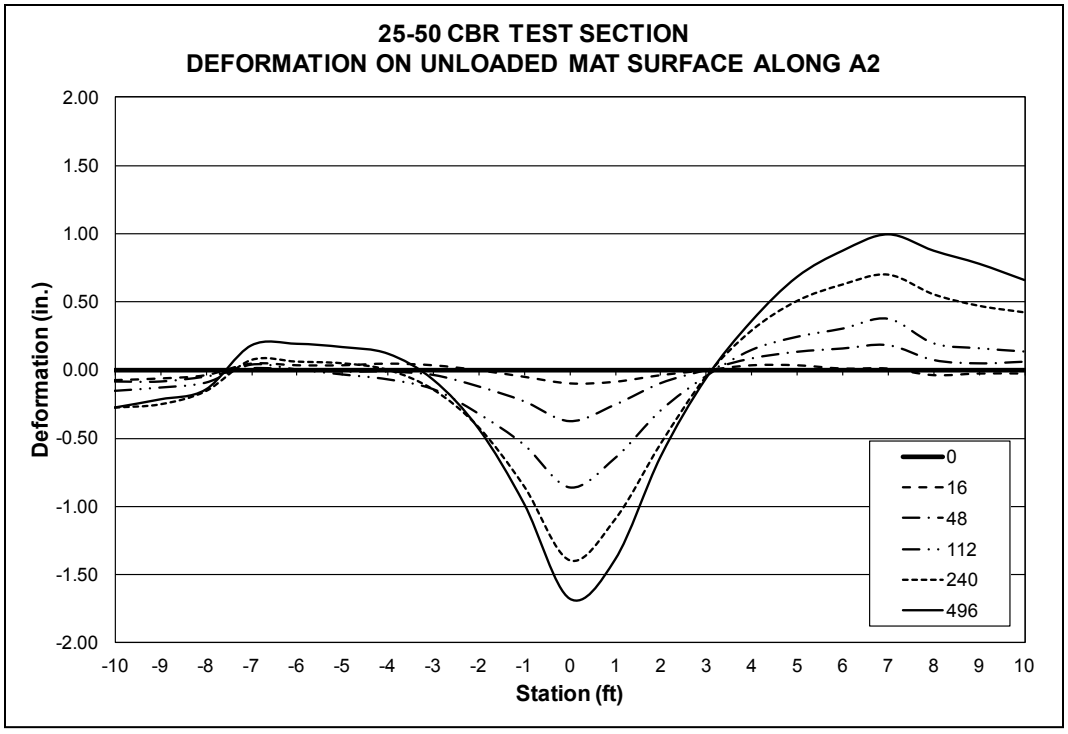

Figure 40. 25-50 CBR deformation on the unloaded mat surface along A3.

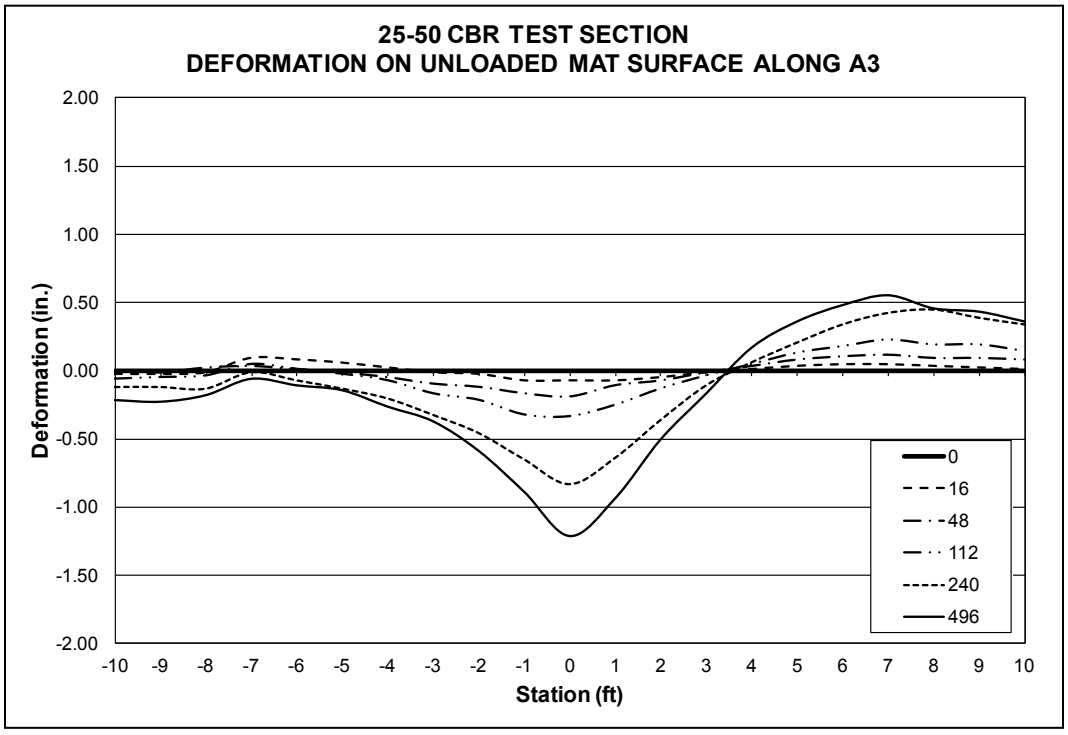

The maximum rut depths measured on the mat surface, both loaded and unloaded, were determined with a straightedge and a ruler. Rut depth measurements are presented in Figures 41 and 42. The rut depth measurements were used to verify values obtained by rod and level cross-section readings.

Table 8 summarizes maximum deformation values measured on each item for profiles, cross sections, and measured rut depths.

3.1.3 Elastic deflection

Elastic deflection was measured on 25-50 CBR test item at scheduled pass intervals. A plot of these data is shown in Figure 43. This plot indicates the elastic deflection, or rebound, of the mat and subgrade as the test wheel moved over the surface.

Elastic deflection was determined by mounting a survey prism on the F-15E load cart just above the center of the load wheel. A continuous survey mode was used with the robotic total station so that elevations were recorded each time the load cart moved 6 in. from the previous measurement. These data were collected dynamically at scheduled pass intervals throughout trafficking. The data were reduced, and measurements within half a tire width (4.5 in.) from the centerline were averaged at each 1-ft station along the centerline of traffic. The average elevation at each station was then subtracted from measurements taken on the unloaded mat surface at the same location. For example, the average of dynamic deflections at each station for passes 16 to 32 was subtracted from the unloaded centerline profile recordings at each station collected at pass 16. The difference in the loaded and unloaded measurements is the elastic deflection, or rebound, of the mat and subgrade as the test wheel moved over the surface. The average elastic deflection at each station for each data collection interval is shown in Figure 43.

3.2 25-50 CBR analysis of results

3.2.1 Mat breakage

Three types of mat damage were noted during trafficking: (1) dishing (plastic deformation) of the mat panels, (2) corner curls along the wheel path, and (3) breaking off of a panel section between the shoot bolt and panel end adjacent to the traffic centerline. The most common damage

Figure 41. 25-50 CBR loaded rut depths measured on the mat surface with a straightedge.

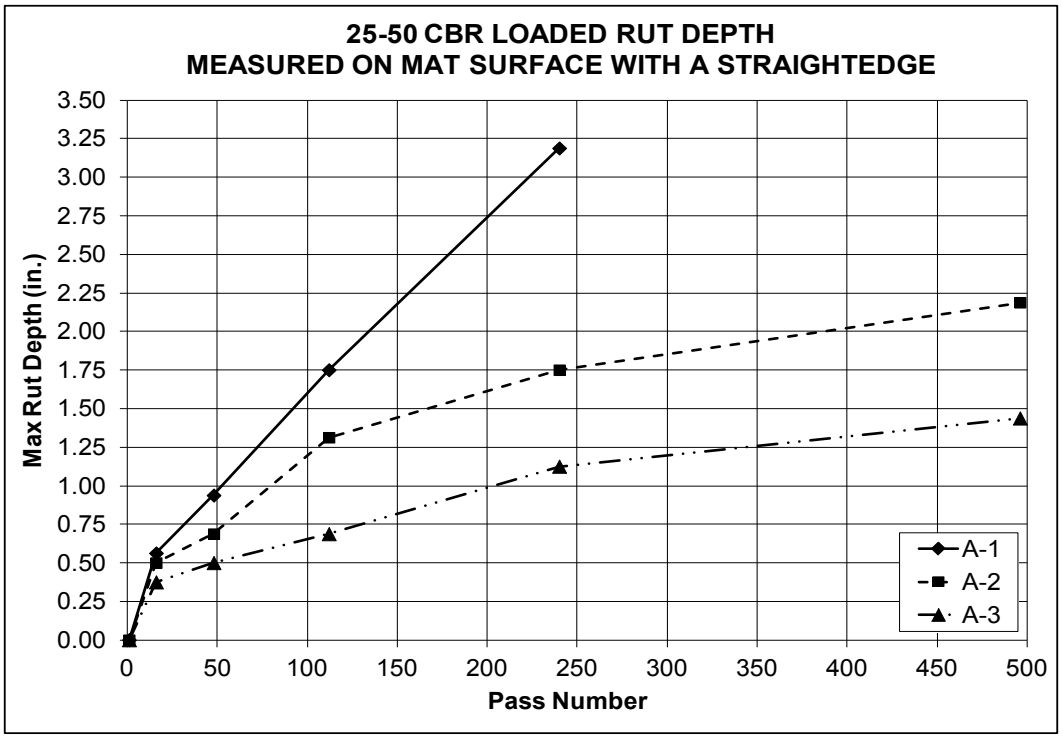

Figure 42. PSA unloaded rut depths measured on the mat surface with a straightedge.

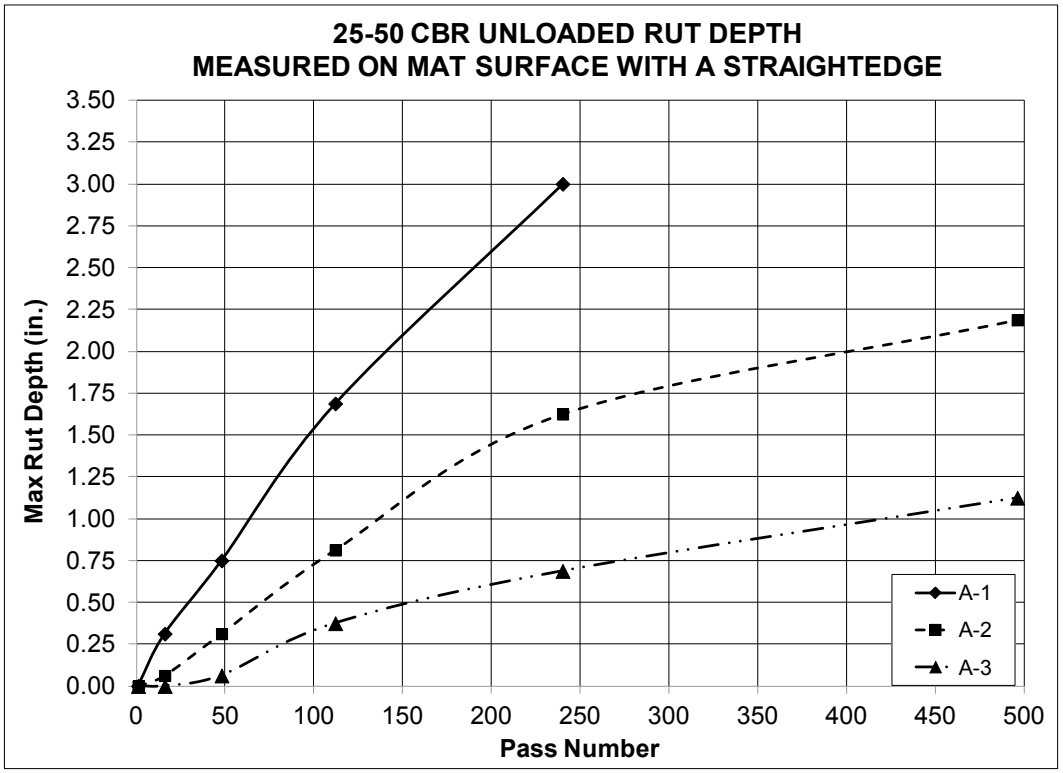

Table 8. PSA permanent deformation maximum values measured for each test item.

Data Collection Location	Pass No.	Subgrade Profile Max Abrupt Change in Elevation (in.)	Mat Surface Profile Max Abrupt Change in Elevation (in.)	Loaded Deformation on Mat Surface (in.)	Unloaded Deformation on Mat Surface (in.)	LoadedRut Depth with Straightedge (in.)	Unloaded Rut Depth with Straightedge (in.)
A1	240	0.74	0.99	2.98	3.15	3.19	3.00
A2	496			2.29	2.26	2.19	2.19
A3	496			1.52	1.49	1.44	1.13

Figure 43. Elastic deflection on mat at various pass levels for the 25-50 CBR item.

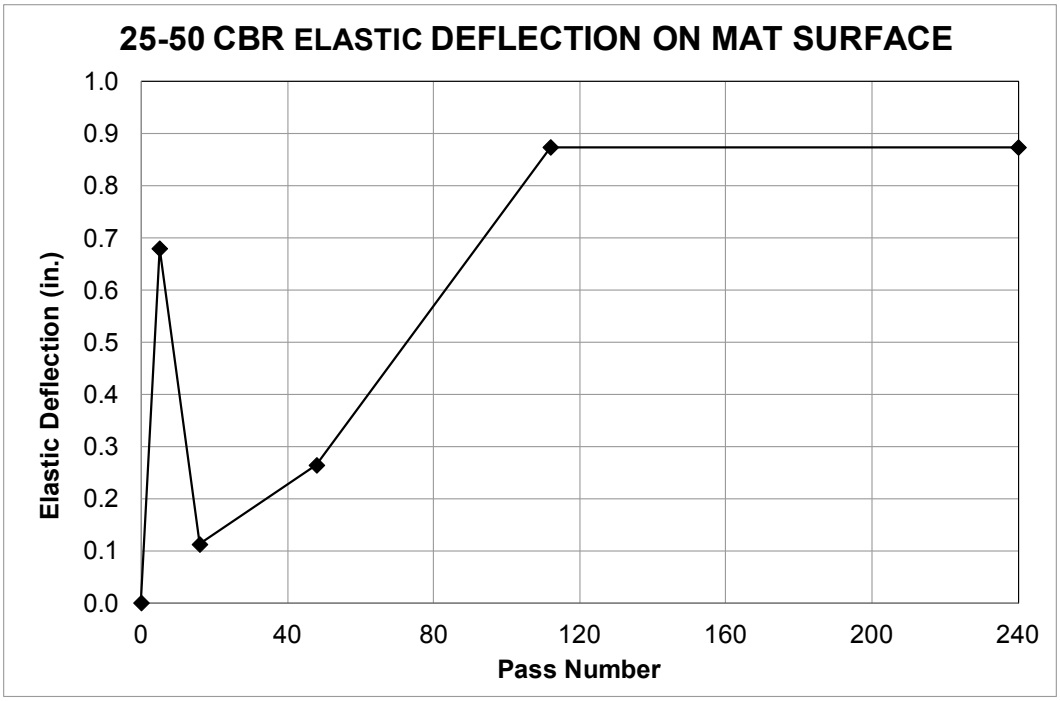

was dishing. TheMLC-70 mat system was not stiff enough to prevent subgrade deformation from occurring. As the subgrade deformed, an air gap began to form between the bottom surface of the mats and the top of the subgrade. Eventually the size of the air gap increased until the strain in the mat exceeded its elastic limit. Once the elastic limit was exceeded, the mat began to yield and plastically deform. Nearly all of the panels in the wheel path had some degree of dishing; however, the dishing did not cause tire hazards nor prevent further operations from occurring and was not counted as mat breakage in terms of the failure criteria. Mat panel dishing is accounted for in the subgrade deformation failure criterion.

The second most prevalent damage was the formation of corner curls at the free ends of panels along the traffic centerline. These corner curls resulted from stresses applied to the outside free corner of the female connector by the male connector of the adjacent panel. As the subgrade deformation increased, the severity of the corner curls also increased, since the freedom of movement at the free end allowed for an increase in the level of applied stress at that location. None of the corner curls presented an isolated tire hazard or limited traffic; therefore, none of the corner curls were noted as mat breakage in terms of the failure criterion.

Only two panels were noted to have broken pieces of the upper section of the mat between the free end and the shoot bolt closest to the traffic centerline. This damage was determined to be a function of subgrade deformation and not solely mat panel fatigue failure. As the subgrade deformation became greater than the failure criterion, the two free panel ends along the centerline began to contact each other and were forced to rotate downward under the test load. The downward force was transferred into the two panels since there was little subgrade support underneath. A crack was incubated and then propagated under low cycle fatigue, until the mat piece broke free from the panel and instantly relieved the stress from its partner piece on the opposite side of the centerline. These two mat breaks were considered failure; however, the 10% mat breakage failure criterion was not reached during the evaluation.

3.2.2 Permanent deformation

3.2.2.1 Centerline profile

The profile plots in Figures 33 and 34 were analyzed to determine whether the roughness criterion was exceeded. The maximum changes in elevation were 0.74 and 0.99 in. for the final subgrade and mat surface profiles, respectively. Since these values were less than the 1.25-in. failure criterion for the F-15E, the MLC-70 Trackway mat system performed adequately to prevent excessive roughness from occurring.

3.2.2.2 Cross sections

Figures 35 through 40 show cross-section values of the mat surface, both loaded and unloaded, for the 25-50 CBR test item. From the values reported in Table 8, the failure criterion of 1.25 in. was exceeded at all three data collection locations after trafficking was concluded. Since all three locations had measurements greater than 1.25 in., the system failed due to excessive

permanent deformation. From Figures 35, 36, and 37, the permanent deformation appeared to have exceeded the failure limit after 112 passes at A1 and A2, and after 240 passes at A3. However, since permanent deformation was measured only at scheduled traffic intervals, the exact number of passes required to reach 1.25 in. is unknown.

Normally, the deformation along the three data collection locations are averaged to determine a single value for comparison to the failure criterion; however, since there was a high degree of variability in the strength of the soil at these locations, they were analyzed independently. After the test was concluded, the posttest soil strength measurements in Table 3 showed a decrease to 10, 15, and 30 CBR, respectively, for A1, A2, and A3. The large drop in strength indicated that the stabilized layer likely pulverized during trafficking and lost strength rapidly. The early strength loss greatly increased the rate of subgrade deformation and led to early failure of the system. For the purpose of predicting the number of passes the system could sustain prior to failure, an effective 15 CBR was assumed to account for the behavior of the stabilized section. A second attempt to meet the test objective was accomplished by constructing another test section using a CH material as described in the 25 CBR sections of this report.

3.2.3 Elastic deflection

The elastic deflection measurements for the 20-50 CBR test section shown in Figure 43 were the sum of the elastic deflection of the mat and the subgrade. The elastic deflection values increased almost immediately from 0 to 0.7 in. in the first 5 passes, decreased back to 0.1 after 21 passes, increased to 0.9 after 112 passes, and remained constant until 496 passes. The initial increase was caused as the mat system's profile allowed it to push into the upper surface of the subgrade and then rebound to its initial position. Once the panels began to strain beyond their yield, the elastic deflection decreased because the panels conformed to the shape of the subgrade. Additional traffic application caused the rate of subgrade deformation to increase faster than the deformation of the matting system. The elasticity of the aluminum panels allowed them to bridge over the air gap when unloaded. After about 112 passes, the system stabilized and the elastic deflection remained constant until the test was concluded. The relatively large elastic deflection values indicate that the MLC-70 system was not stiff enough to prevent subgrade deformation once the stabilized layer began to break up. Since the results did not appear to be indicative of a 25 CBR subgrade, an additional test section was constructed of CH material as described in the 25 CBR sections of this report.

4 25 CBR Results and Analysis

The 25 CBR test section was constructed in May 2012 in the Hangar 4 pavement test facility at the ERDC. The following sections describe the observations during trafficking by simulated F-15E aircraft loads; results of data collection; and analysis of the results.

4.1 25 CBR trafficking results

4.1.1 Behavior of mat under traffic: Visual observations

Trafficking began May 31, 2012, on the 25 CBR test section. After the test vehicle completed 16 passes, data were collected, and no damage was noted to the mat surface. Traffic continued with data collected at the scheduled intervals shown in Table 6 with no damage reported. After 1,008 passes, the test section was considered failed due to permanent deformation in excess of the 1.25-in. allowable limit for the F-15E aircraft; however, since the only mat damage was dishing (plastic deformation) in the traffic area, and no tire hazards were present, traffic was continued. After 2,032 passes, traffic was concluded, because the permanent deformation on the test section had greatly exceeded the 1.25-in. limit. The only panel damage observed upon conclusion of traffic was dishing of the mat panels in the wheel path. Figure 44 shows the condition of the test section after 2,032 passes. A summary of the results from system trafficking is shown in Table 9.

4.1.2 Permanent deformation

Permanent deformation was measured on the subgrade before and after the test and on the mat surface before trafficking; at intervals during trafficking shown in Table 6; and after trafficking was concluded. The pre-traffic data were subtracted from all subsequent data in attempt to normalize the data, or to show only the changes that occurred because of trafficking. The discussions that follow are based on normalized data.

Plots of the centerline profile data for the 25 CBR section, as determined from robotic total-station readings, are shown in Figures 45 and 46. Maximum abrupt changes in elevation were determined by observing the difference in elevation of data points within two stations of each other and choosing the maximum value for each plot. Each maximum value was then used for comparison to the roughness criterion. Beginning and ending

Figure 44. Final condition of 25 CBR F-15E test section after 2,032 passes.

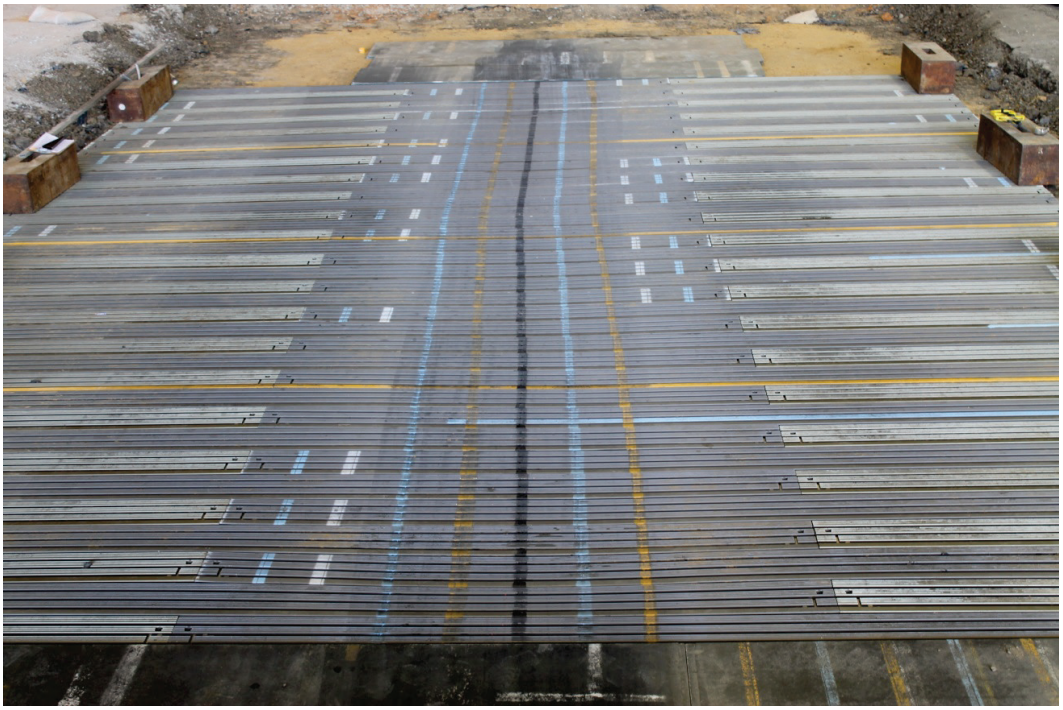

Table 9. 25 CBR mat damage summary.

Number of Passes at Failure	Failure Type	Damage Description	Loaded Deformation (in.)
1,008	Permanent Deformation	Loaded deformation >1.25 in.	1.32
2,032			1.69

stations were ignored because of changing boundary conditions at the interface of the test section and the AM2 ramps. Since the two mat types were not physically connected and the AM2 panels were installed over a much stiffer material, ruts began to form under the ends of the test section, and an elevation difference was apparent at the interface of the ramps. The abrupt change in elevation caused the load cart to dynamically impact the ends of the test section and increase the rate of deformation of the subgrade in these areas. Therefore, the impact areas displayed behavior significantly different from that of the interior portions of the test section. Since these end effects are not representative of normal field conditions, they are largely ignored for data analysis. An example of this behavior can be seen in Figure 45 from Stations 0 to 2 and from Stations 26 to 28.

Figure 45. Centerline profile on the subgrade for the 25 CBR section.

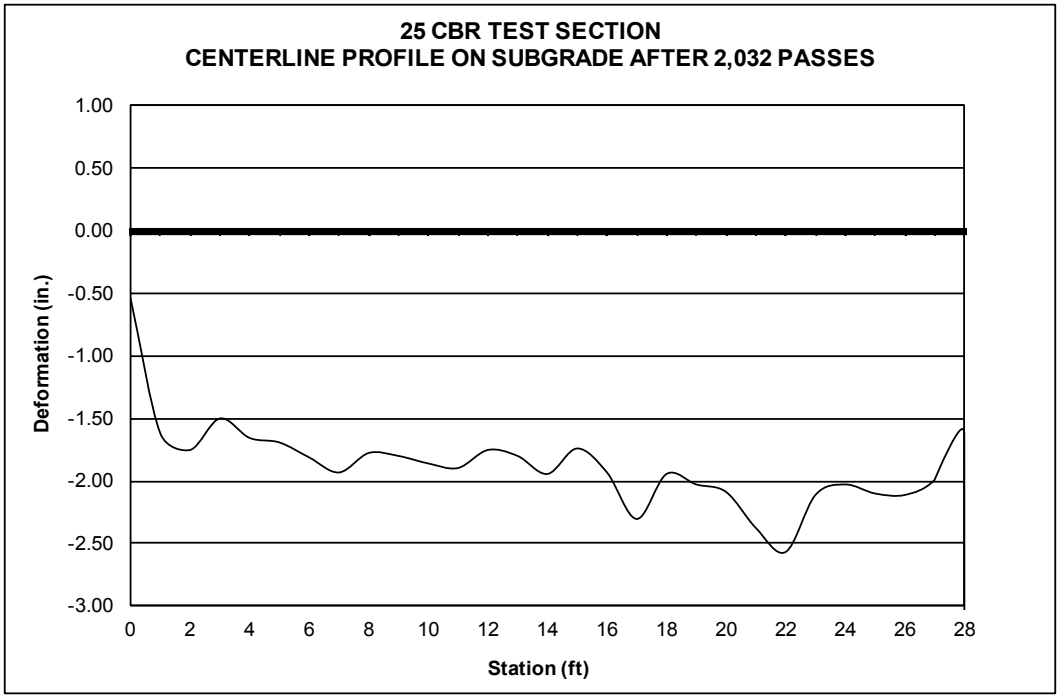

Figure 46. Centerline profile on mat surface for the 25 CBR section.

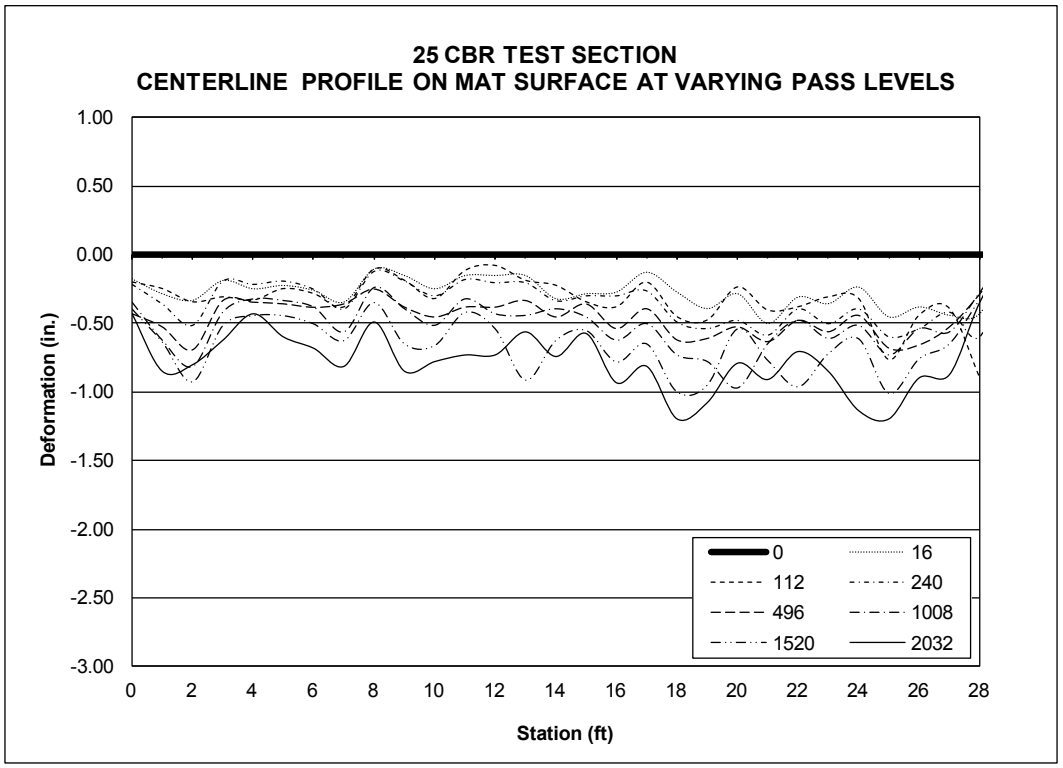

Plots of the average cross-section data, collected along lines in Figure 2, are shown in Figures 47 through 49. Maximum deformation values for the subgrade, loaded, and unloaded cross sections were determined as the difference in elevation from the average height of the elevated material on each side of the trough to the deepest point in the bottom of the trough.

The maximum rut depths measured on the mat surface, both loaded and unloaded, were determined with a straightedge and a ruler. Rut depth measurements are presented in Figure 50 with a logarithmic scale along the x-axis for clarity. Pass 0 was changed to pass 1 in this figure, so the initial point could be displayed on the logarithmic scale. The rut depth measurements were used to verify values obtained by robotic total-station cross-section readings.

Table 10 summarizes maximum deformation values measured after trafficking was concluded for profiles, cross sections, and measured rut depths.

4.1.3 Elastic deflection

Elastic deflection was measured on the 25 CBR test section at scheduled pass intervals shown in Table 6. A plot of these data is shown in Figure 51. This plot indicates the elastic deflection, or rebound, of the mat and subgrade as the test wheel moved over the surface.

Figure 47. Average subgrade deformation in the 25 CBR section.

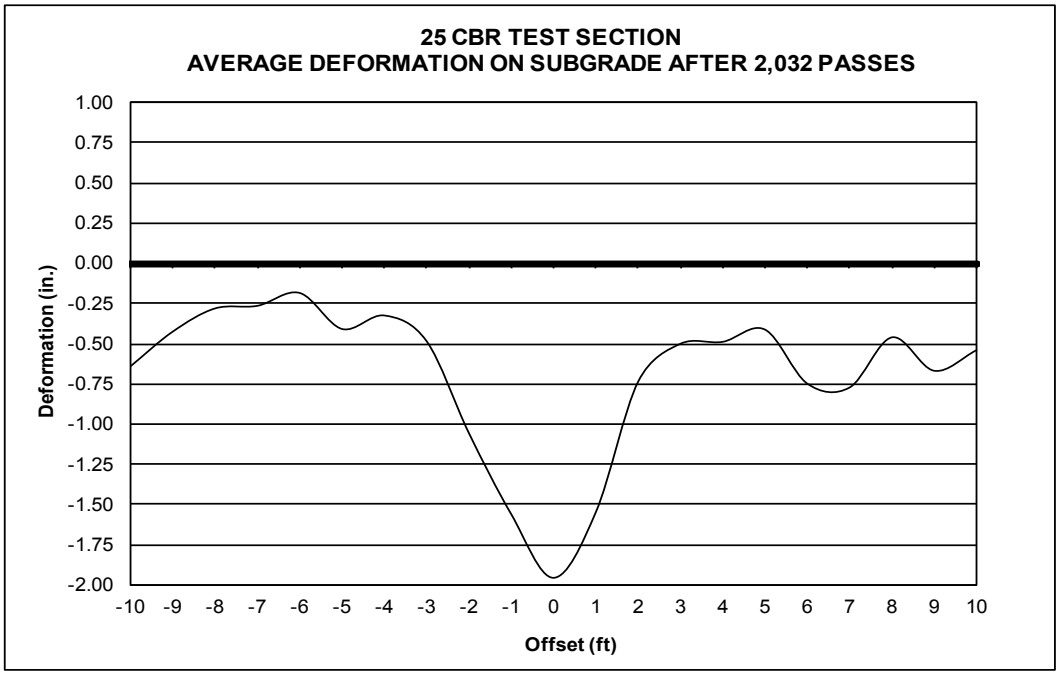

Figure 48. Average deformation on the loaded mat surface in the 25 CBR section.

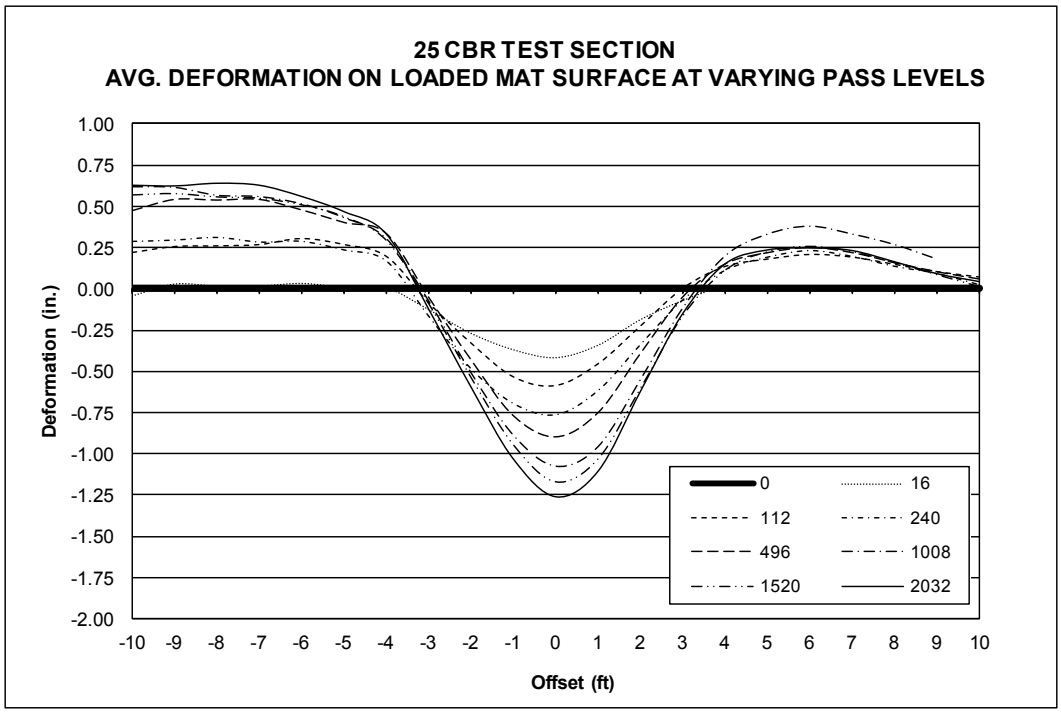

Figure 49. Average deformation on the unloaded mat surface in the 25 CBR section.

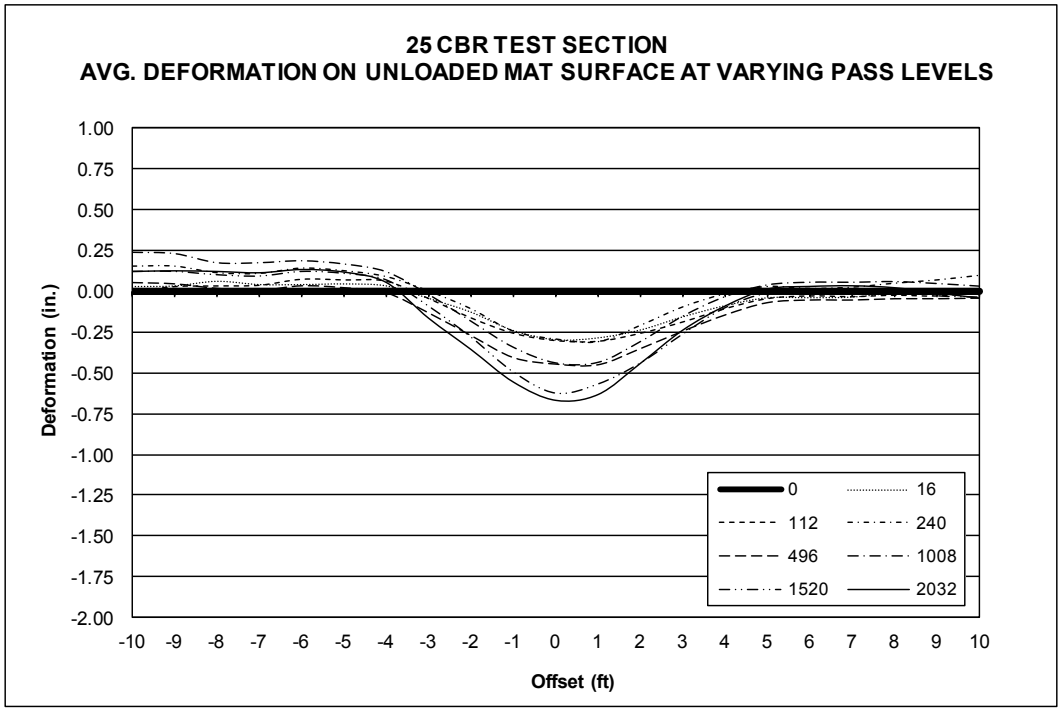

Figure 50. Rut depths measured on mat surface in the 25 CBR section.

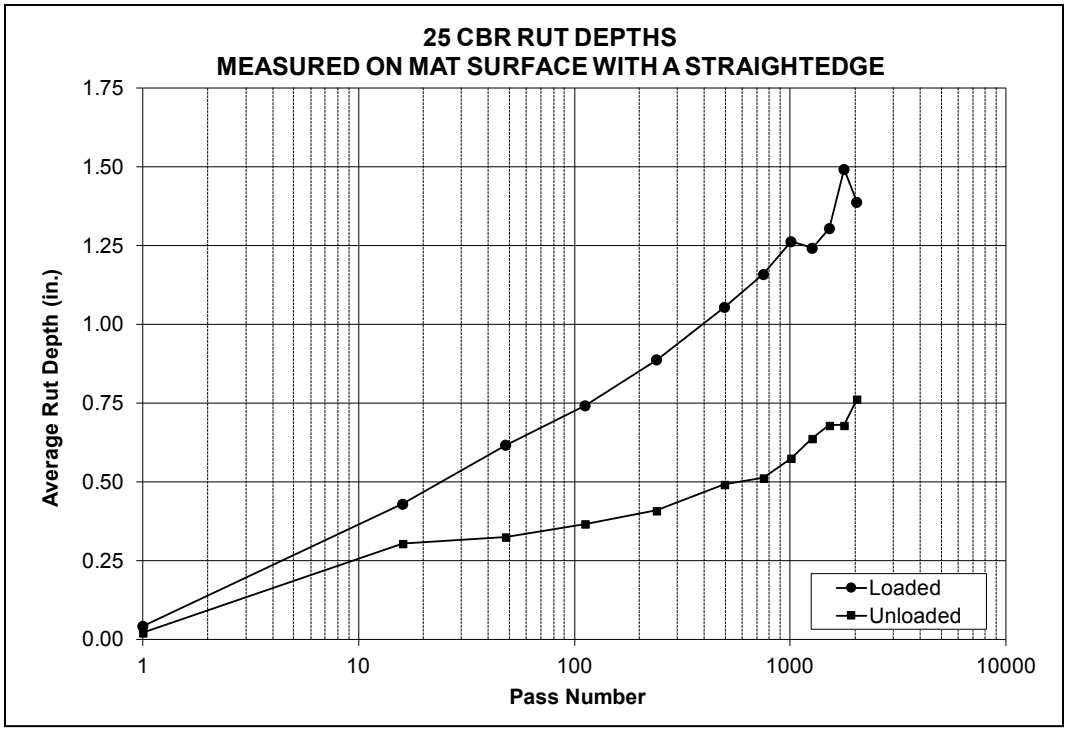

Table 10. 25 CBR permanent deformation maximum values.

Test Item	Pass No.	Subgrade Profile Max Abrupt Change in Elevation (in.)	Mat Surface Profile Max Abrupt Change in Elevation (in.)	Subgrade Permanent Deformation (in.)	Loaded Deformation on Mat Surface (in.)	Unloaded Deformation on Mat Surface (in.)	Loaded Rut Depth with Straightedge (in.)	Unloaded Rut Depth with Straightedge (in.)
25 CBR	2,032	0.56	0.38	1.95	1.69	0.73	1.49	0.76

Elastic deflection was determined by mounting a survey prism on the F-15E load cart just above the center of the load wheel. A continuous survey mode was used with the robotic total station so that elevations were recorded each time the load cart moved 6 in. from the previous measurement point. These data were collected dynamically at scheduled pass intervals throughout trafficking. The data were reduced, and measurements within a half-tire width (4.5 in.) from the centerline were averaged at each 1-ft station along the centerline of traffic. The average elevation at each station was then subtracted from measurements taken on the unloaded mat surface at the same location. For example, the average of dynamic deflections at each station for passes 17 to 32 was subtracted from the unloaded centerline profile recordings at each station collected at pass 16. The difference in the

loaded and unloaded measurements is the elastic deflection, or rebound, of the mat and subgrade as the test wheel moved over the surface. The average elastic deflection at each station for each data collection interval is shown in Figure 51.

Figure 51. Elastic deflection on the mat surface in the 25 CBR section.

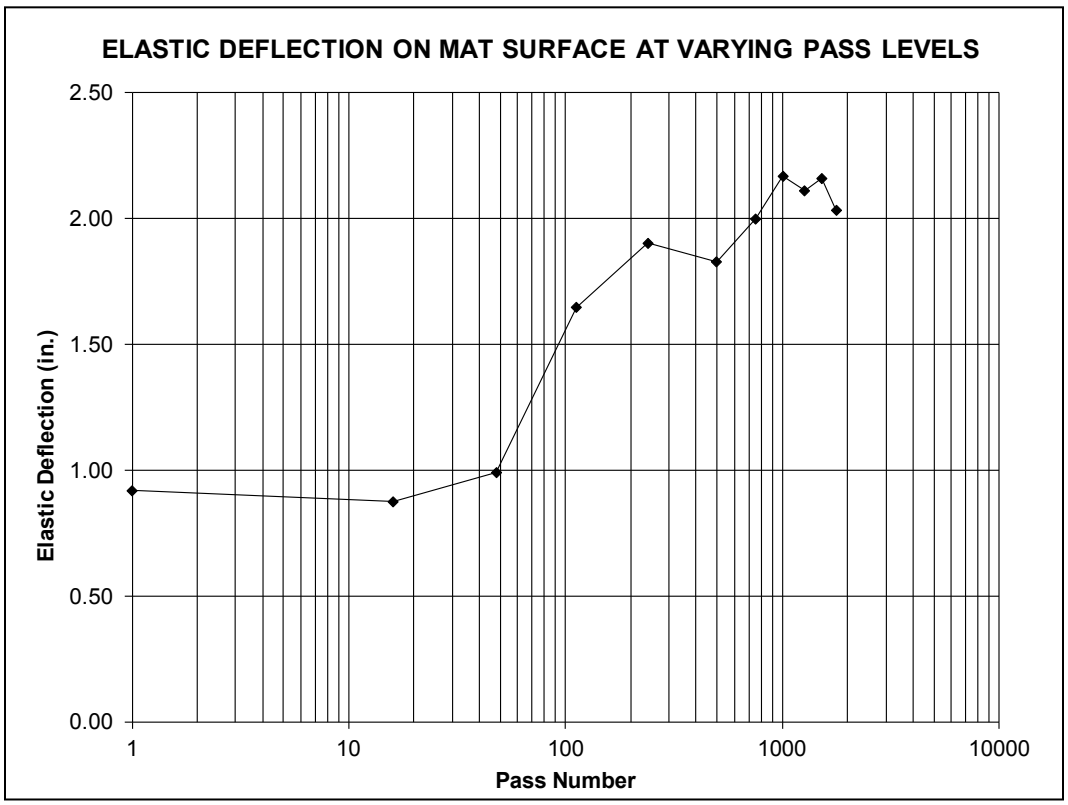

4.2 25 CBR analysis of results

4.2.1 Mat breakage

Visual inspection of the MLC-70 panels at the conclusion of the 25 CBR F-15E traffic test revealed no damage other than about 3/4 in. of dishing. Therefore, the system was able to sustain 2,032 simulated F-15E passes without breaking or becoming a tire hazard, even though the panels were deformed. The MLC-70 mat system was not stiff enough to prevent subgrade deformation from occurring. As the subgrade deformed, an air gap began to form between the bottom surface of the mats and the top of the subgrade. Eventually the size of the air gap increased until the strain in the mat exceeded its elastic limit. Once the elastic limit was exceeded, the mat began to yield and plastically deform. Nearly all of the panels in the wheel path had some degree of dishing; however, the dishing did not cause

tire hazards nor prevent further operations from occurring and was not counted as mat breakage in terms of the failure criteria. Mat panel dishing is accounted for in the subgrade deformation failure criterion.

4.2.2 Permanent deformation

4.2.2.1 Centerline profile

The profile plots in Figures 45 and 46 were analyzed to determine whether the roughness criterion was exceeded. The maximum changes in elevation were 0.56 and 0.38 in. for the final subgrade and mat surface profiles, respectively. Since these values were less than the 1.25-in. failure limit for the F-15E, the MLC-70 Trackway mat system performed adequately to prevent excessive roughness from occurring.

4.2.2.2 Cross sections

Figures 47 through 49 show cross-section values of the subgrade and the mat surface, both loaded and unloaded. From these figures, the maximum deformation values were determined and the numbers were reported in Table 10. As shown, permanent deformations of 1.95, 1.69, and 0.73 were measured on the subgrade, loaded mat surface, and unloaded mat surface, respectively. Based on these values, the failure criterion of 1.25 in. was exceeded for both the subgrade and the loaded mat surface after 2,032 passes; therefore, the 25 CBR section failed by exceeding the limits for permanent deformation of the subgrade. From Figures 48 and 50, failure had occurred after 1,008 passes, and the deformation continued to increase in severity as the test progressed.

4.2.3 Elastic deflection

The elastic deflection measurements for the 25 CBR test section shown in Figure 51 were the sum of the elastic deflection of the mat and the elastic deflection of the subgrade. The elastic deflection values stayed constant at about 0.9 in. for the first 16 passes and then increased slightly to 1.0 in. after 48 passes. The elastic deflection then began to increase significantly and remained 2.0 to 2.2 in. from about 750 to 2,032 passes. Since the elastic deflection values increased for the majority of the test, the air gap between the bottom of the panels and the top of the subgrade continued to increase. The permanent deformation of the subgrade occurred at a faster rate than the permanent deformation of the matting system, and the elasticity of the aluminum panels allowed them to bridge over the air gap when unloaded.

The elastic deflection exceeded 2 in. from 496 passes through the conclusion of the test at 2,032 passes. This 2-in. value exceeded even the permanent deformation of the final subgrade surface of 1.95 in. It would be difficult for the difference in the loaded and unloaded deflection values to exceed the total deformation of the subgrade unless the soil was highly elastic. The trend of the deformation follows historic testing trends; however, the reported values appear to be somewhat elevated. The error may have been induced in the installation height of the prism over the test wheel, or, more likely, a combination of the tire pressure and sidewall movement in the test wheel. The elastic deflection values in previous reports were used as predictors of landing mat panel fatigue failure and not as limiting criteria, resulting in failure of an entire mat section.

5 100 CBR Results and Analysis

The 100 CBR test section was constructed in September 2012 in the Hangar 4 pavement test facility at the ERDC. The following sections describe the observations during trafficking by simulated F-15E aircraft loads; results of data collection; and analysis of the results.

5.1 100 CBR trafficking results

5.1.1 Behavior of mat under traffic: Visual observations

Trafficking began September 6, 2012, on the 100 CBR test section. As the traffic progressed, no damage was noted to any of the panels, regardless of the assembled configuration. As the load cart moved across the surface, some lateral shifting of the mat was caused by the turning of the drive wheels on the mat surface; however, the change of alignment did not cause any operational concerns. After 3,716 passes, there was still no evidence of mat damage and less than one-half inch of deformation in the subgrade. Some of the smaller aggregates in the limestone base had worked their way through the mat joints and were lying on the surface of the mat. Although the migration of the material did not result in tire hazards or structural problems, it resulted in the presence of particles that could cause foreign object damage to jet engines. The aggregate migration could likely be avoided by the installation of a geotextile over the surface prior to installation of the mat. Since the number of passes to failure of the system was predicted to exceed 10,000 passes, and the concept of using MLC-70 for fighter traffic was for expedient repairs, the traffic was stopped and the test was concluded. A summary of the results from system trafficking is shown in Table 11.

Table 11. 100 CBR mat damage summary.

Item	Number of Passes at Conclusion	Failure Type	Damage Description	Loaded Deformation (in.)
A	3,716	NA	NA	0.39
B	3,716	NA	NA	0.45

5.1.2 Permanent deformation

Permanent deformation was measured on the subgrade before and after the test and on the mat surface before trafficking, during trafficking at intervals

shown in Table 6, and after trafficking was concluded. The pre-traffic data were subtracted from all subsequent data in attempt to normalize the data, or to show only the changes that occurred because of trafficking. The discussions that follow are based on normalized data.

Figures 52 and 53 show plots of the centerline profile data for Items A and B as determined from robotic total-station readings. Maximum abrupt changes in elevation were determined by observing the difference in elevation of data points within two stations of each other and choosing the maximum value for each plot. Each maximum value was then used for comparison to the roughness criterion. Beginning and ending stations for both test configurations were ignored because of changing boundary conditions at the interface of the test items and the AM2 ramps. Since the two mat types were not physically connected, the movement of the AM2 panels under F-15E loads was possibly different than that of the test items. Since the test subgrade was very strong, this effect was limited and was only slightly noticeable for the first 2 ft of the test section as shown in Figure 52.

Plots of the average cross-section data collected along lines shown in Figure 3 for Items A and B are shown in Figures 54 through 59. Maximum deformation values for the subgrade, loaded, and unloaded cross sections were determined as the difference in elevation from the average height of the elevated material on each side of the rut to the deepest point in the bottom of the rut.

Figure 52. Centerline profile on the subgrade for the 100 CBR section.

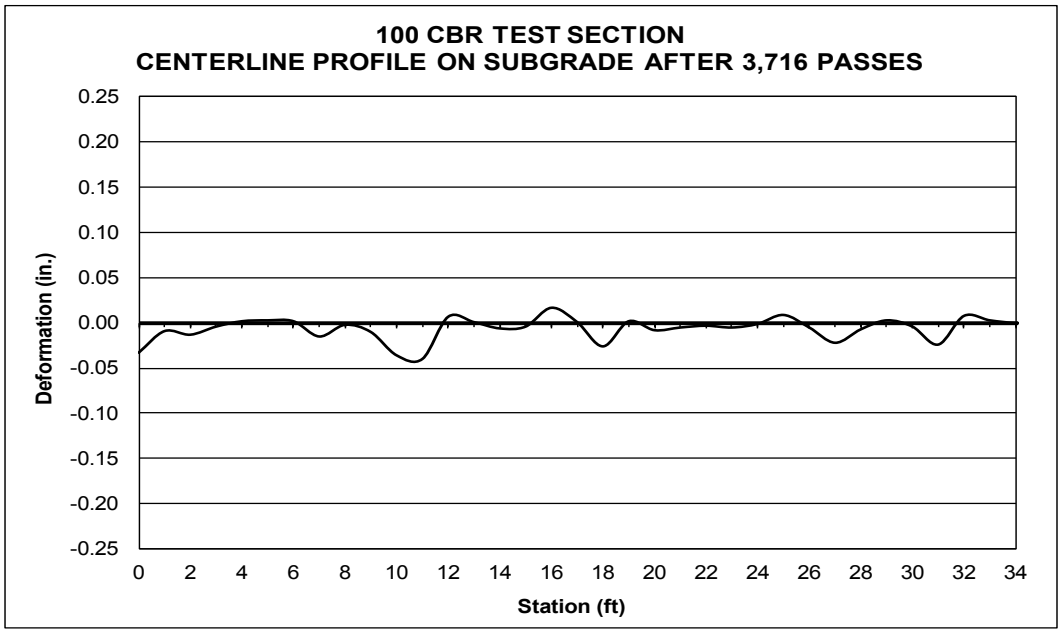

Figure 53. Centerline profile on mat for the 100 CBR section.

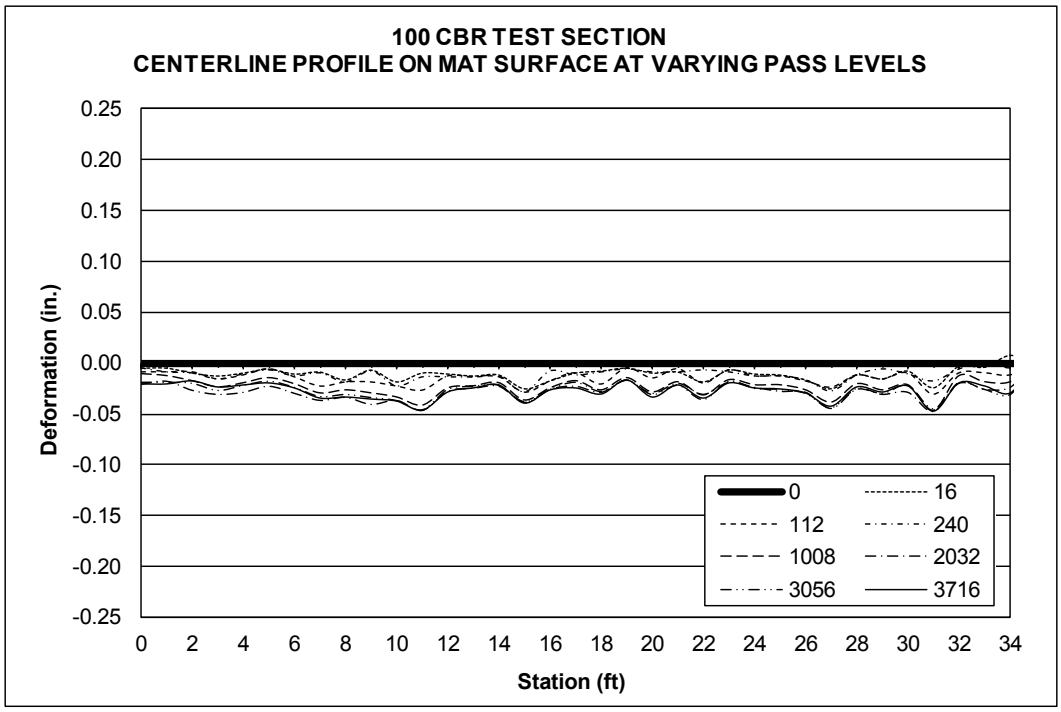

Figure 54. Average subgrade deformation in the 100 CBR section, Item A.

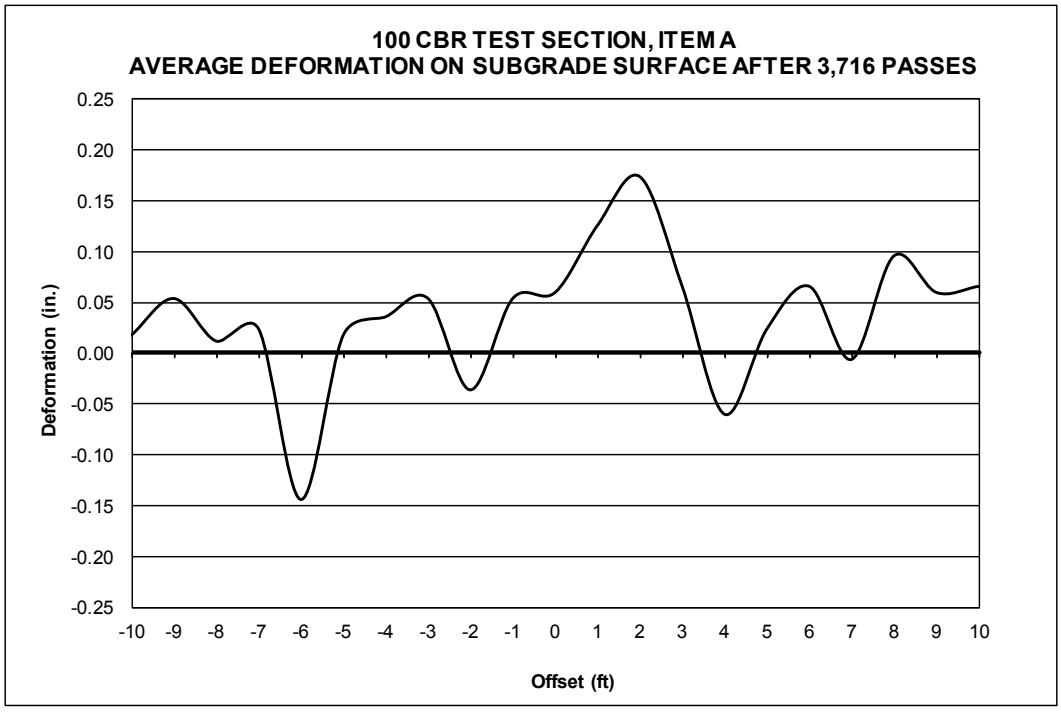

Figure 55. Average subgrade deformation in the 100 CBR section, Item B.

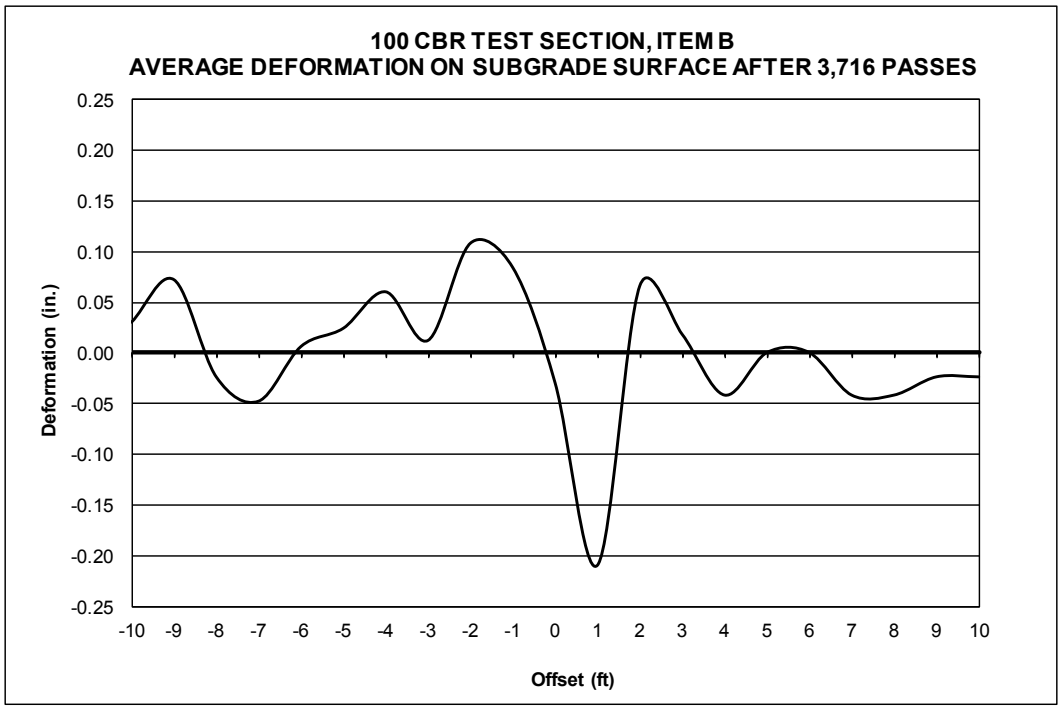

Figure 56. Average deformation on loaded mat in 100 CBR, Item A.

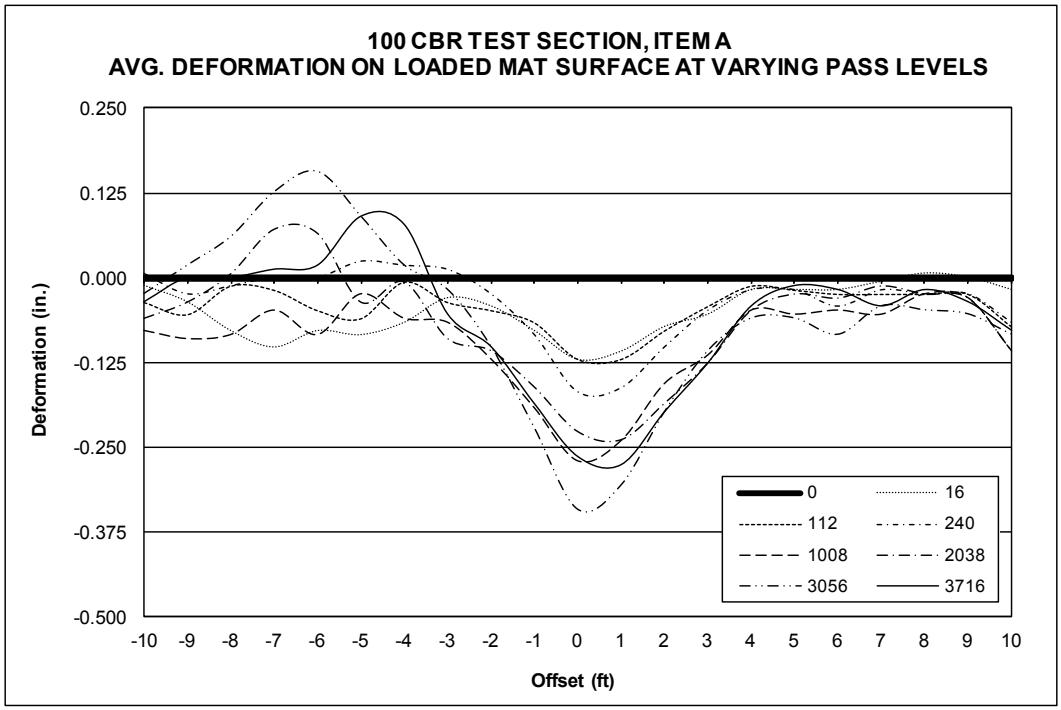

Figure 57. Average deformation on loaded mat in 100 CBR section, Item B.

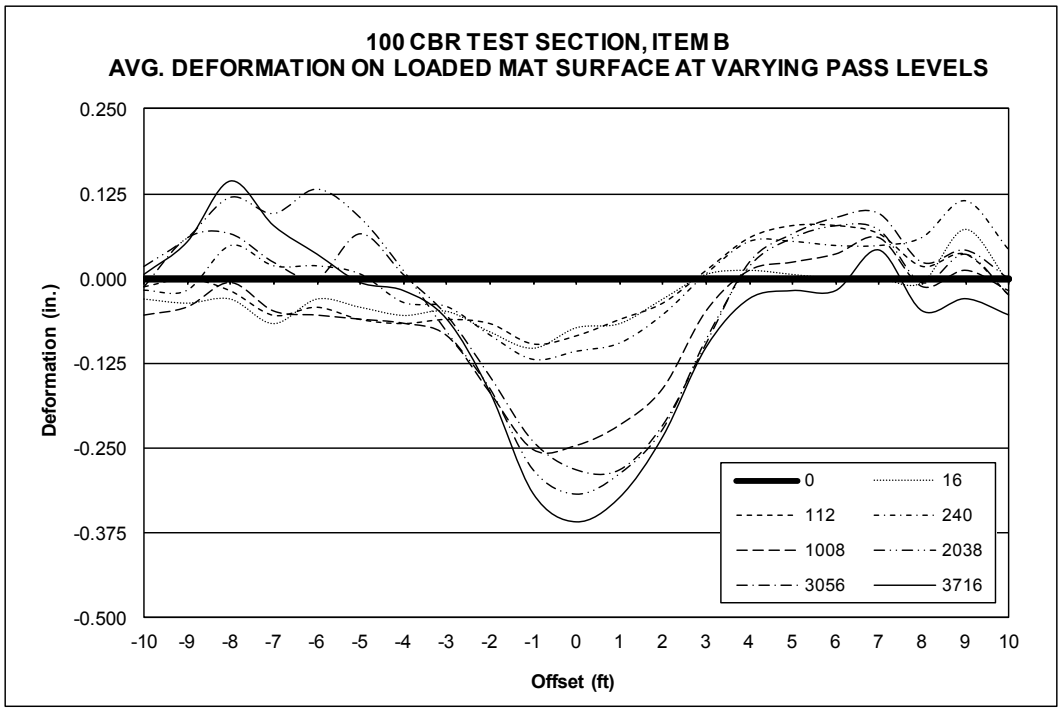

Figure 58. Average deformation on unloaded mat in 100 CBR section, Item A.

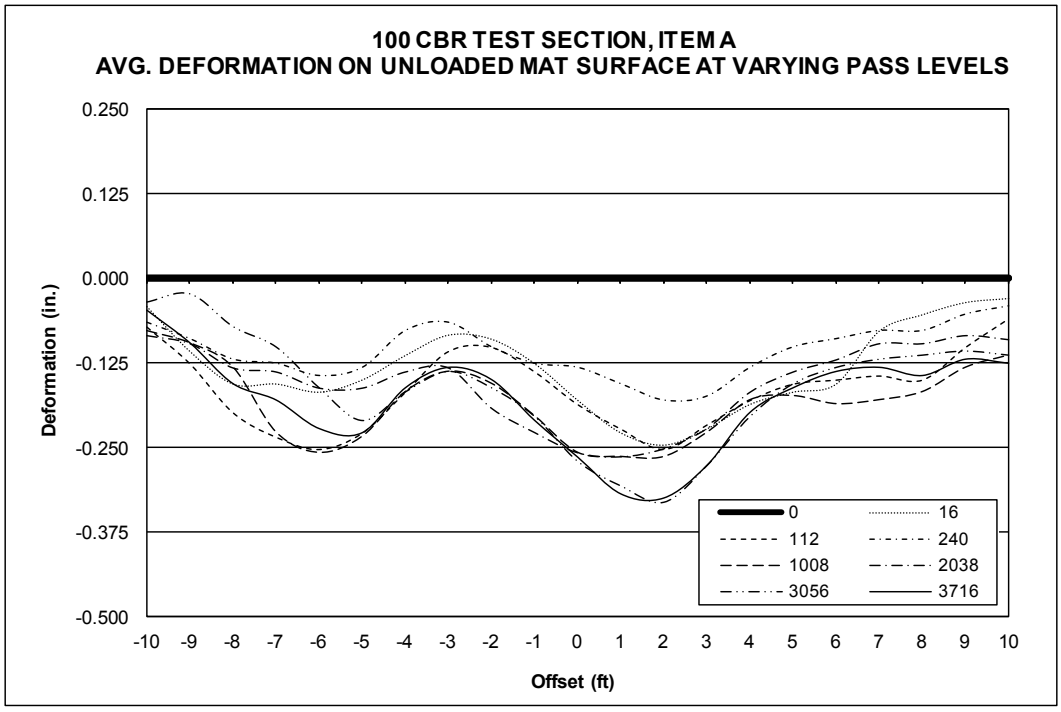

Figure 59. Average deformation on unloaded mat in 100 CBR section, Item B.

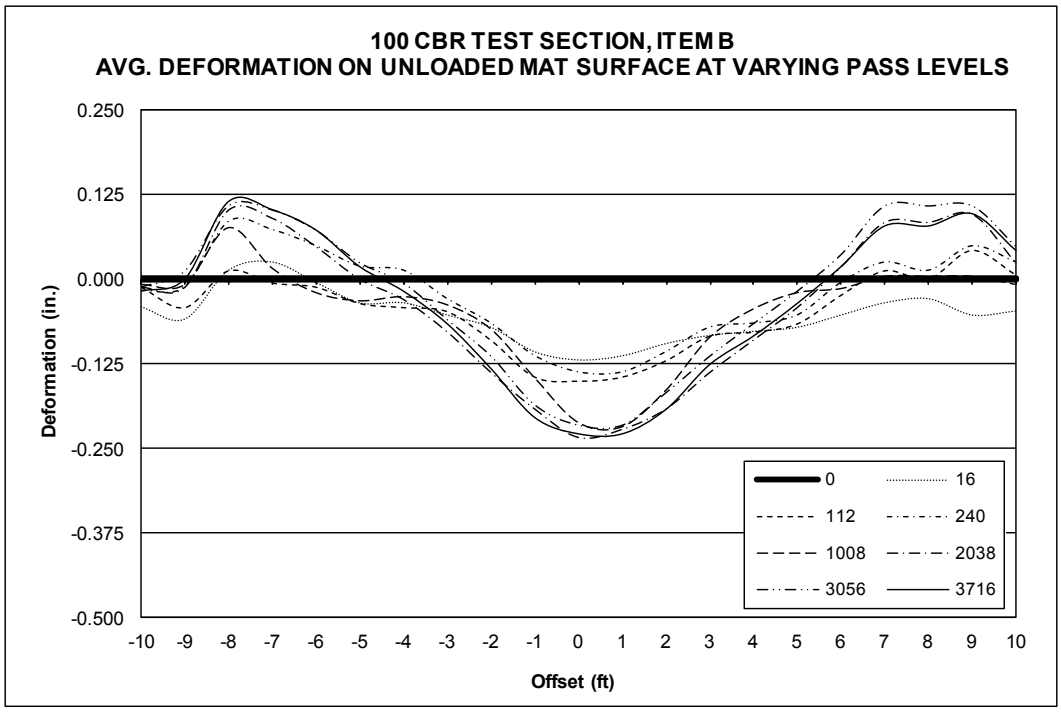

The maximum rut depths measured on the mat surfaces, both loaded and unloaded, were determined with a straightedge and a ruler. Rut depth measurements are presented in Figures 60 and 61 with a logarithmic scale along the x-axis for clarity. Pass 0 was changed to Pass 1 in these figures so the initial point could be displayed on the logarithmic scale. The rut depth measurements were used to validate values determined from the cross sections.

Table 12 summarizes maximum deformation values measured for Items A and B for profiles, cross sections, and measured rut depths.

5.1.3 Elastic deflection

Elastic deflection was measured on the 100 CBR section at scheduled pass intervals shown in Table 6. A plot of these data is shown in Figure 62. This plot indicates the elastic deflection, or rebound, of the mat and subgrade as the test wheel moved over the surface.

Elastic deflection was determined by mounting a survey prism on the F-15E load cart just above the center of the load wheel. A continuous survey mode was used with the robotic total station so that elevations were recorded each time the load cart moved 6 in. from the previous measurement. These data

Figure 60. Item A rut depths measured on mat surface in the 100 CBR section.

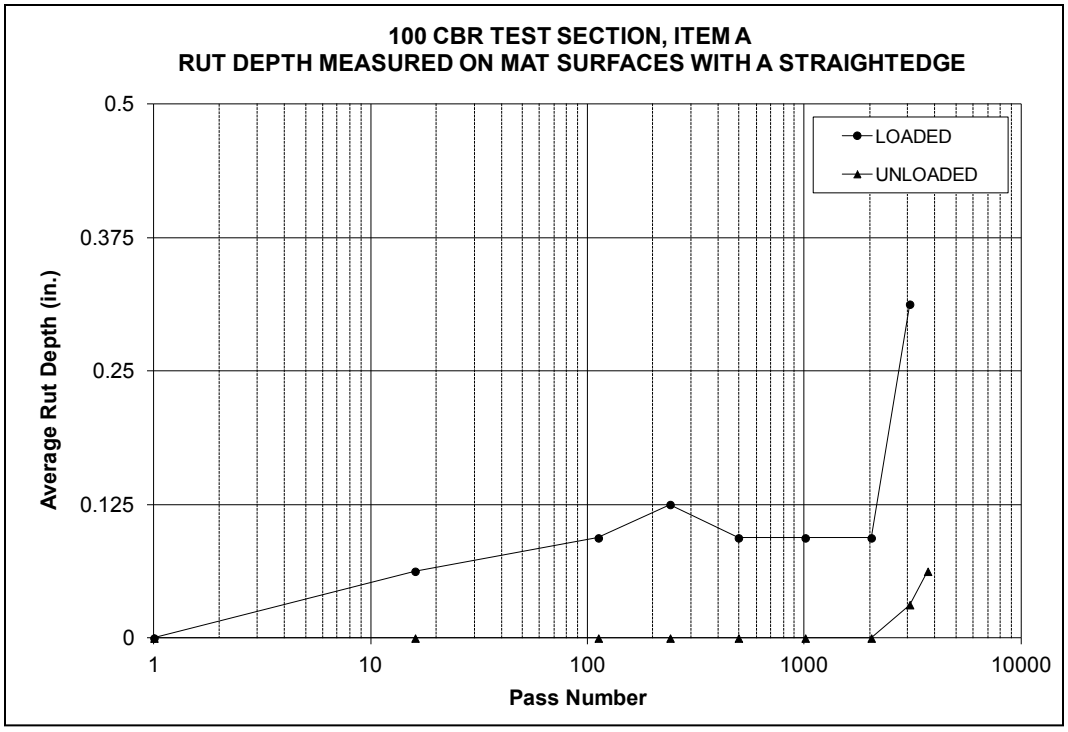

Figure 61. Item B rut depths measured on mat surface in the 100 CBR section.

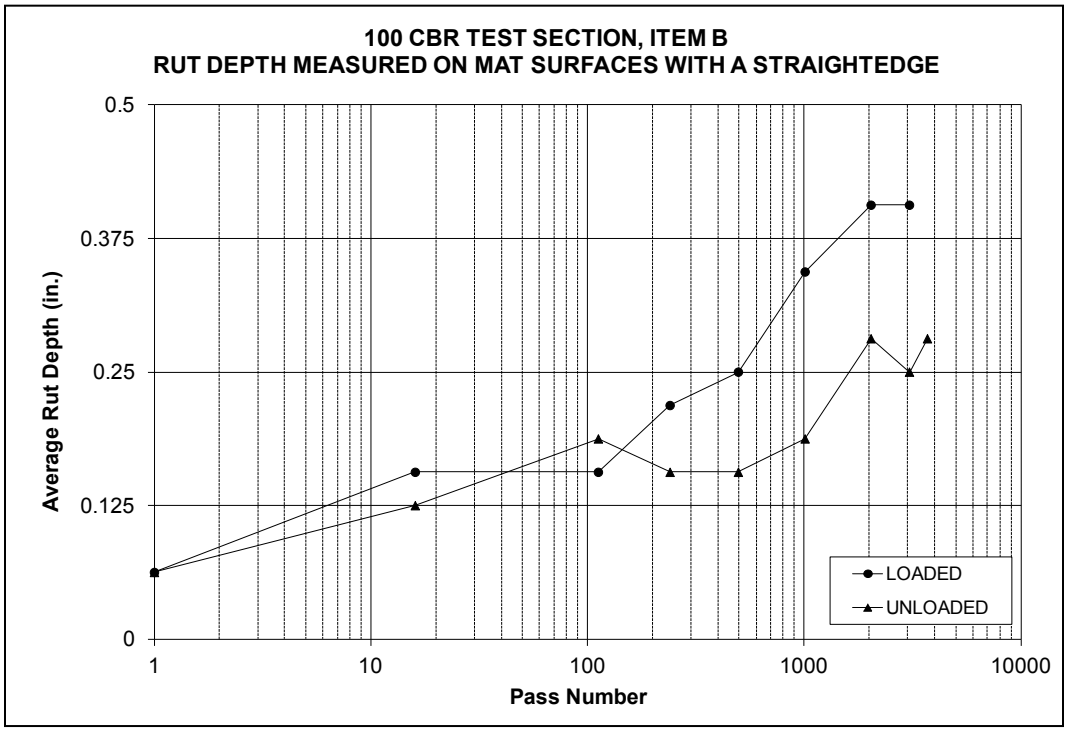

Table 12. 100 CBR section permanent deformation maximum values.

Test Item	Pass No.	Subgrade Profile Max Abrupt Change in Elevation (in.)	Mat Surface Profile Max Abrupt Change in Elevation (in.)	Subgrade Permanent Deformation (in.)	Loaded Permanent Deformation on Mat Surface (in.)	Unloaded Permanent Deformation on Mat Surface (in.)	Loaded Rut Depth with Straightedge (in.)	Unloaded Rut Depth with Straightedge (in.)
A (center)	3,716	0.05	0.02	0.00	0.39	0.33	0.31	0.06
B (joint)	3,716	0.03	0.02	0.28	0.45	0.32	0.44	0.31

Figure 62. Elastic deflection on the mat surface in the 100 CBR test section.

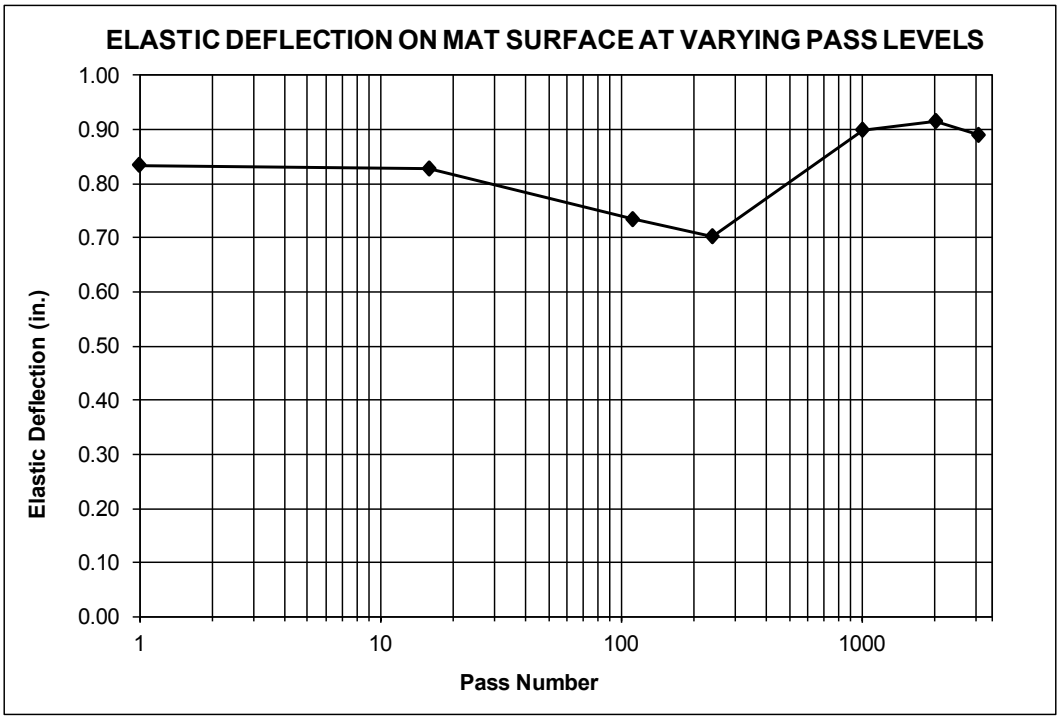

were collected dynamically at scheduled pass intervals throughout trafficking. The data were reduced, and measurements within half a tire width (4.5 in.) from the centerline were averaged at each 1-ft station along the centerline of traffic. The average elevation at each station was then subtracted from measurements taken on the unloaded mat surface at the same location. For example, the average of dynamic deflections at each station for passes 17 to 32 was subtracted from the unloaded centerline profile recordings at each station collected at pass 16. The difference in the loaded and unloaded measurements is the elastic deflection, or rebound, of the mat and subgrade as the test wheel moved over the surface. The average elastic deflection at each station for each data collection interval is shown in Figure 62.

5.1.4 Earth pressure cell data

EPCs were installed in the subgrade in the locations shown in Figure 23. The gauges labeled S1, S2, and S3 were located underneath Item A and gauges N1, N2, and N3 were located underneath Item B. Data points were collected at a rate of 250 Hz by a Campbell Scientific CR5000 measurement and data logger system operated by an experienced instrumentation technician. Examples of the data collected for each instrument are shown in Figures 63 through 70. Each of the examples represents approximately 58,000 data points collected by the EPCs during passes 1 through 16. For the examples shown, each of the large peaks represents one pass by the F-15E load cart. The wander pattern used during trafficking is evident from the peaks' increase as the load cart moved toward the gauge location and their decrease as the load cart moved away from the gauge. Because of the enormous content of the data captured during the trafficking, the data were reduced and summarized in the Appendix.

Figure 63. EPC N1 data for passes 1-16 on the 100 CBR section.

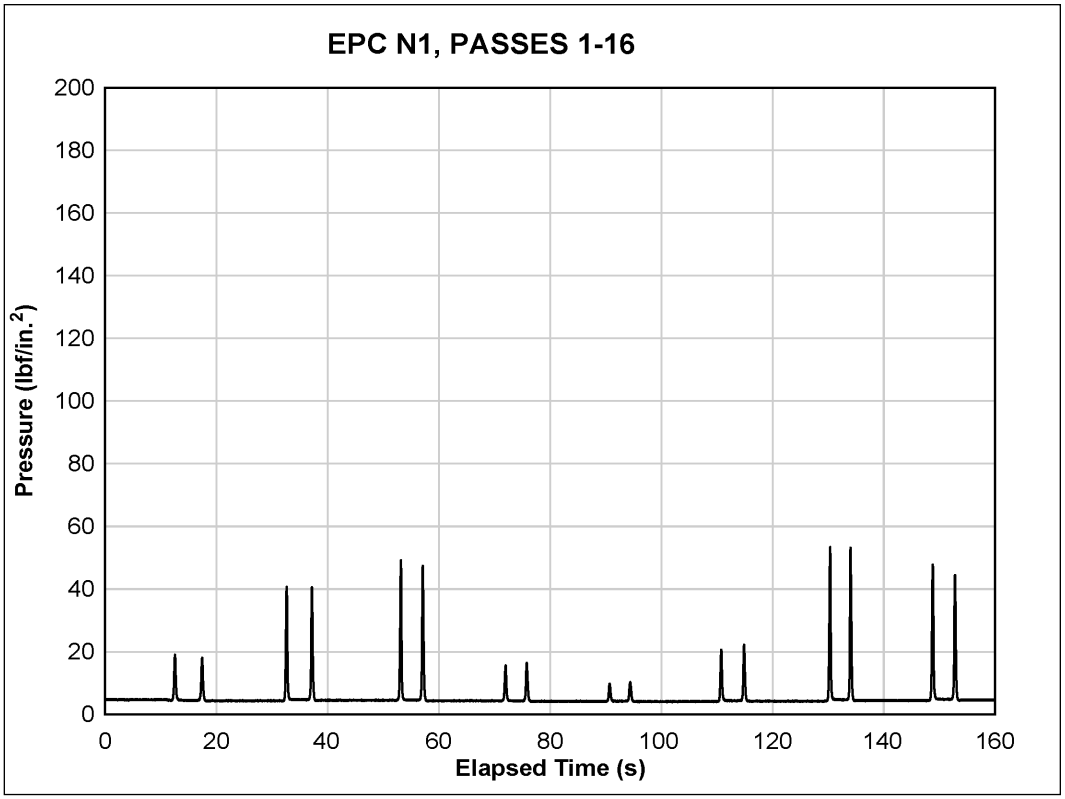

Figure 64. EPC N2 data for passes 1-16 on the 100 CBR section.

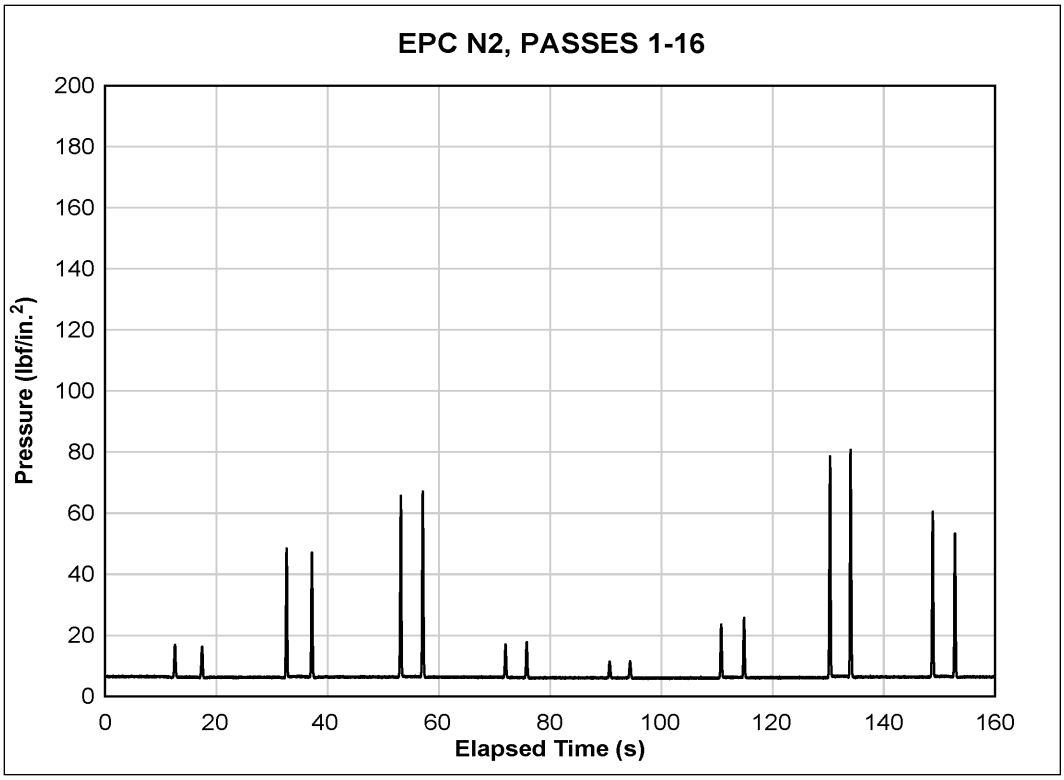

Figure 65. EPC N3 data for passes 1-16 on the 100 CBR section.

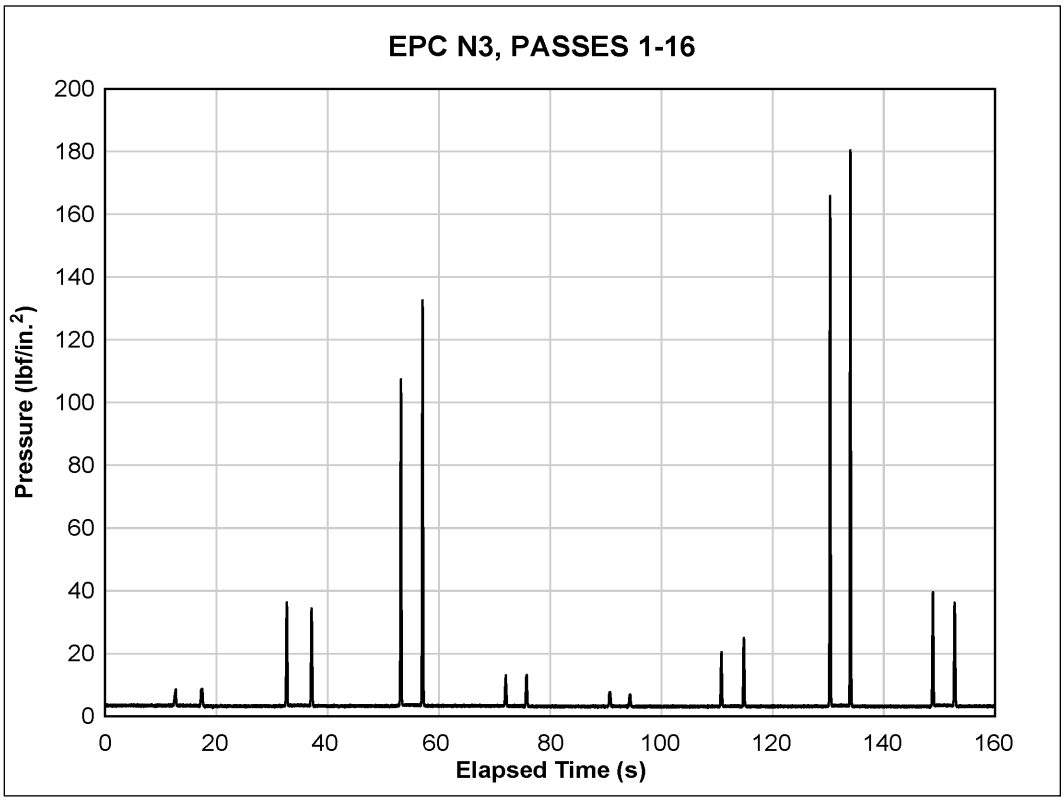

Figure 66. EPC S1 data for passes 1-16 on the 100 CBR section.

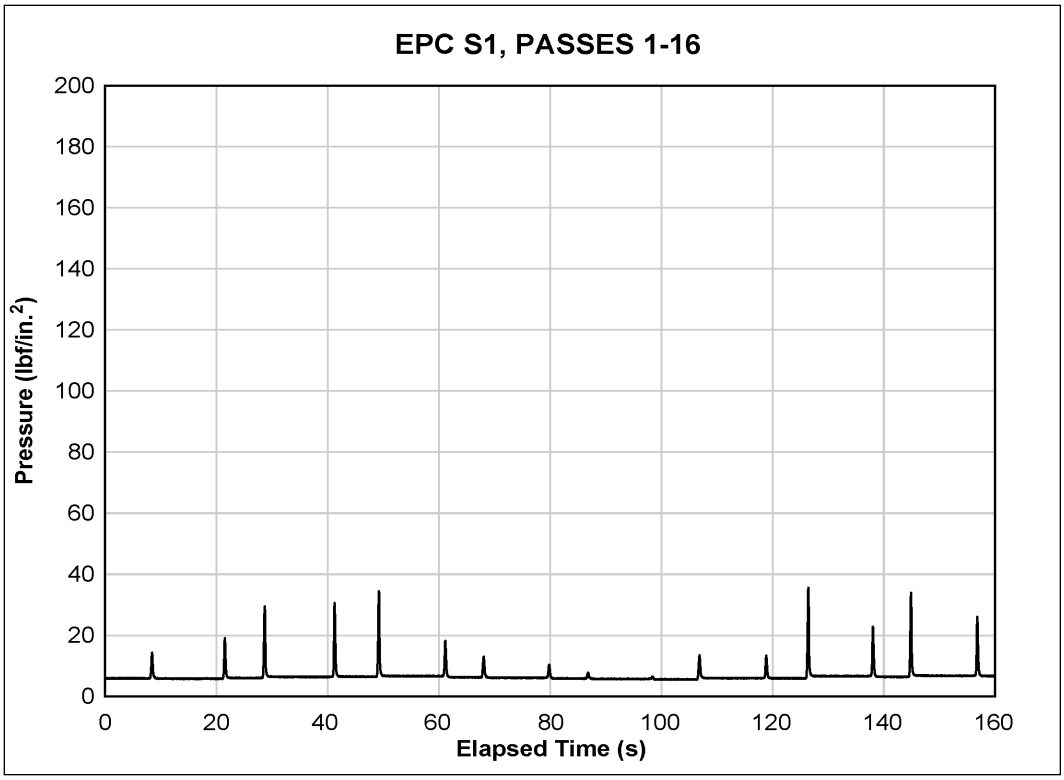

Figure 67. EPC S2 data for passes 1-16 on the 100 CBR section.

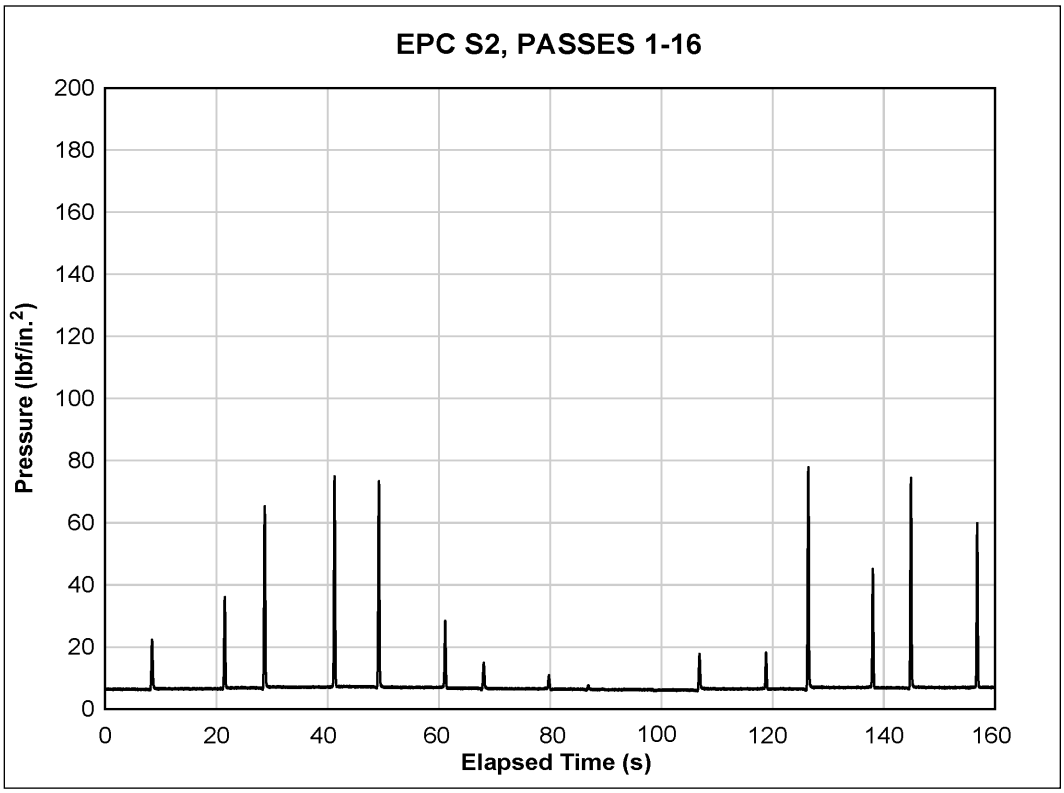

Figure 68. EPC S3 data for passes 1-16 on the 100 CBR section.

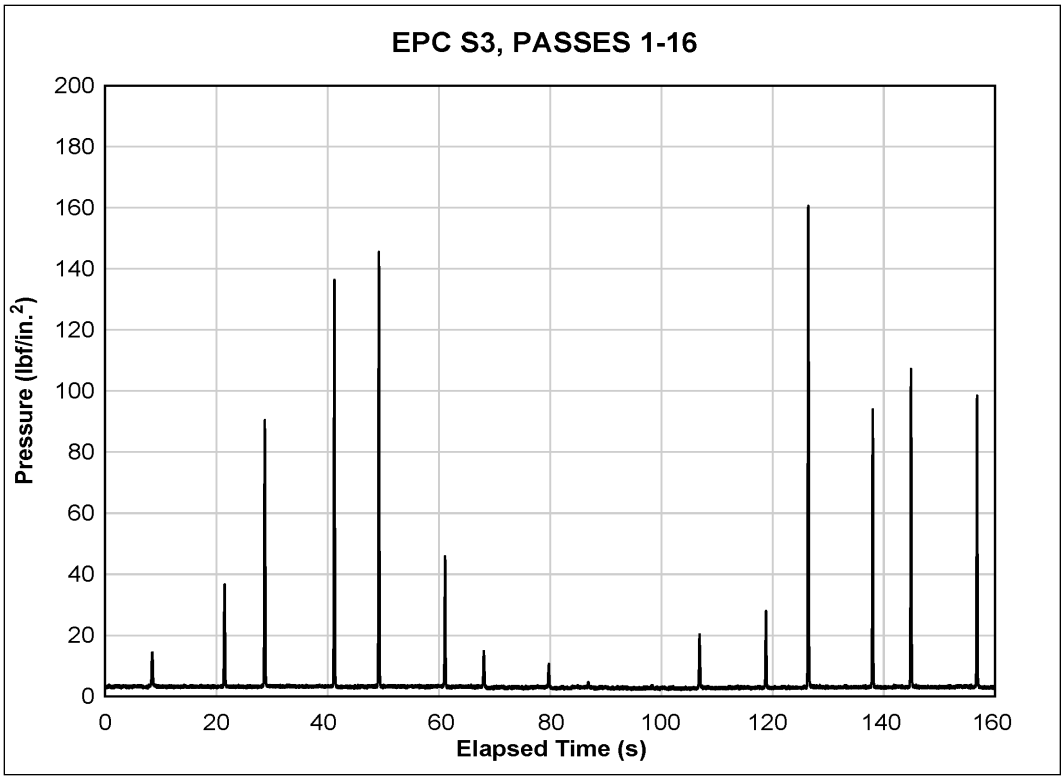

Figure 69. EPC O1 data for passes 1-16 on the 100 CBR section.

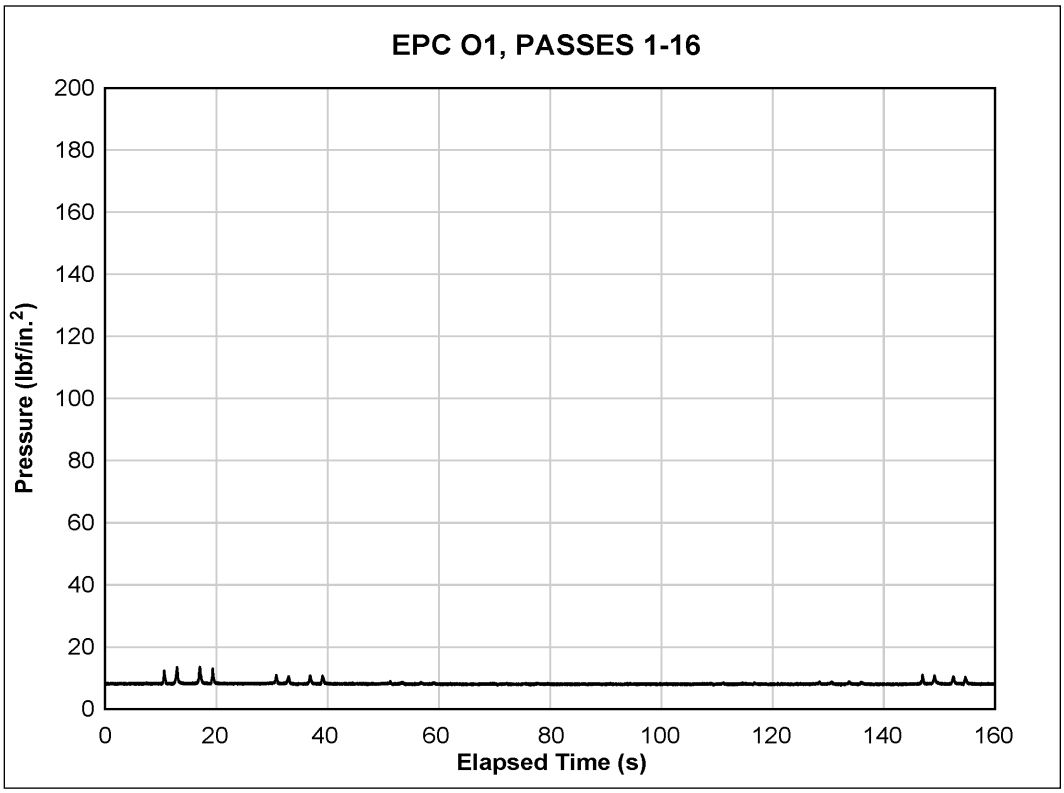

Figure 70. EPC O2 data for passes 1-16 on the 100 CBR section.

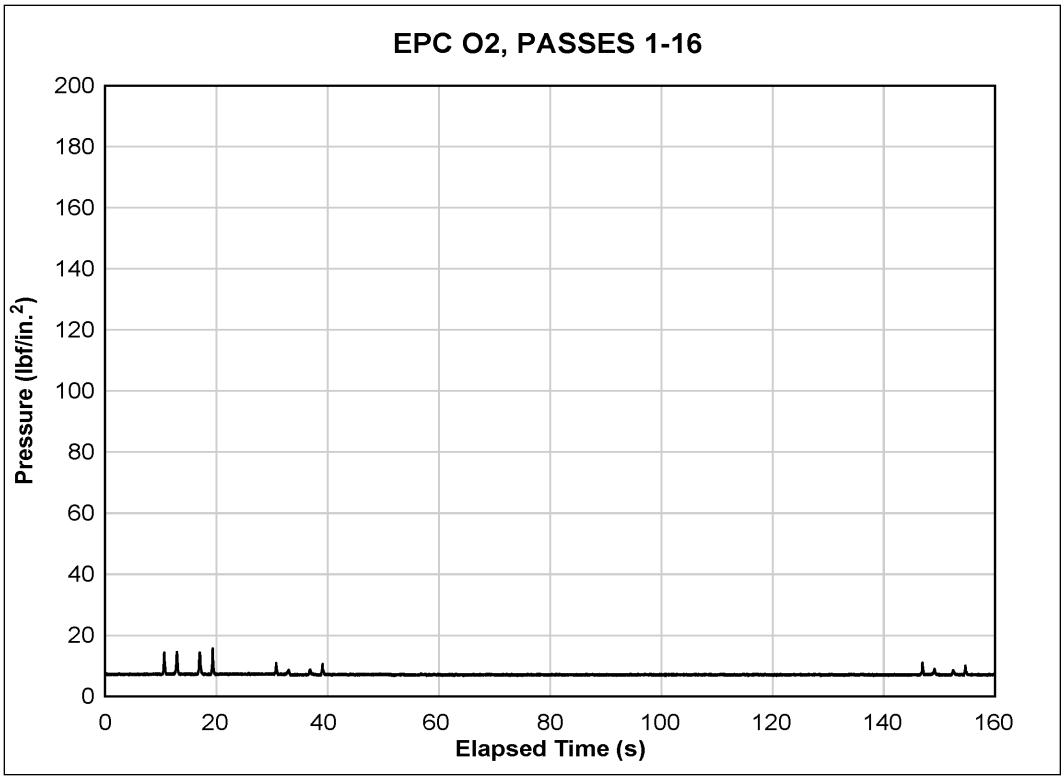

Figure 71 represents a graphical summary of the maximum vertical pressure measured for each data collection interval. The pressures measured under Item A were noticeably smaller than those measured at the same depths under Item B. This was expected since the joints along the centerline of Item B reduce the stiffness of the mat system and therefore its ability to distribute the applied load evenly across the subgrade. Maximum pressure values ranged from 110 to 180 lbf/in.^{2}, 61 to 82 lbf/in.^{2}, and 21 to 32 lbf/in.^{2} for depths of 6, 12, and 24 in., respectively, for gauges underneath Item A. Underneath Item B, centerline pressures ranged from 178 to 238 lbf/in.^{2}, 74 to 115 lbf/in.^{2}, and 49 to 78 lbf/in.^{2} for depths of 6, 12, and 24 in., respectively.

The horizontal distribution of pressures can also be inferred from the examples of the raw data. For example, looking at Figure 63, passes 1 through 16 were recorded, starting from an outside lane, working across the test section, and then traveling back towards the center. The first two peaks show the load cart traveling back and forth in a lane about 18 in. from the centerline with pressure values approximately 20 lbf/in.^{2} recorded, depending on the actual tire location with respect to the EPC gauge. The third and fourth peaks represent the load cart traveling in the

Figure 71. Maximum EPC values for each traffic interval under the 100 CBR test section.

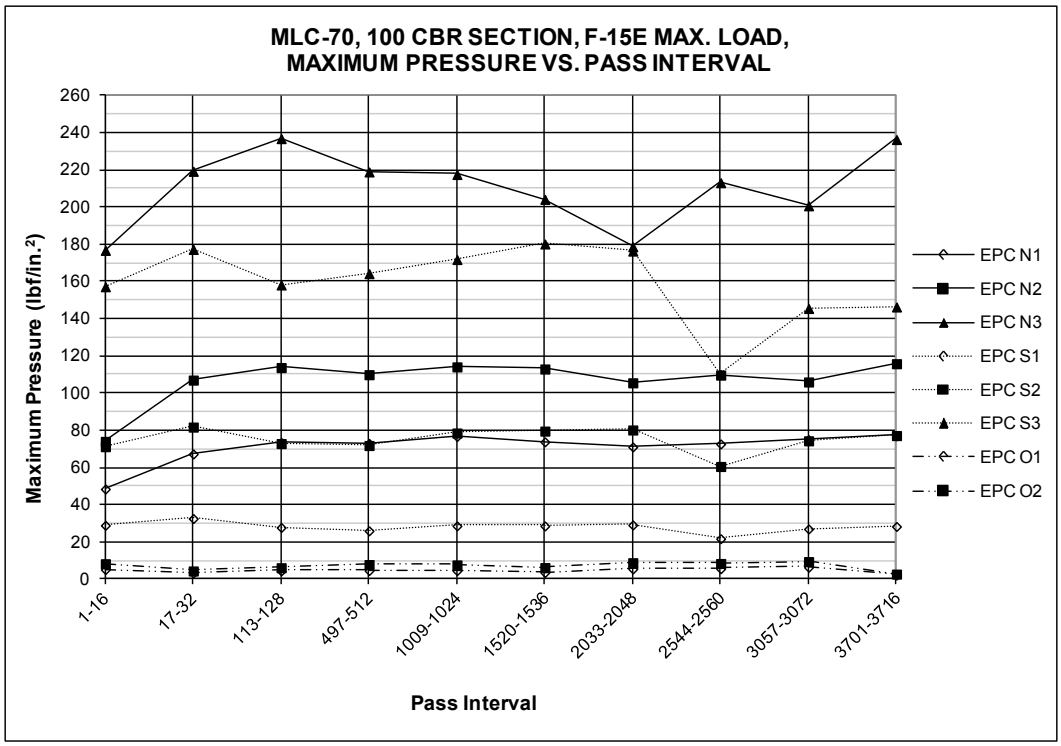

traffic lane adjacent to the center, about 9 in. from the centerline. Pressure values in this location were approximately 40 lbf/in.². The fifth and sixth peaks represent the load moving directly over the gauge location with pressures measuring about 50 lbf/in.². The peak pressures recorded in the entire data set are included in the appendix.

5.2 100 CBR analysis of results

5.2.1 Mat breakage

Visual inspection of the MLC-70 panels at the conclusion of the 100 CBR F-15E traffic test revealed no damage other than about 0.25 in. of dishing. Therefore, the system was able to sustain 3,716 simulated F-15E passes without breaking or becoming a tire hazard. The subgrade was so strong that very little strain or fatigue was induced in the mat panels, therefore, no mat breakage failure resulted.

5.2.2 Permanent deformation

5.2.2.1 Centerline profile

The profile plots in Figures 52 and 53 were analyzed to determine whether the roughness criterion was exceeded. The maximum changes in elevation were 0.05 and 0.02 in. for the final subgrade and mat surface profiles, respectively. Since these values were much less than the 1.25-in. failure limit for the F-15E, the MLC-70 Trackway mat system performed adequately to prevent excessive roughness from occurring.

5.2.2.2 Cross sections

Figures 54 through 59 show cross-section values of the subgrade and the mat surface, both loaded and unloaded for Items A and B. From these figures, the maximum deformation values were determined and the numbers were reported in Table 12. As shown, maximum permanent deformations for the two items of 0.28, 0.45, and 0.33 in. were measured on the subgrade, loaded mat surface, and unloaded mat surface, respectively. Based on these values, the failure criterion of 1.25 in. was not exceeded for either item; therefore, the 100 CBR section was not failed after 3,716 passes.

5.2.3 Elastic deflection

The elastic deflection measurements for the 100 CBR test section shown in Figure 62 were the sum of the elastic deflection of the mat and the elastic deflection of the subgrade. The elastic deflection values remained relatively constant throughout the test and only varied from about 0.7 to 0.9 in. The initial value of about 0.8 in. likely indicated that the mat was positioned slightly above the subgrade at the beginning of the test, since only about 0.25 in. of permanent deformation occurred in the subgrade during trafficking. Based on the data, the 100 CBR subgrade was considered largely inelastic, and the movement was determined to be caused by a pretest air gap between the mat and subgrade surface that only slightly increased during trafficking.

5.2.4 Earth pressure cell Data

For Item A and B in the 100 CBR test section, the EPC data collected during trafficking show the stresses measured in the subgrade 6, 12, and 24 in. under the traffic centerline and 12 and 24 in. under Item A offset 6 ft from the centerline. The maximum EPC values averaged approximately

180 lbf/in.^{2} at 6 in., 90 lbf/in.^{2} at 12 in., and 50 lbf/in.^{2} at 24 in. underneath the traffic centerline. Using measured deflections from a 4-point bending test, the composite modulus of elasticity of the matting system was back-calculated using a two-dimensional finite element implementation of the Mindlin plate theory. The composite modulus of the MLC-70 system was found to be approximately 550,000 lbf/in.^{2}. Using the back-calculated modulus of elasticity, the measured pressure values were compared to predicted values using a layered elastic analysis computer program, WinLEA. Predicted stresses from layered elastic analysis using a 100 CBR simulated subgrade were 202, 88, and 27 lbf/in.^{2} for depths of 6, 12, and 24 in., respectively. The predicted value nearly equaled the measurement at 12 in., but overestimated the average stress at 6 in. by about 20 psi and under predicted by the same amount at 24 in. After examining the values in Figure 71, the 6-in. and 24-in. predictions fell within the range of measured values. Therefore, the layered elastic analysis method may prove useful for predicting approximate subgrade stresses over high strength subgrade materials for mat-surfaced airfields.

6 Summary of MLC-70 Trackway Results

This report describes three unique test sections with subgrade strengths ranging from 25 to 100 CBR for the MLC-70 Trackway mat system. A fourth test section over a 6 CBR subgrade was described by Rushing, T. W. et al., 2012. All four test sections were evaluated under simulated F-15E traffic. The following chapter compiles some of the data collected during these four tests.

6.1 Mat breakage

Based on the results from all four test sections, mat breakage, in terms of tire hazards, sharp edges, and loose pieces, for the MLC-70 Trackway mat system should not be a concern for the user. However, when placed over weak soils, the panels deformed plastically as the subgrade deformation increased. Therefore, the most relevant way to compare the system's performance in terms of passes to failure is to compare the subgrade deformation for the different subgrade strengths.

6.2 Permanent deformation

For a direct comparison, the loaded rut depths for all four test sections were plotted on a log base 10 scale as shown in Figure 72. Values for the 25-50 CBR test section described in this report were adjusted to a 15 CBR based on the posttest condition of the subgrade. Since the initial CBR values ranged from 35 to 50, the rate of deformation for the first 50 passes closely followed the path of the 25 CBR test section. After 50 passes, the stabilized surface began to break up, thus lowering the strength of the soil to an effective 15 CBR. Since the trend falls between the 6 and 25 CBR values, it is considered a reasonable representation of the behavior of a soil having a 15 CBR strength.

If greater than 1,000 passes are required for a given operational scenario under F-15E or similar heavy fighter operations, a minimum of a 25 CBR subgrade should be required. As the strength of the subgrade increases beyond 25, a significant improvement in the number of allowable passes should be expected.

Figure 72. Comparison of the rate of deformation for various CBR values.

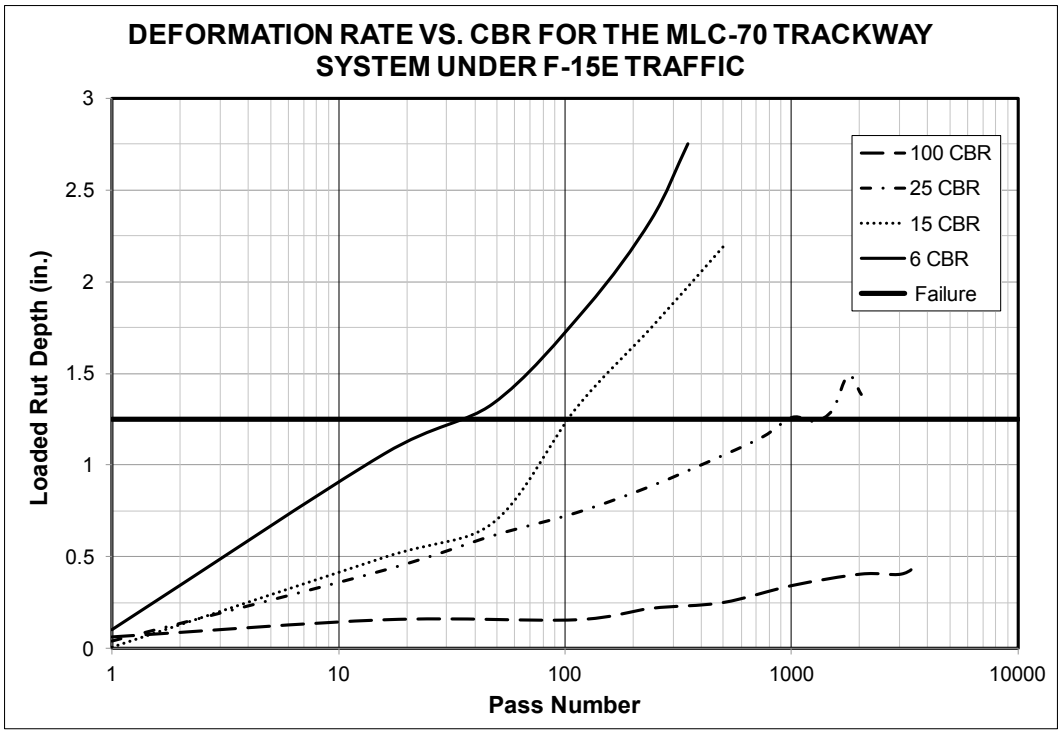

The number of passes to failure for each of the tested subgrade strength conditions is shown in Figure 73. As described for Figure 72, an effective strength of 15 CBR was projected for the 25-50 CBR test section for analysis purposes. Since failure by deformation did not occur for the 100 CBR test section, a projected number of passes to failure of 10,000 passes is shown to indicate a more likely failure trend. The prediction is thought to be conservative in terms of deformation failure; however, there is not enough data to determine if local fatigue in the mat panels may lead to failure by mat breakage before 10,000 passes is reached. Therefore, the prediction shown should be used with caution. As with any airfield mat system, routine inspections are required during use to ensure it is functioning properly and without safety concerns. The data is presented to assist the user in making educated decisions about the number of allowable operations achievable with the MLC-70 Trackway system for soils with strength values outside of those specifically tested.

Figure 73. Prediction of the number of passes to failure for F-15E traffic.

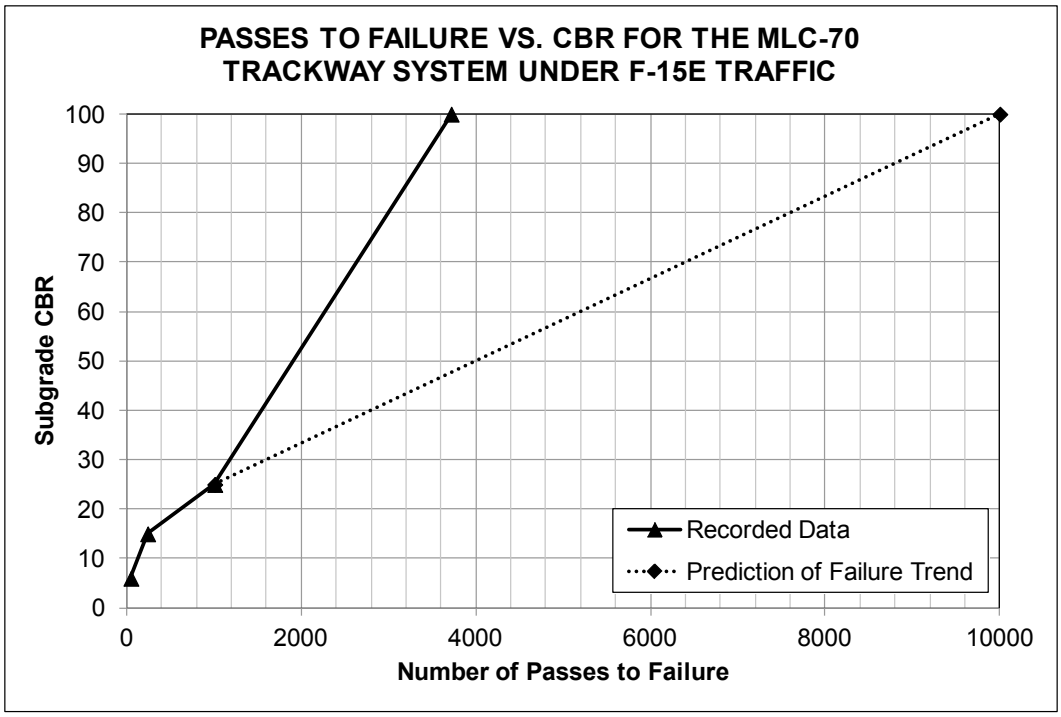

7 Conclusions and Recommendations

7.1 Conclusions

The purpose of the investigations described herein was to determine the ability of Faun Trackway's MLC-70 matting system to carry US military aircraft loads. Simulated F-15E traffic was applied to represent the worst-case loading conditions expected to be applied to a mat-surfaced airfield facility. The following conclusions were derived from accelerated traffic testing of the MLC-70 Trackway airfield matting system:

1. An 8-in.-deep cement-stabilized soil, such as the one described for the 25-50 CBR test section, was only able to support 112 F-15E aircraft passes when surfaced with the MLC-70 system. The profile of the mat likely aided in the breaking of the upper surface of the stabilized soil and accelerated its deterioration. One third of the test section was able to support 240 passes of simulated F-15E traffic before failure by excessive rutting. Additional traffic was applied until 496 passes were completed across two-thirds of the test section. Mat damage was limited to dishing in the wheel path, corner curls along end joints along the traffic lane, and two broken ends near the shoot bolt location. Since the stabilized material was broken up during traffic application, the effective CBR after trafficking was most likely closer to a 15 CBR; therefore, a second 25 CBR test was conducted.
2. A 24-in.-deep 25 CBR CH soil is capable of supporting 1,008 passes of simulated F-15E traffic before failure by permanent deformation. Traffic continued until 2,032 passes were completed and the deformation was well beyond failure. The only mat damage noted was dishing along the traffic wheel path.
3. A 24-in.-deep 100 CBR crushed limestone soil can support greater than 3,716 passes of simulated F-15E traffic without exceeding any failure limits. Time constraints caused trafficking to be concluded prior to failure. Based on the deformation data collected and lack of mat damage, several thousand more passes likely could have been achieved. A prediction of the failure trend indicated that at least 10,000 passes may be reached; however, failure by mat breakage could occur before failure by permanent deformation of the subgrade.
4. The MLC-70 Trackway mat system is capable of carrying heavy fighter aircraft traffic when placed over a soil having greater than or equal to a 25 CBR for a depth of 24 in.

7.2 Recommendations

Based on the airfield mat testing completed by the ERDC, the following recommendations are provided:

1. The MLC-70 Trackway mat system is not recommended for sustained fighter or heavy cargo aircraft operations over soils with less than 25 CBR.
2. The MLC-70 Trackway mat system is recommended only for emergency or expedient use by fighter and heavy cargo aircraft over soils with strengths between 6 CBR and 25 CBR because of the limited number of operations it can support before exceeding rut limits.
3. The installation of a non-woven geotextile fabric underneath the MLC-70 Trackway mat is recommended for fighter operations to prevent migration of soil and fine aggregates onto the mat surface.

References

ASTM International. 2009. *Standard test method for use of the dynamic cone penetrometer in shallow pavement applications*. Designation D6951/6591M -09. West Conshohocken, PA: ASTM.

_____. 2009. *Standard test method for in-place density and water content of soil and soil-aggregate by nuclear methods (shallow depth)*. Designation D6938-10. West Conshohocken, PA: ASTM.

_____. 2009. *Standard test methods for laboratory determination of water (moisture) content of soil and rock by mass*. Designation D2216-10. West Conshohocken, PA: ASTM.

Burgmann, R. A., and C. O. Ingebretson. 1969. *Military potential test of Class 60 assault trackway*. USATECOM Project No. 7-6-0642-01. Fort Knox, KY: US Army Armor & Engineer Board.

Garcia, L., and T. W. Rushing. 2014. *AM2 25 CBR subgrade sensitivity test*. ERDC/GSL TR-14-7. Vicksburg, MS: US Army Engineer Research and Development Center.

Garcia, L., and T. W. Rushing. 2013. *AM2 100 CBR subgrade sensitivity test*. ERDC/GSL TR (in preparation). Vicksburg, MS: US Army Engineer Research and Development Center

Handbook for Concrete and Cement. 1995. *Standard test method for determining the California Bearing Ratio of soils*. CRD-C 654-95. US Army Corps of Engineers.

Rollings, R. S. 1975. *Comparison of the British class 60 trackway and AM-2 mat for bomb damage repair applications*. AFWL-TR-75-149. Kirtland Air Force Base, NM: Air Force Weapons Laboratory.

Rushing, T. W., L. Garcia, and Q. S. Mason. 2012. *Evaluation of Faun Aluminum Mat Systems*. ERDC/GSL TR-12-32. Vicksburg, MS: US Army Engineer Research and Development Center.

Appendix: Earth Pressure Cell Data for the 100 CBR MLC-70 Test Section

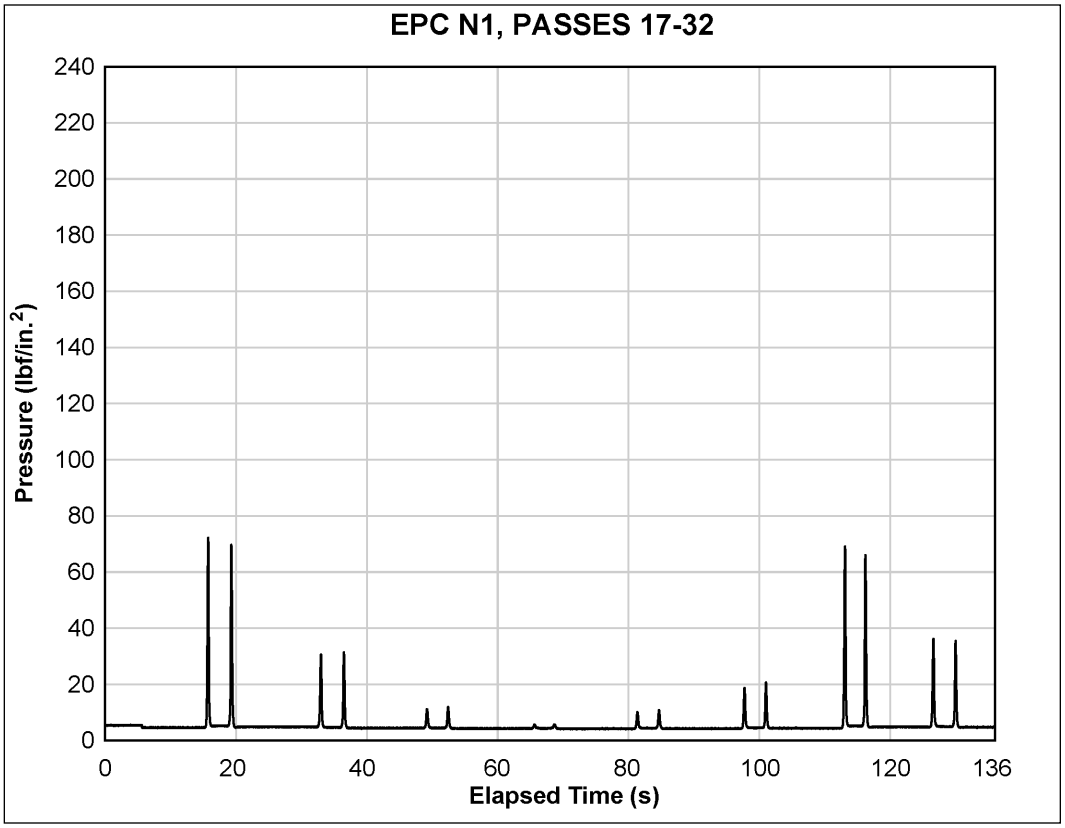

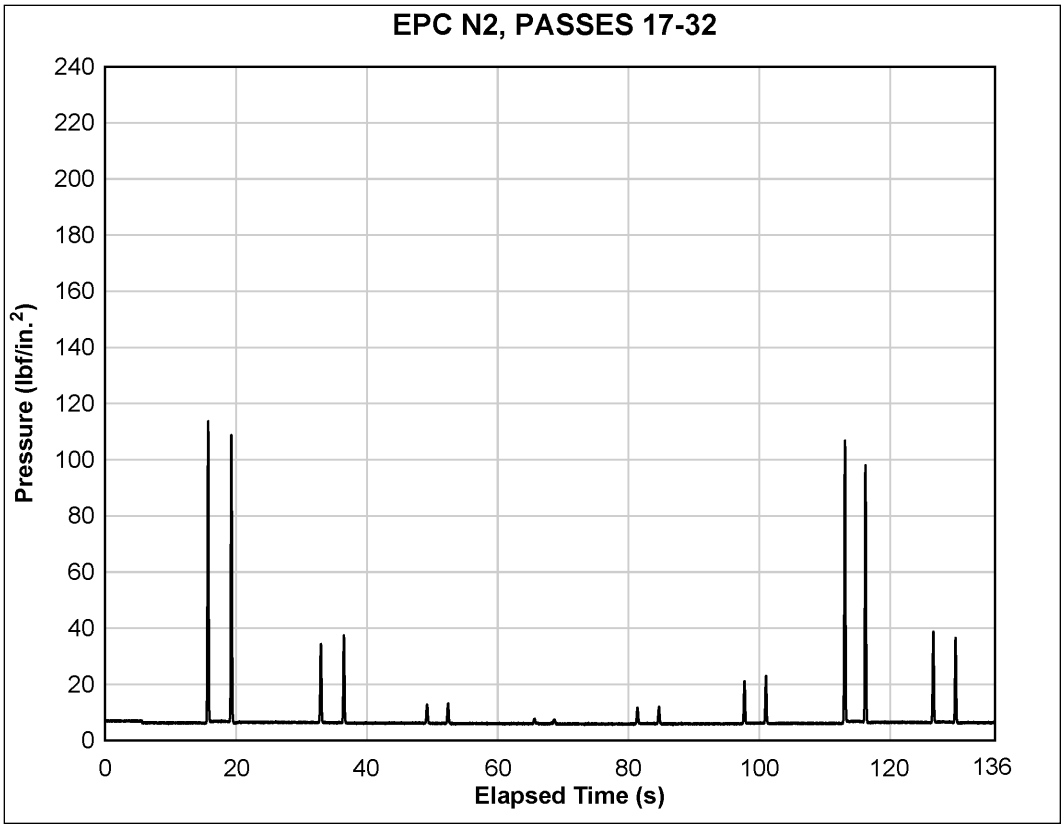
EPC N2, PASSES 17-32
Pressure (lbf/in.2)
240
220
200
180
160
140
120
100
80
60
40
20
0
0
20
40
60
80
100
120
136
Elapsed Time (s)

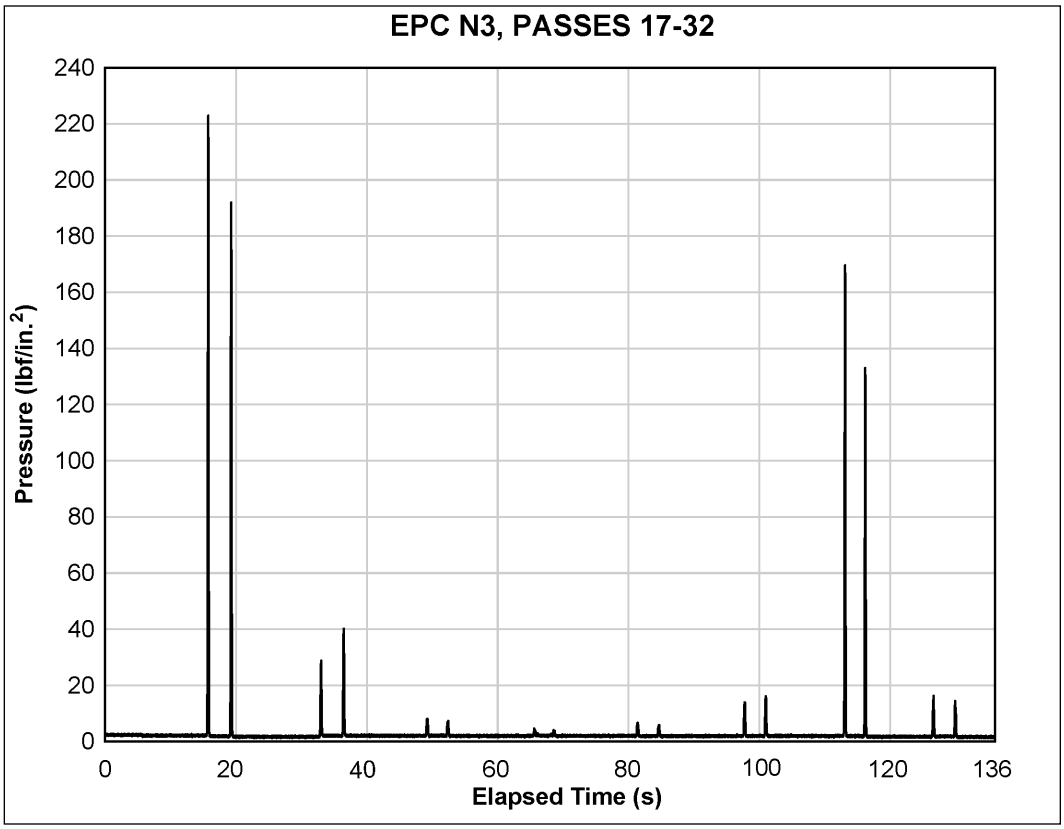
EPC N3, PASSES 17-32
Pressure (lbf/in.2)
240
220
200
180
160
140
120
100
80
60
40
20
0
0
20
40
60
80
100
120
136
Elapsed Time (s)

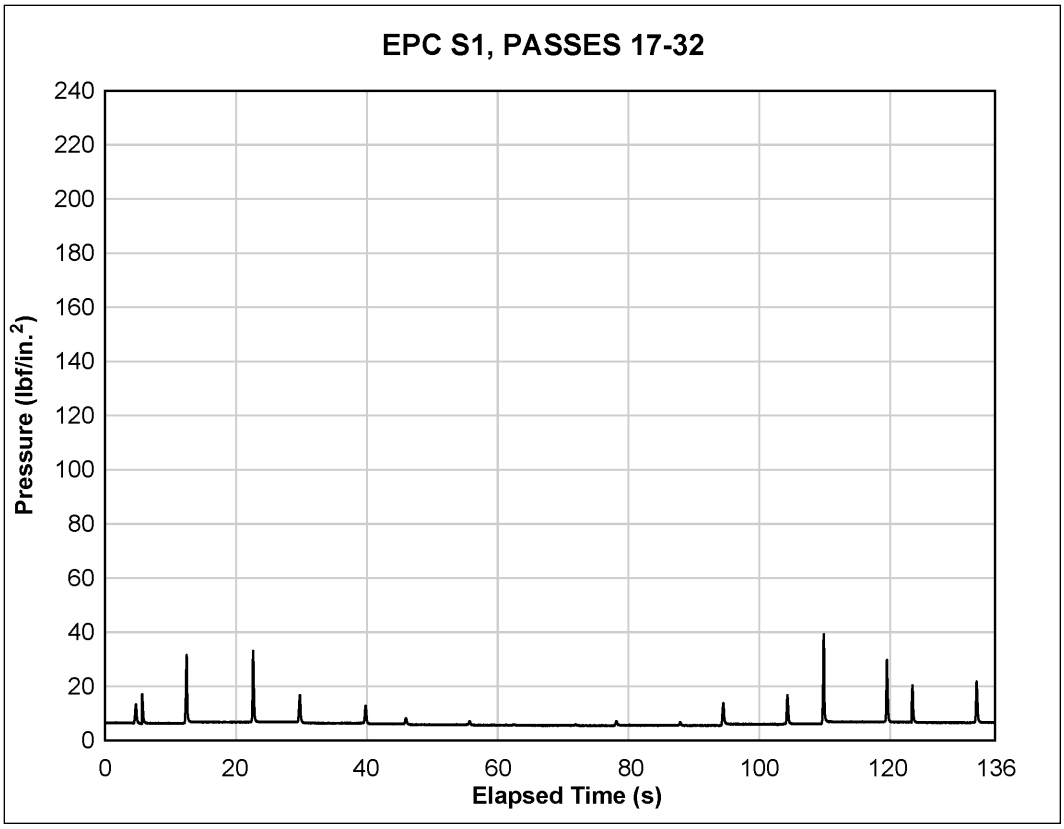
EPC S1, PASSES 17-32
Pressure (lbf/in.2)
240
220
200
180
160
140
120
100
80
60
40
20
0
0
20
40
60
80
100
120
136
Elapsed Time (s)

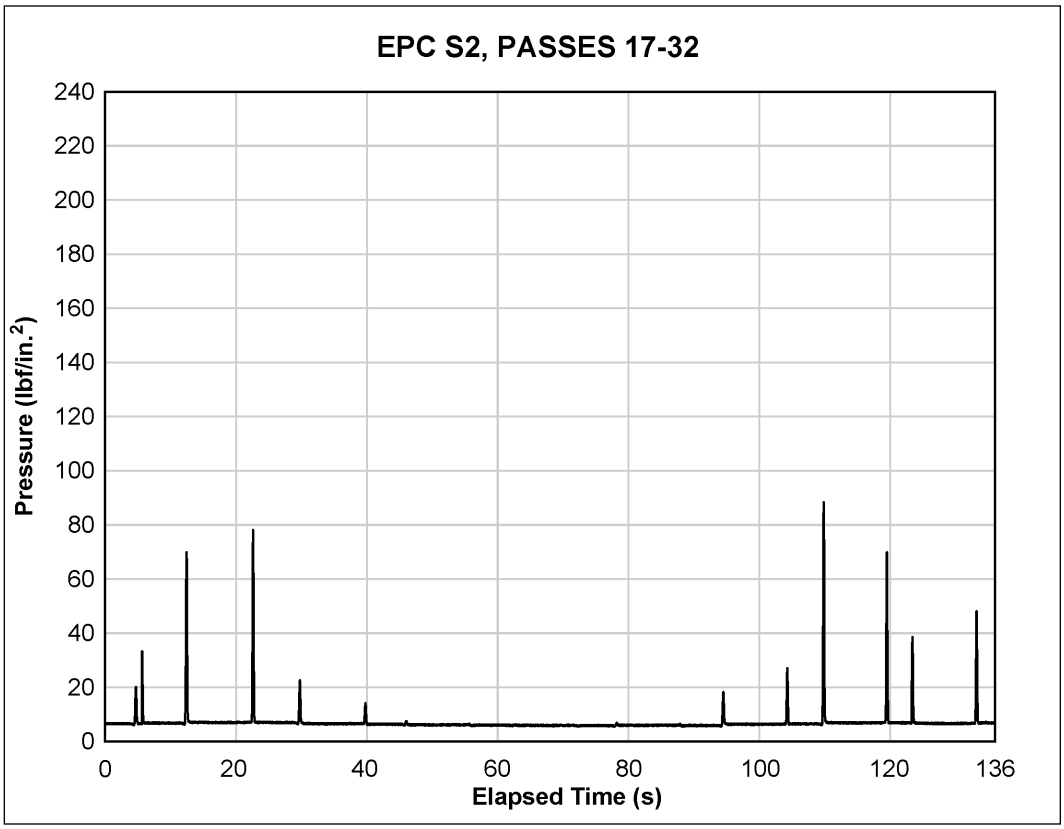
EPC S2, PASSES 17-32
Pressure (lbf/in.2)
240
220
200
180
160
140
120
100
80
60
40
20
0
0
20
40
60
80
100
120
136
Elapsed Time (s)

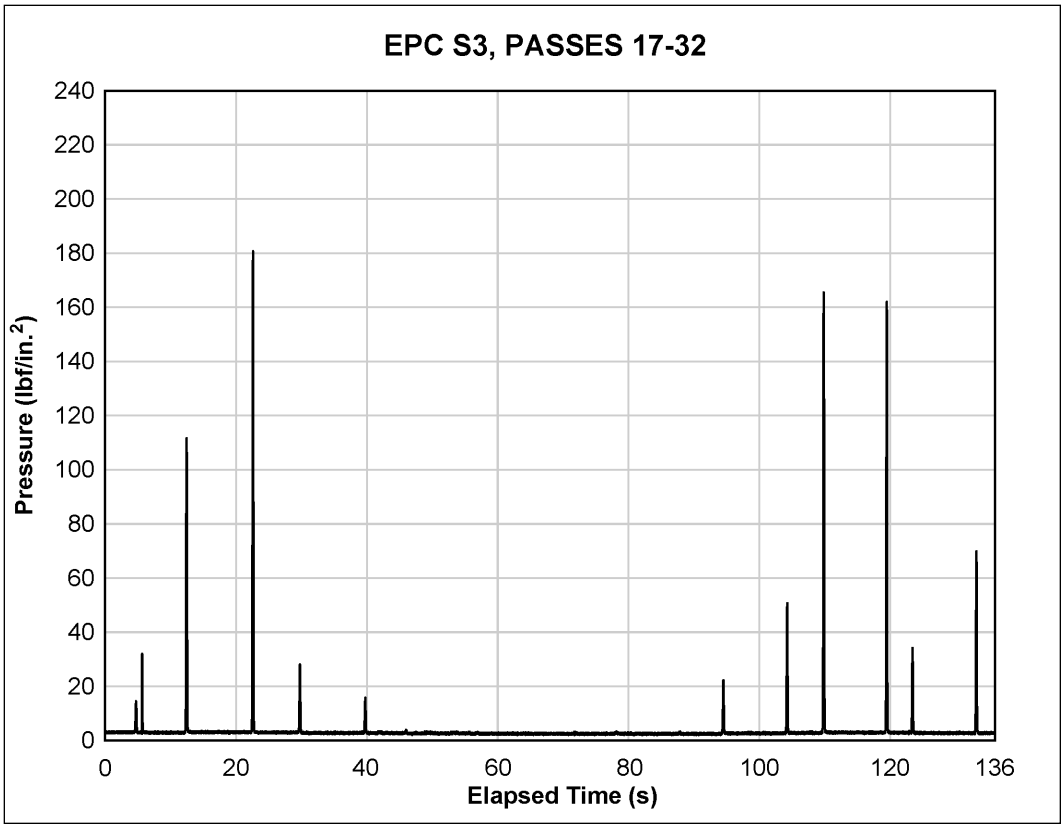
EPC S3, PASSES 17-32
Pressure (lbf/in.2)
240
220
200
180
160
140
120
100
80
60
40
20
0
0
20
40
60
80
100
120
136
Elapsed Time (s)

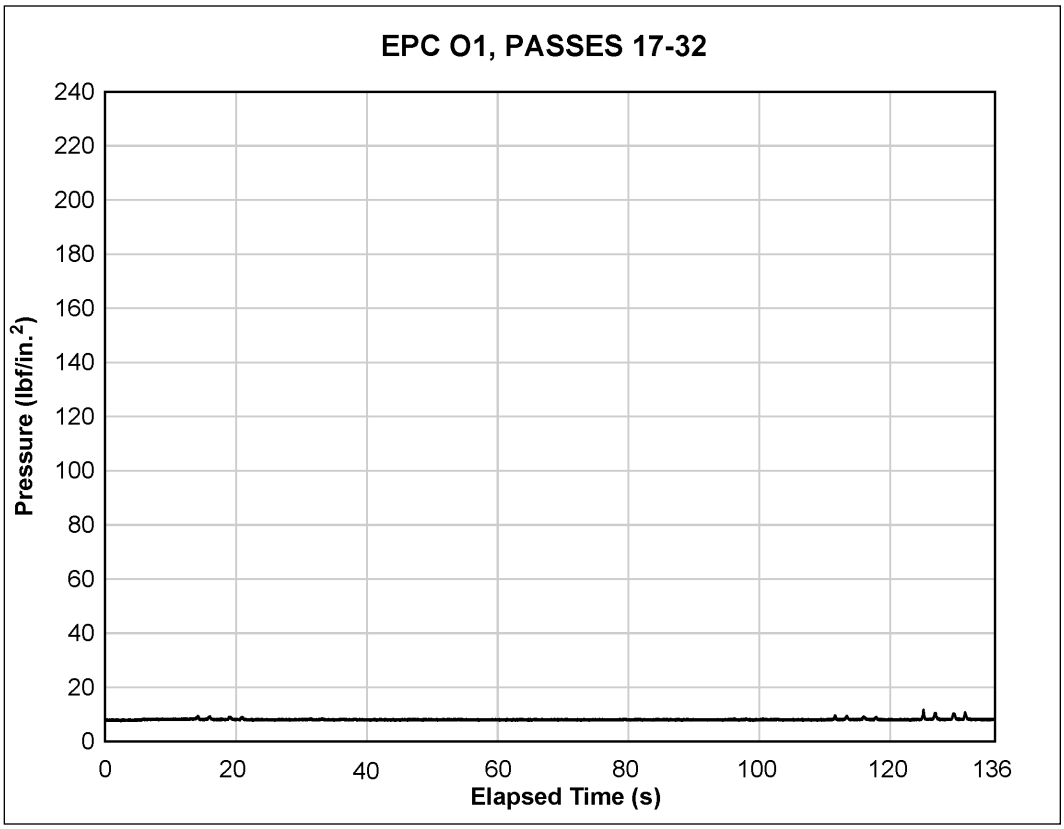
EPC O1, PASSES 17-32
Pressure (lbf/in.2)
240
220
200
180
160
140
120
100
80
60
40
20
0
0
20
40
60
80
100
120
136
Elapsed Time (s)

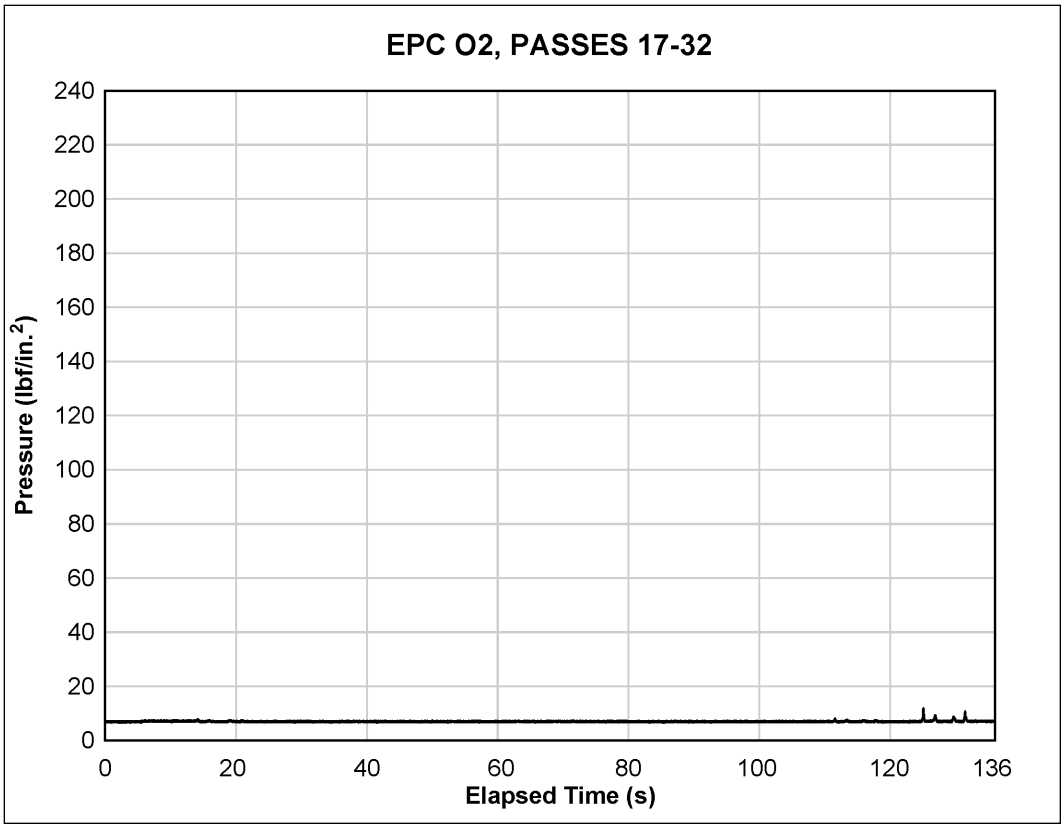
EPC O2, PASSES 17-32
Pressure (lbf/in.2)
240
220
200
180
160
140
120
100
80
60
40
20
0
0
20
40
60
80
100
120
136
Elapsed Time (s)

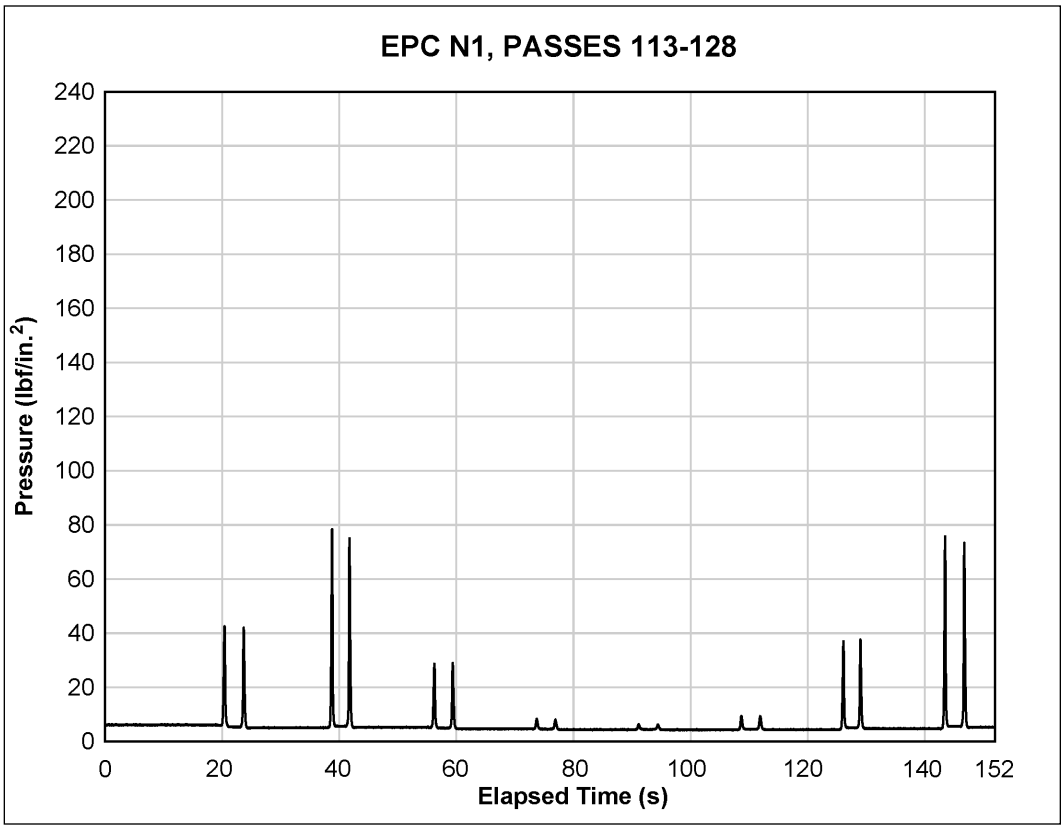
EPC N1, PASSES 113-128
Pressure (lbf/in.2)
240
220
200
180
160
140
120
100
80
60
40
20
0
0
20
40
60
80
100
120
140
152
Elapsed Time (s)

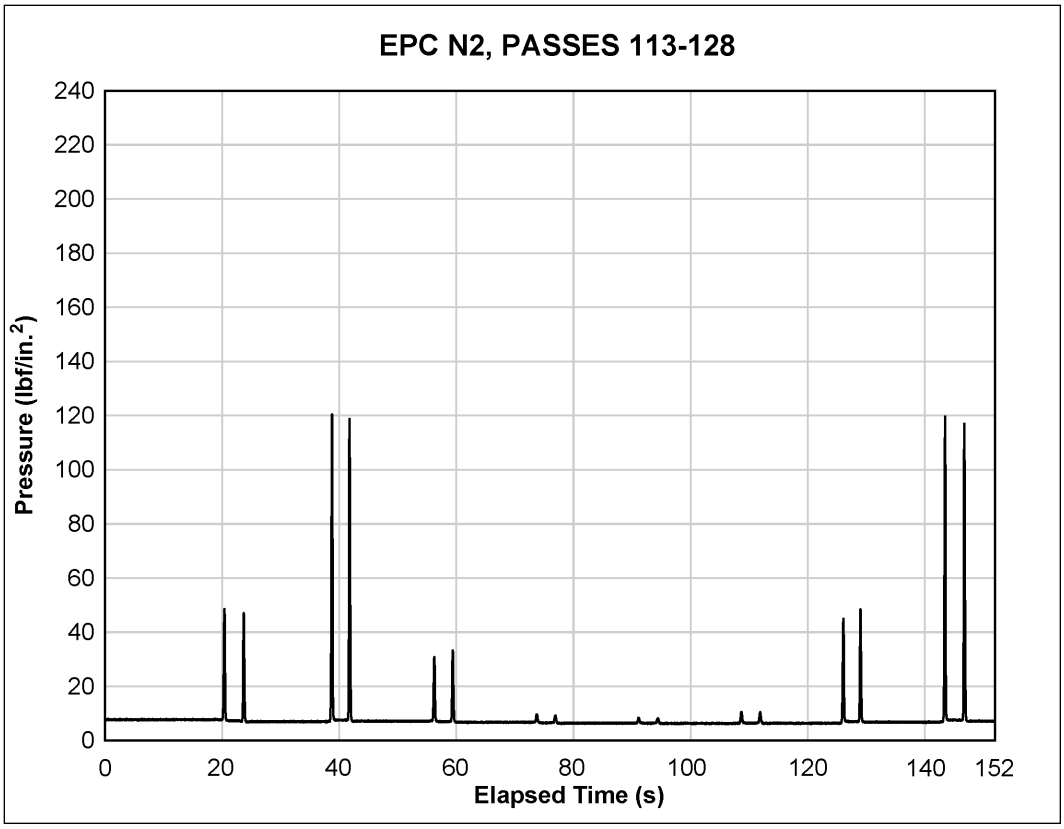
EPC N2, PASSES 113-128
Pressure (lbf/in.2)
240
220
200
180
160
140
120
100
80
60
40
20
0
0
20
40
60
80
100
120
140
152
Elapsed Time (s)

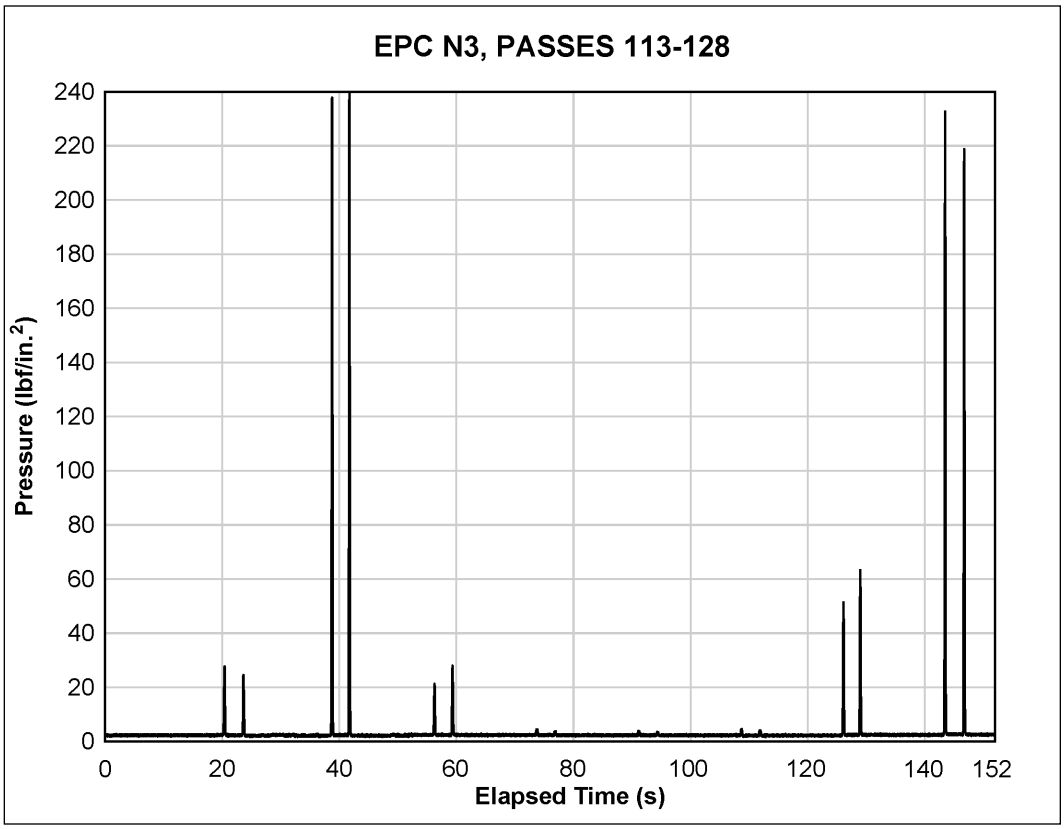
EPC N3, PASSES 113-128
Pressure (lbf/in.2)
240
220
200
180
160
140
120
100
80
60
40
20
0
0
20
40
60
80
100
120
140
152
Elapsed Time (s)

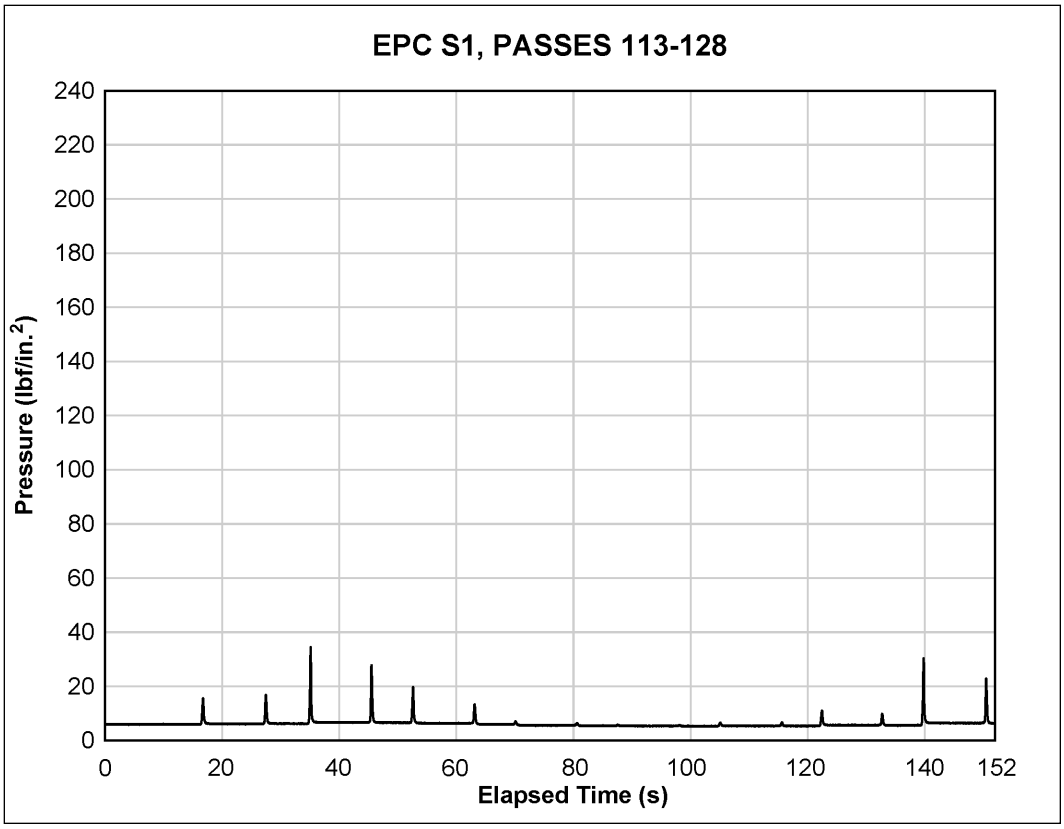
EPC S1, PASSES 113-128
Pressure (lbf/in.2)
240
220
200
180
160
140
120
100
80
60
40
20
0
0
20
40
60
80
100
120
140
152
Elapsed Time (s)

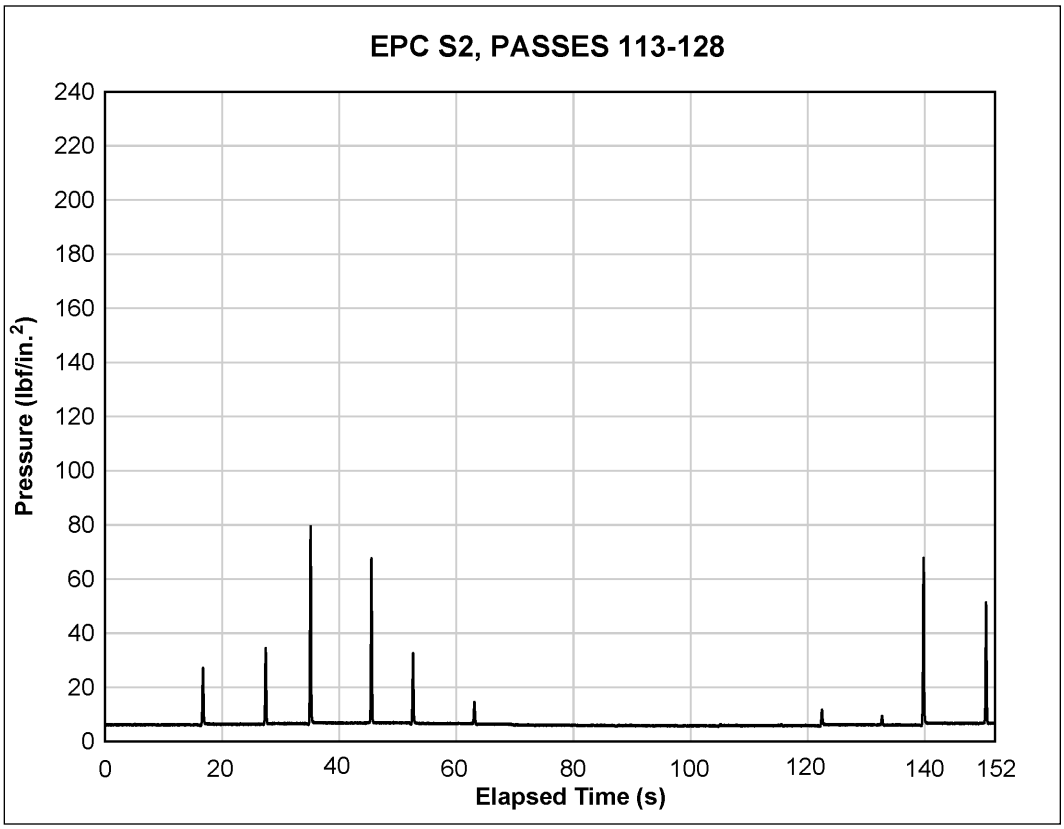
EPC S2, PASSES 113-128
Pressure (lbf/in.2)
240
220
200
180
160
140
120
100
80
60
40
20
0
0
20
40
60
80
100
120
140
152
Elapsed Time (s)

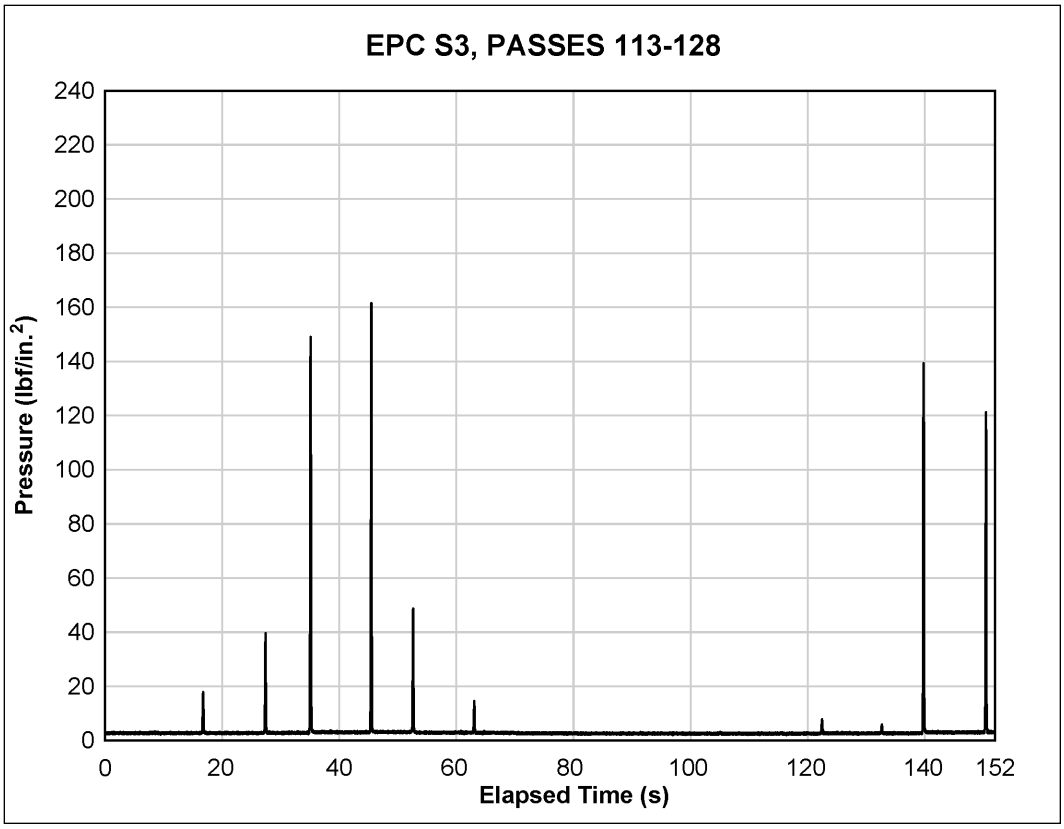
EPC S3, PASSES 113-128
Pressure (lbf/in.2)
240
220
200
180
160
140
120
100
80
60
40
20
0
0
20
40
60
80
100
120
140
152
Elapsed Time (s)

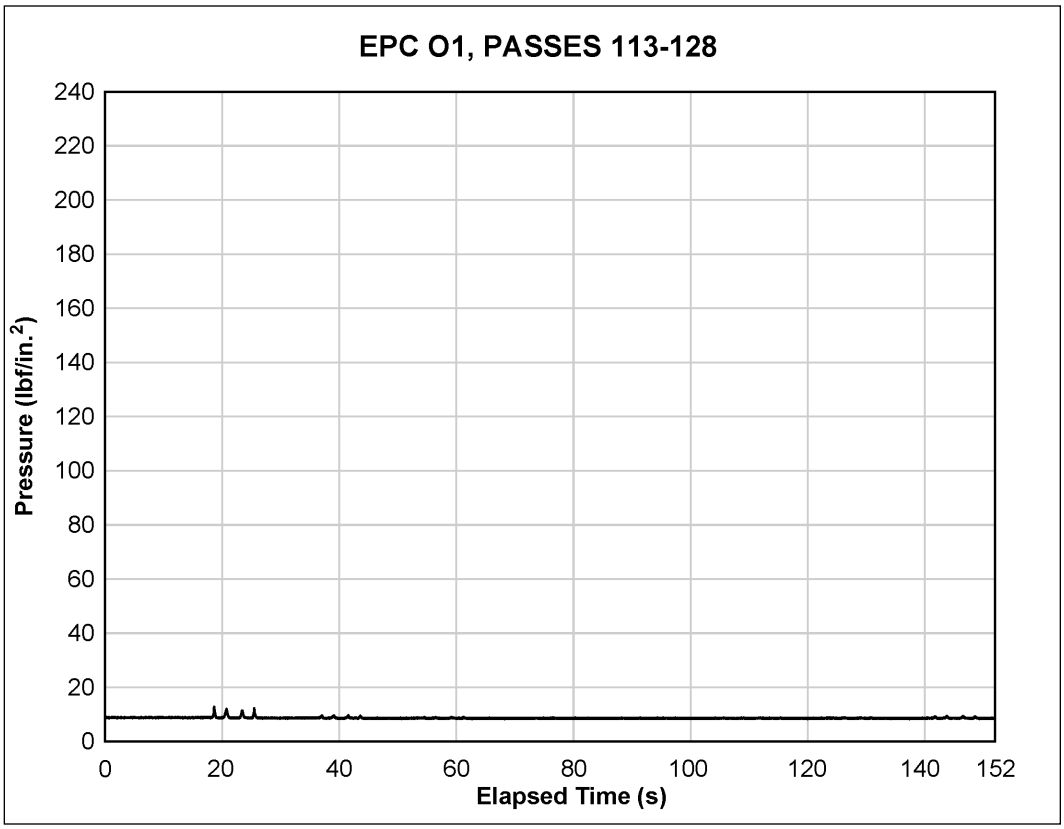
EPC O1, PASSES 113-128
Pressure (lbf/in.2)
240
220
200
180
160
140
120
100
80
60
40
20
0
0
20
40
60
80
100
120
140
152
Elapsed Time (s)

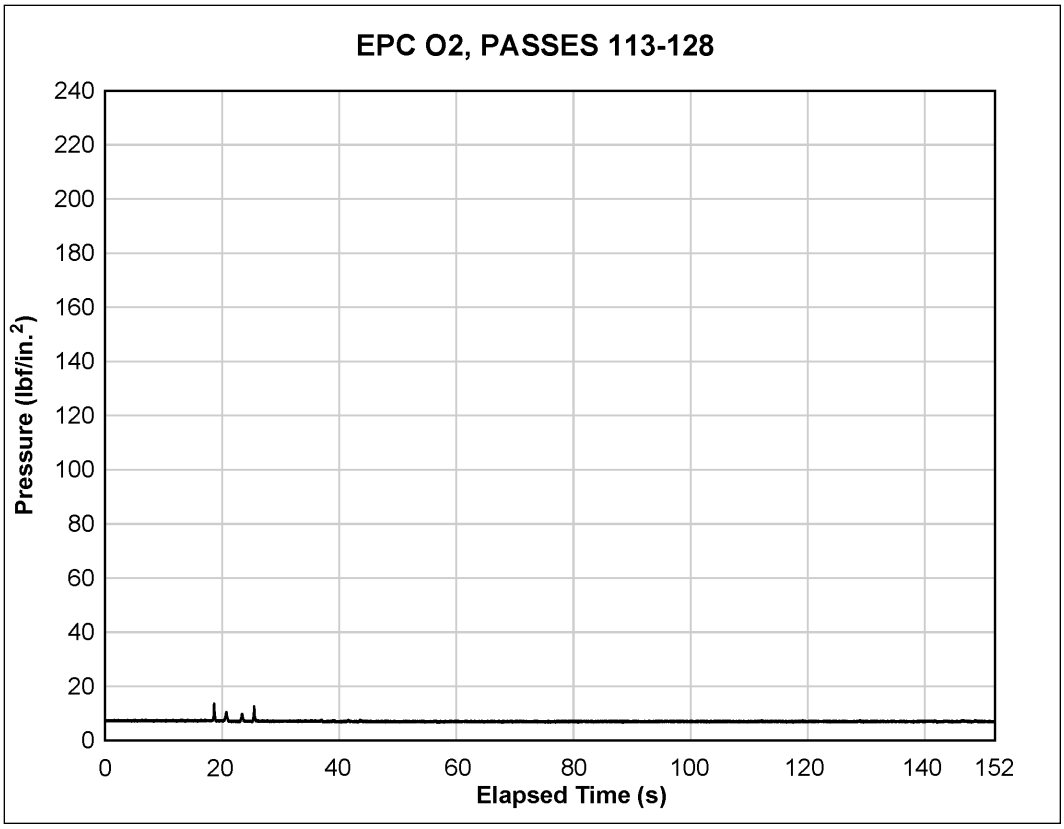
EPC O2, PASSES 113-128
Pressure (lbf/in.2)
240
220
200
180
160
140
120
100
80
60
40
20
0
0
20
40
60
80
100
120
140
152
Elapsed Time (s)

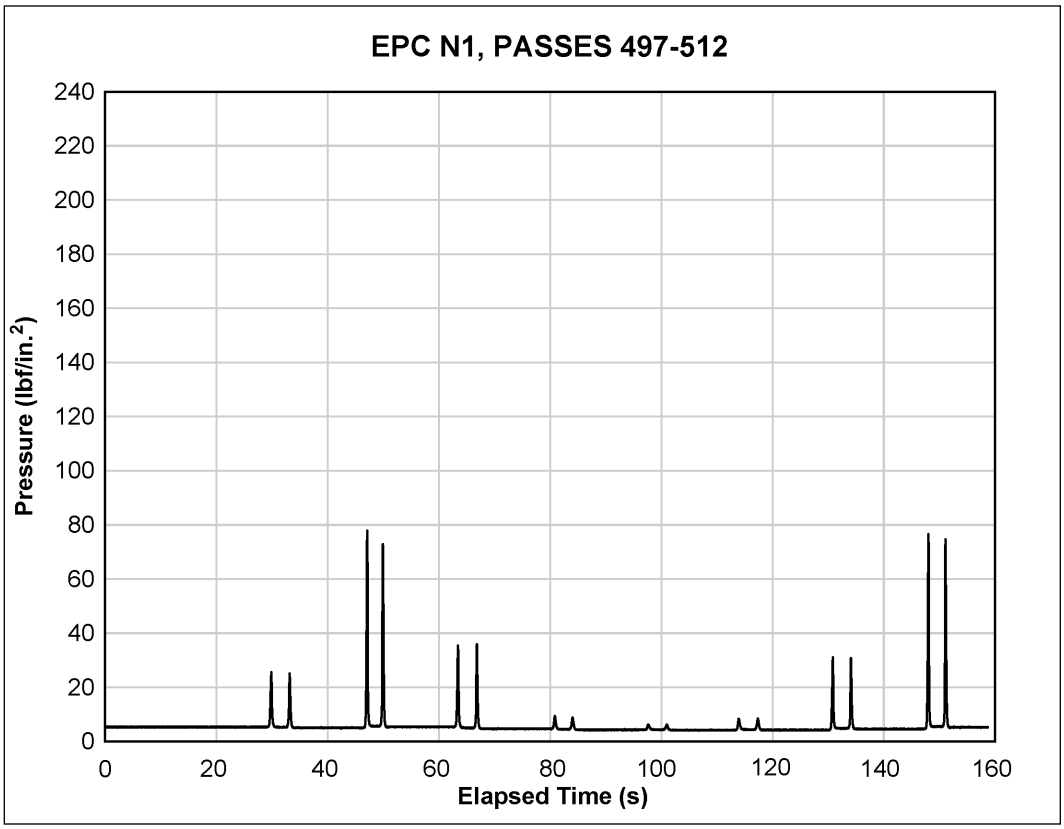
EPC N1, PASSES 497-512
Pressure (lbf/in.2)
240
220
200
180
160
140
120
100
80
60
40
20
0
0
20
40
60
80
100
120
140
160
Elapsed Time (s)

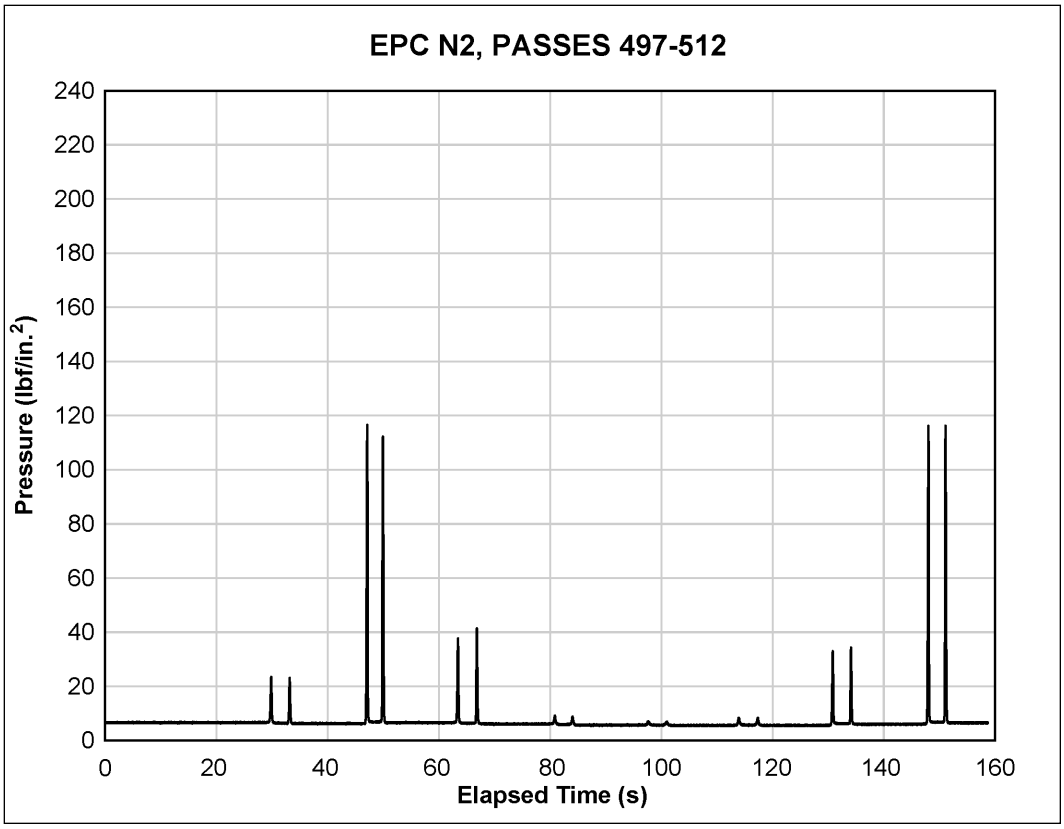
EPC N2, PASSES 497-512
Pressure (lbf/in.2)
Elapsed Time (s)
0
20
40
60
80
100
120
140
160
180
200
220
240

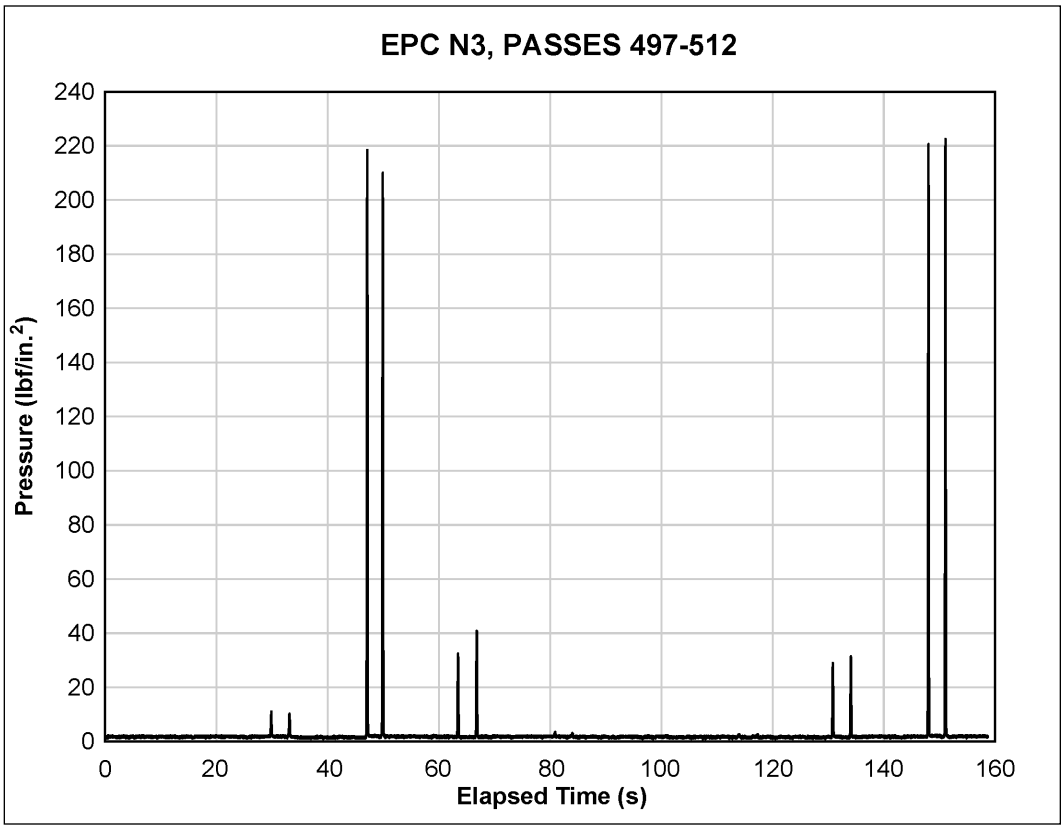
EPC N3, PASSES 497-512
Pressure (lbf/in.2)
Elapsed Time (s)
0
20
40
60
80
100
120
140
160
180
200
220
240

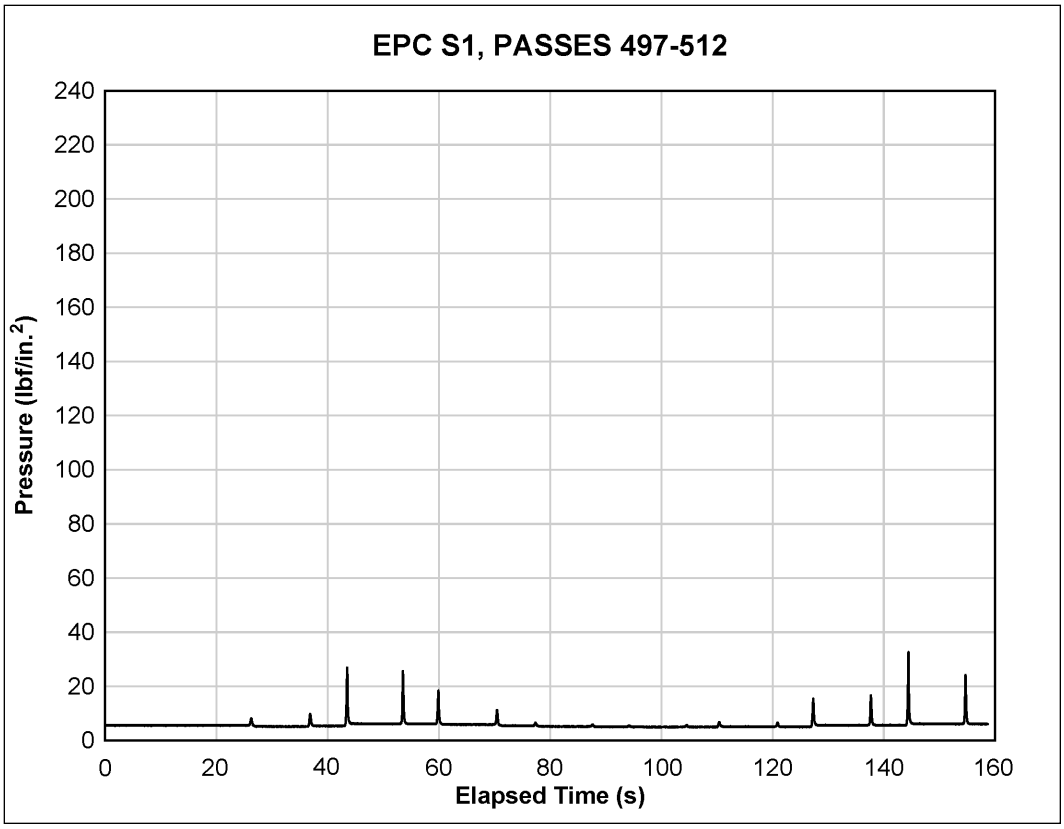
EPC S1, PASSES 497-512
Pressure (lbf/in.2)
0
20
40
60
80
100
120
140
160
180
200
220
240
0
20
40
60
80
100
120
140
160
Elapsed Time (s)

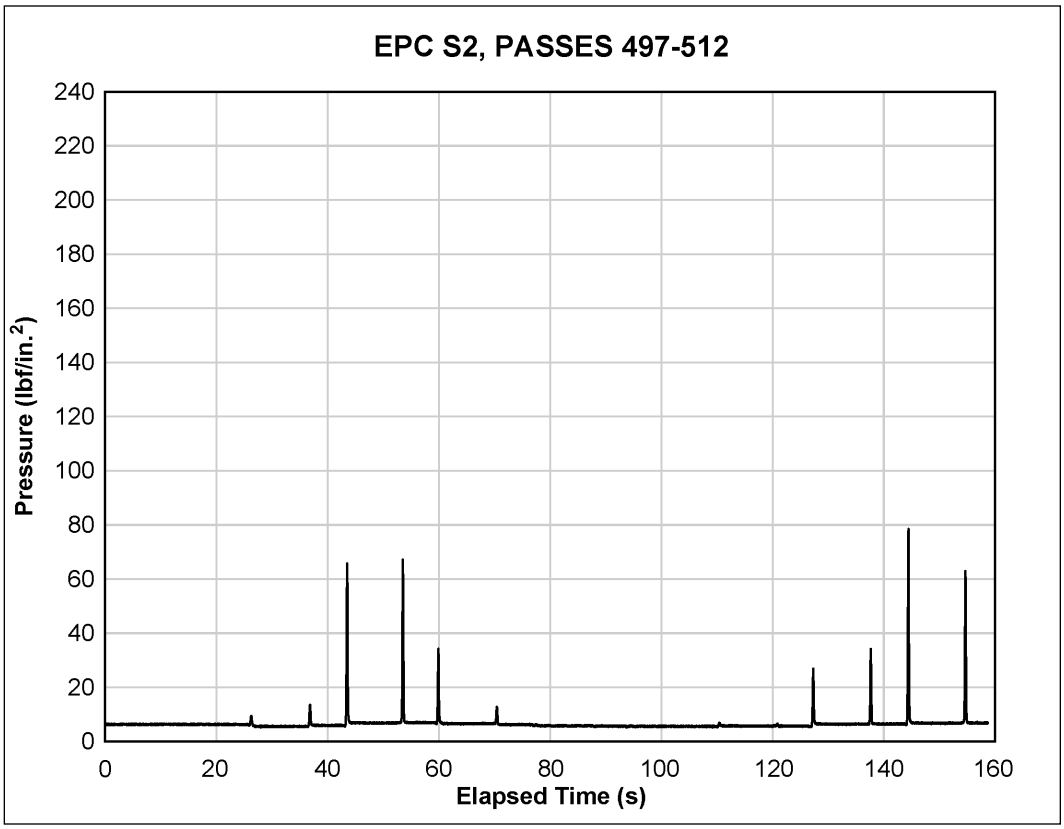
EPC S2, PASSES 497-512
Pressure (lbf/in.2)
0
20
40
60
80
100
120
140
160
180
200
220
240
0
20
40
60
80
100
120
140
160
Elapsed Time (s)

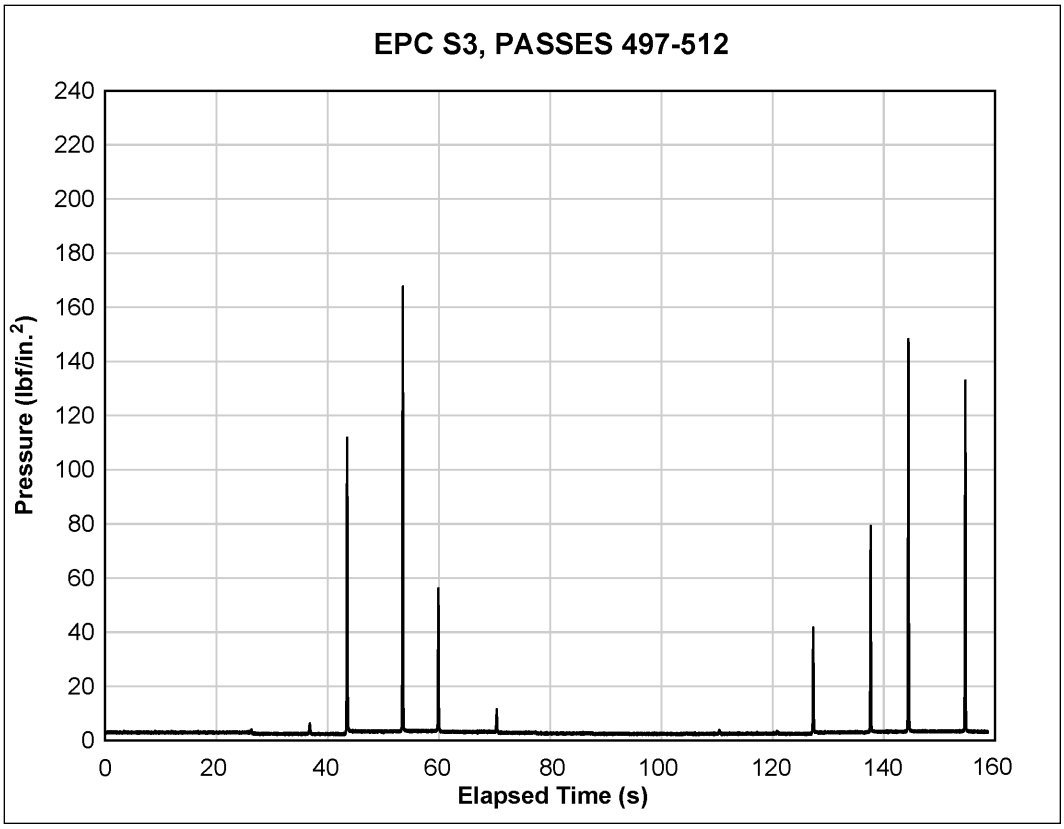
EPC S3, PASSES 497-512
Pressure (lbf/in.2)
0
20
40
60
80
100
120
140
160
180
200
220
240
0
20
40
60
80
100
120
140
160
Elapsed Time (s)

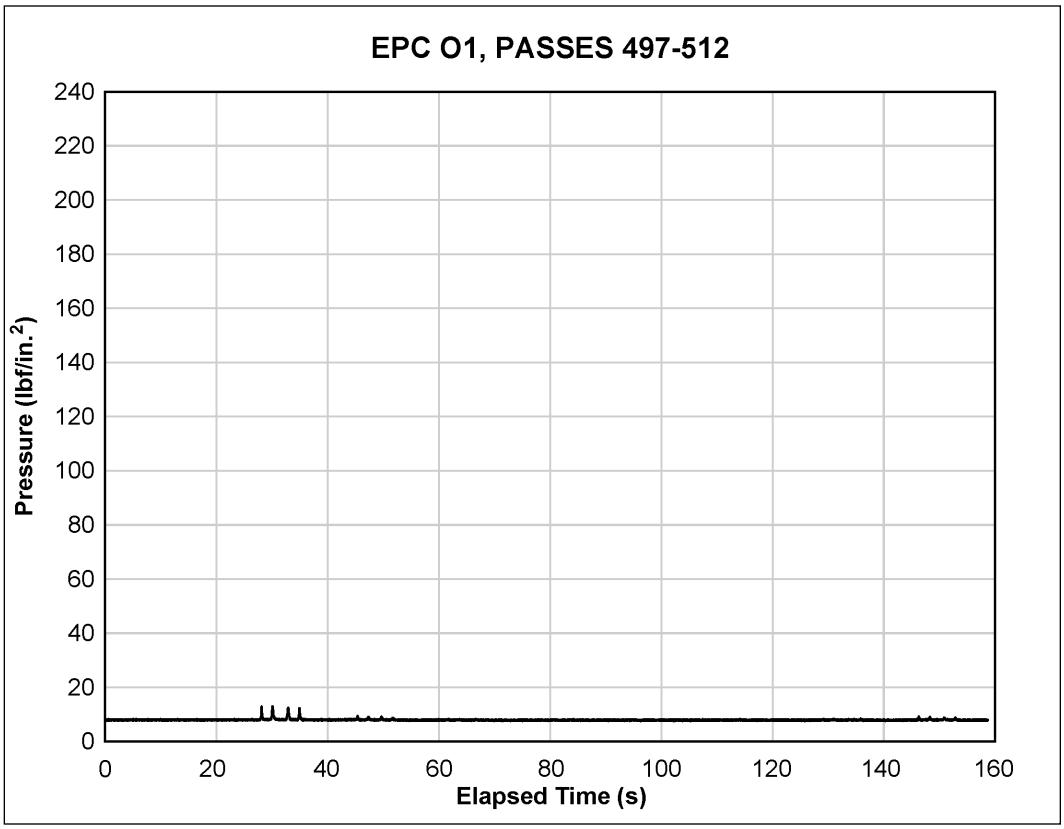
EPC O1, PASSES 497-512
Pressure (lbf/in.2)
0
20
40
60
80
100
120
140
160
180
200
220
240
0
20
40
60
80
100
120
140
160
Elapsed Time (s)

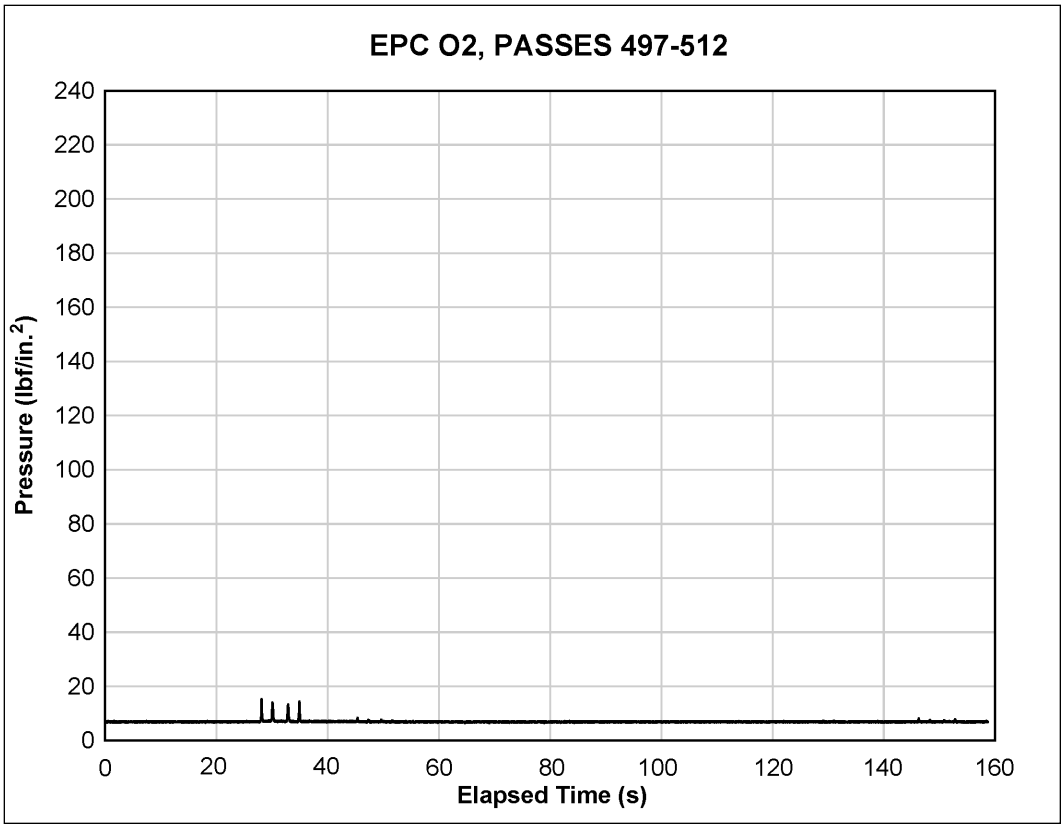
EPC O2, PASSES 497-512
Pressure (lbf/in.2)
240
220
200
180
160
140
120
100
80
60
40
20
0
0
20
40
60
80
100
120
140
160
Elapsed Time (s)

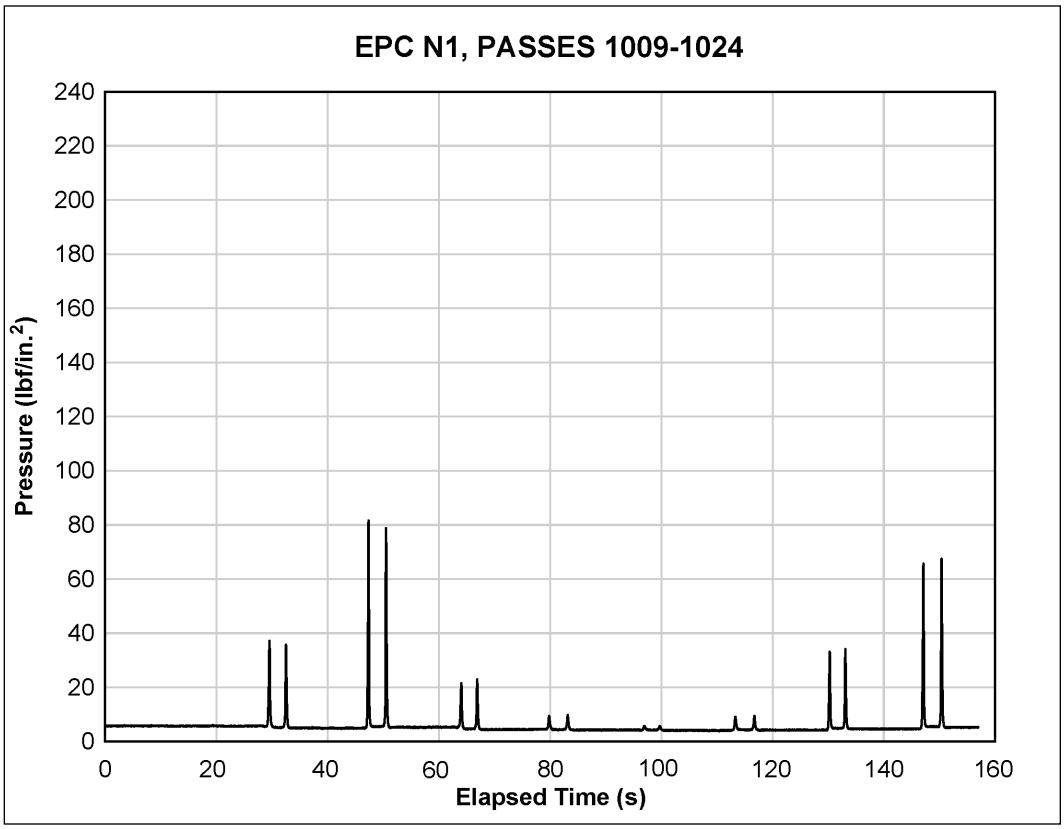
EPC N1, PASSES 1009-1024
Pressure (lbf/in.2)
240
220
200
180
160
140
120
100
80
60
40
20
0
0
20
40
60
80
100
120
140
160
Elapsed Time (s)

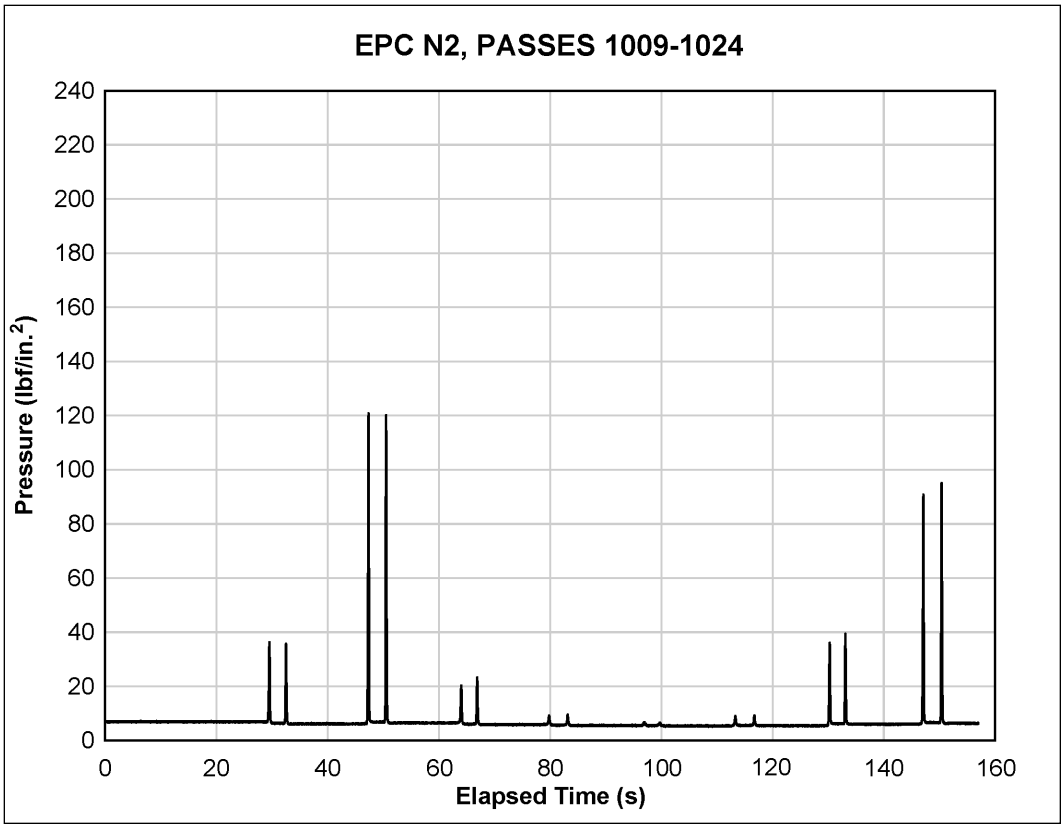
EPC N2, PASSES 1009-1024
Pressure (lbf/in.2)
240
220
200
180
160
140
120
100
80
60
40
20
0
0
20
40
60
80
100
120
140
160
Elapsed Time (s)

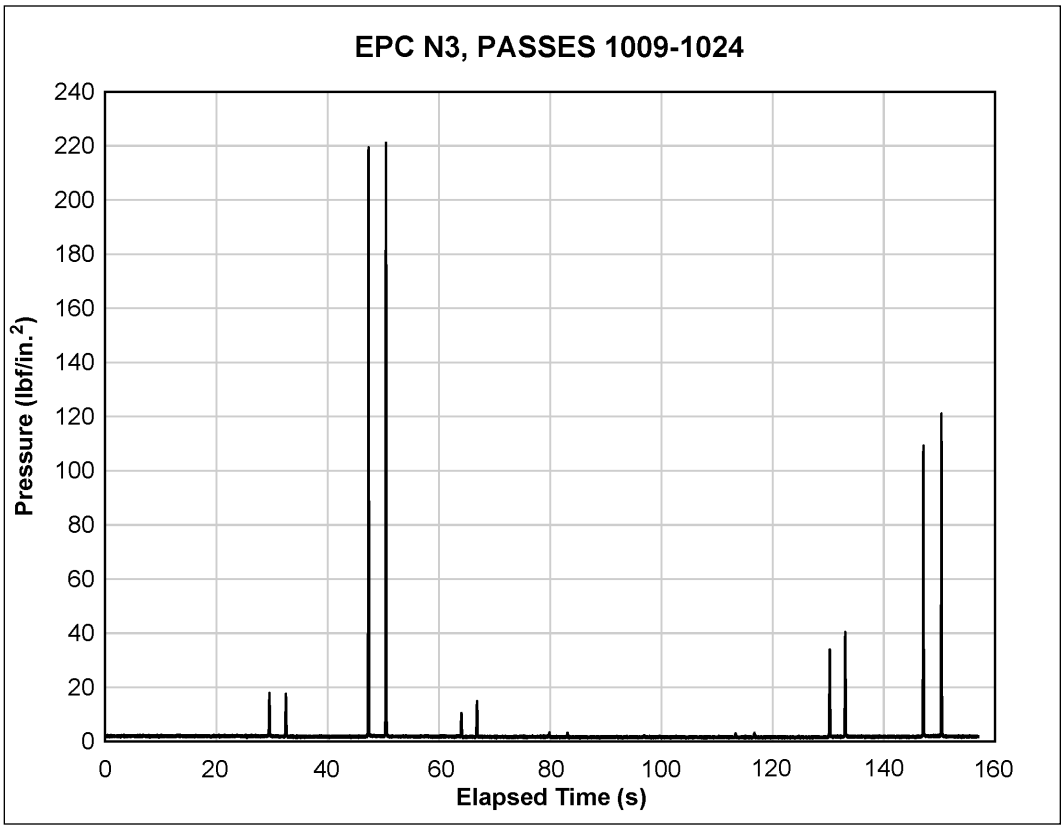
EPC N3, PASSES 1009-1024
Pressure (lbf/in.2)
240
220
200
180
160
140
120
100
80
60
40
20
0
0
20
40
60
80
100
120
140
160
Elapsed Time (s)

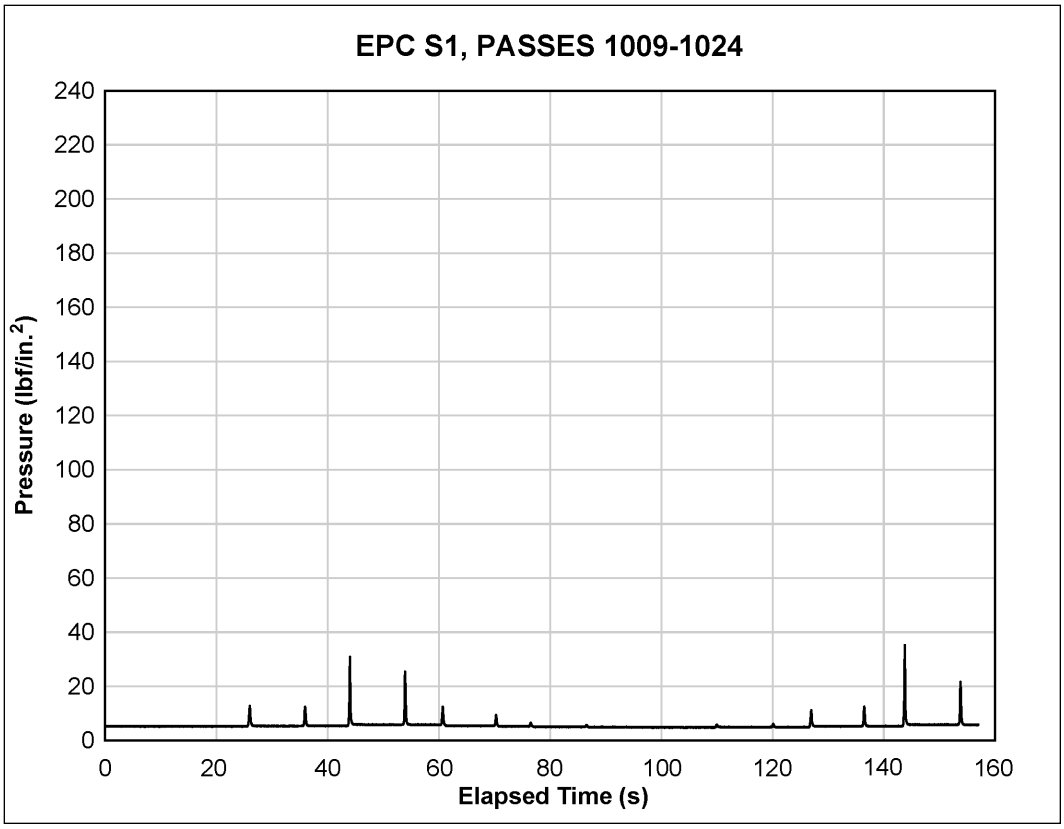
EPC S1, PASSES 1009-1024
Pressure (lbf/in.2)
0
20
40
60
80
100
120
140
160
180
200
220
240
0
20
40
60
80
100
120
140
160
Elapsed Time (s)

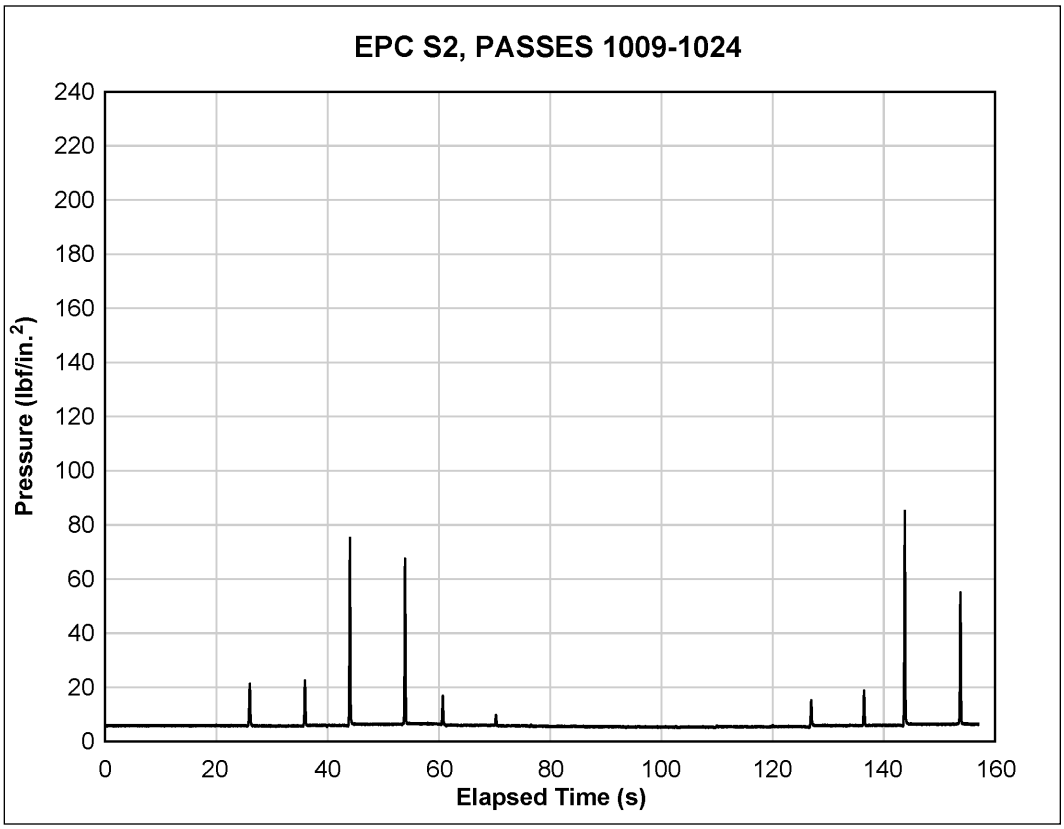
EPC S2, PASSES 1009-1024
Pressure (lbf/in.2)
0
20
40
60
80
100
120
140
160
180
200
220
240
0
20
40
60
80
100
120
140
160
Elapsed Time (s)

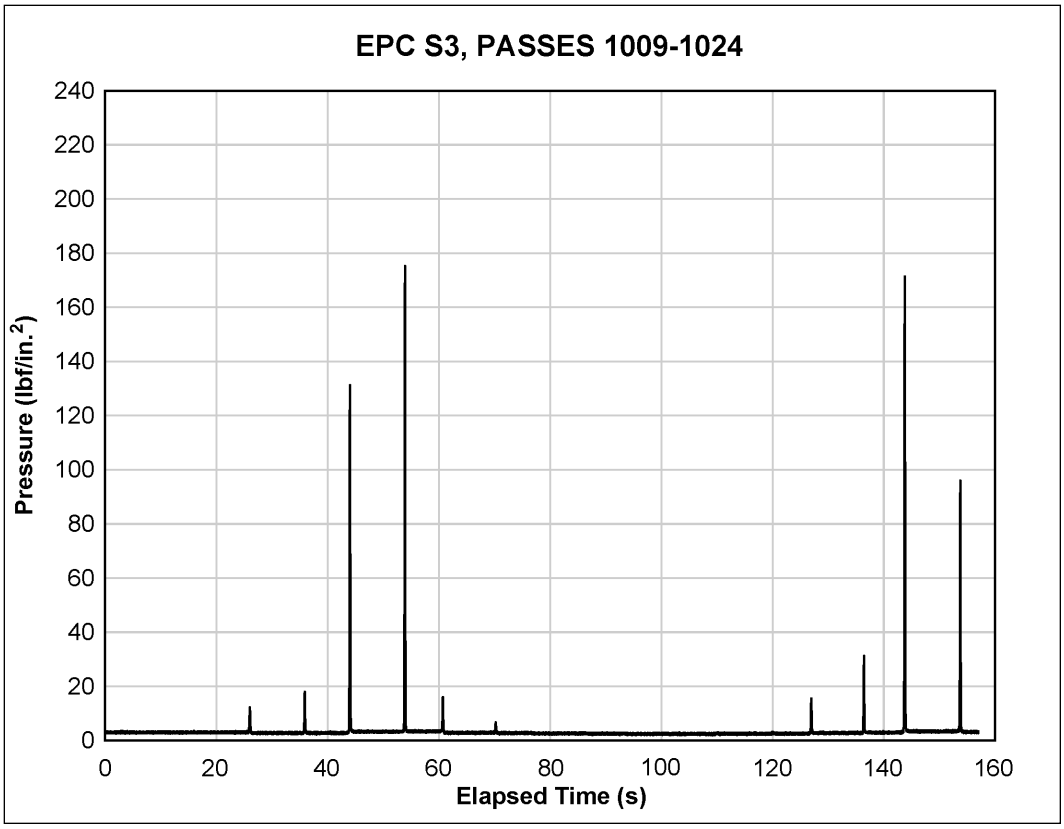
EPC S3, PASSES 1009-1024
Pressure (lbf/in.2)
0
20
40
60
80
100
120
140
160
180
200
220
240
0
20
40
60
80
100
120
140
160
Elapsed Time (s)

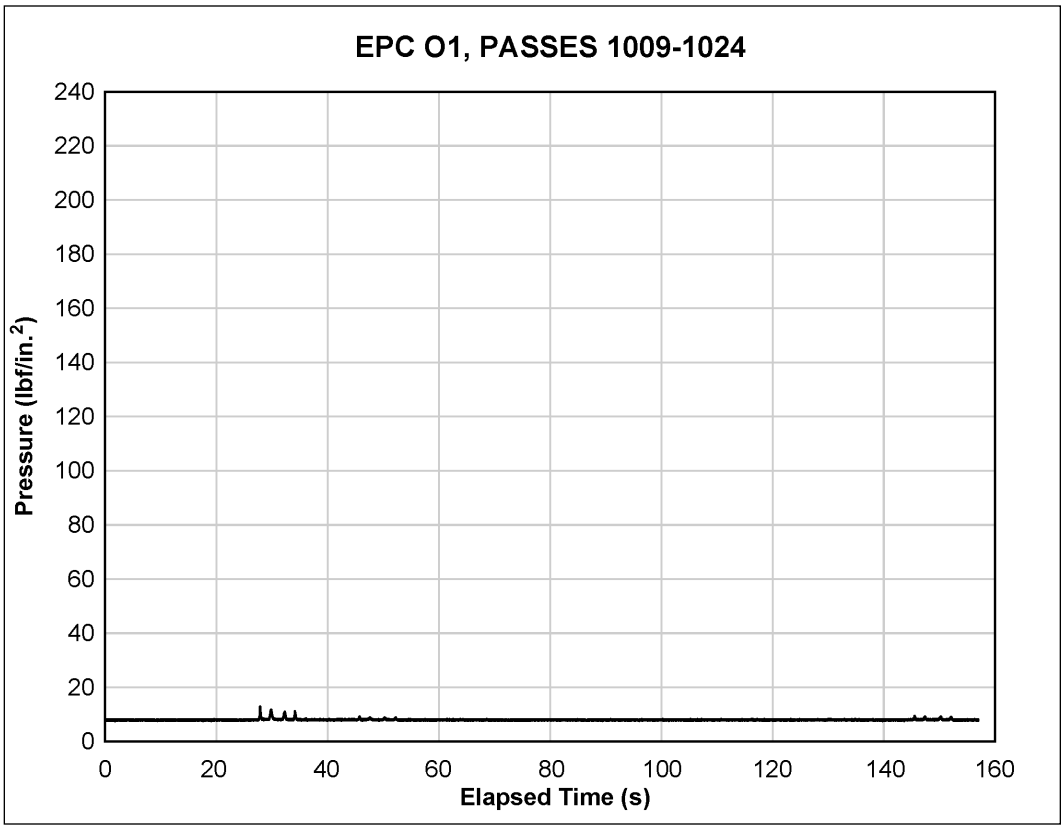
EPC O1, PASSES 1009-1024
Pressure (lbf/in.2)
0
20
40
60
80
100
120
140
160
180
200
220
240
0
20
40
60
80
100
120
140
160
Elapsed Time (s)

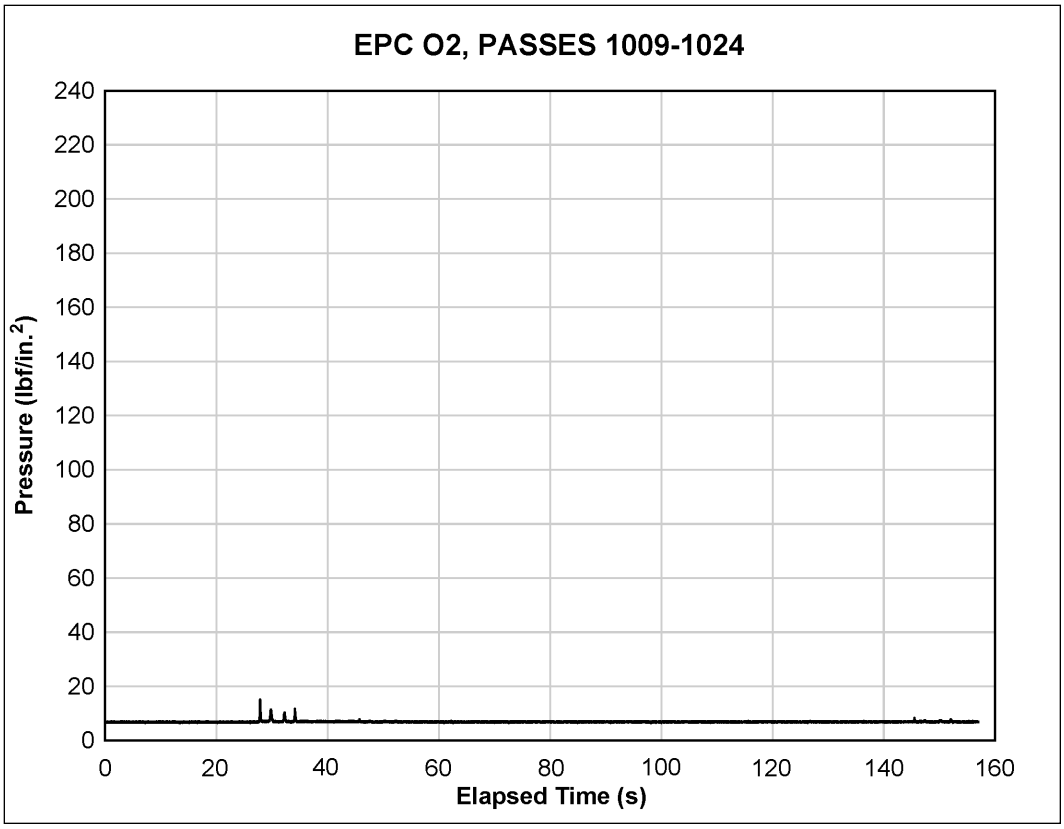
EPC O2, PASSES 1009-1024
Pressure (lbf/in.2)
240
220
200
180
160
140
120
100
80
60
40
20
0
0
20
40
60
80
100
120
140
160
Elapsed Time (s)

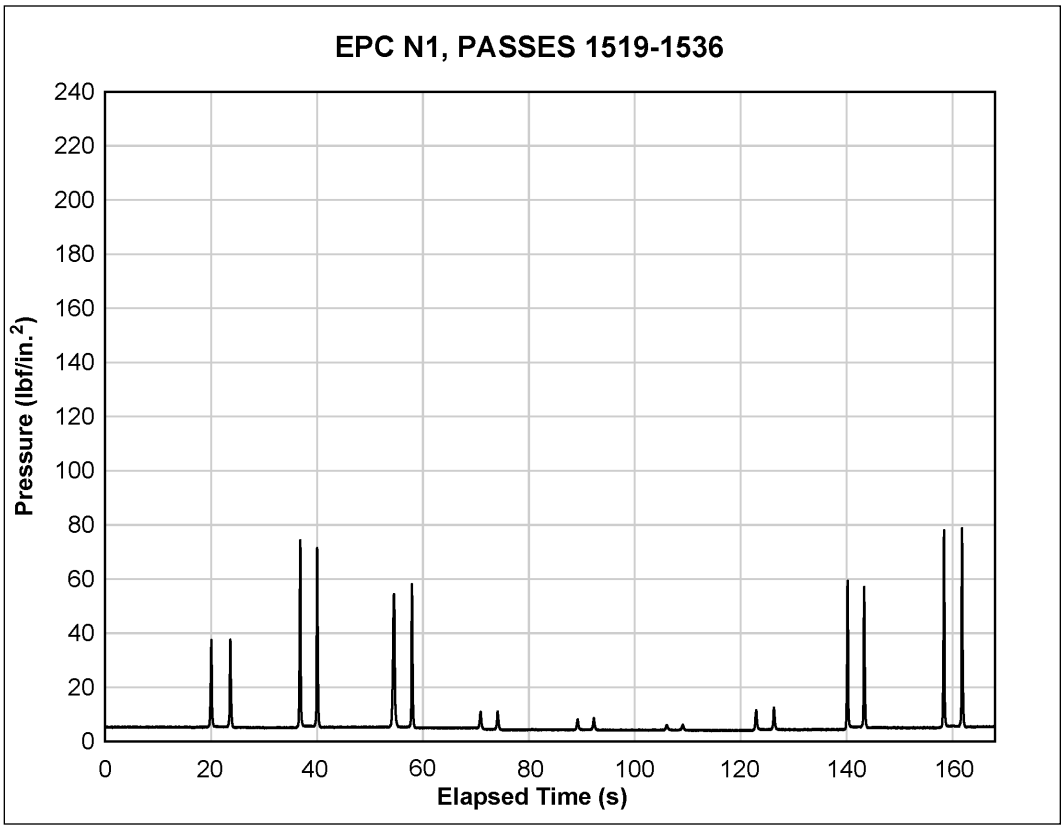
EPC N1, PASSES 1519-1536
Pressure (lbf/in.2)
240
220
200
180
160
140
120
100
80
60
40
20
0
0
20
40
60
80
100
120
140
160
Elapsed Time (s)

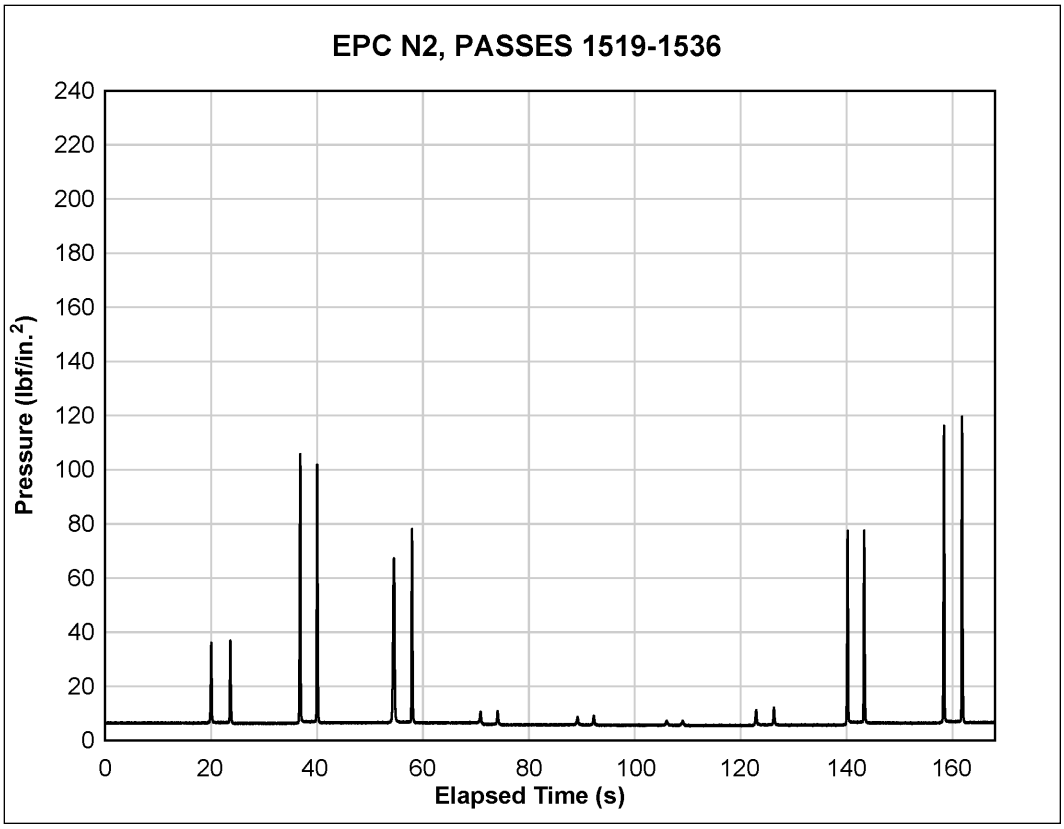
EPC N2, PASSES 1519-1536
Pressure (lbf/in.2)
0
20
40
60
80
100
120
140
160
180
200
220
240
0
20
40
60
80
100
120
140
160
Elapsed Time (s)

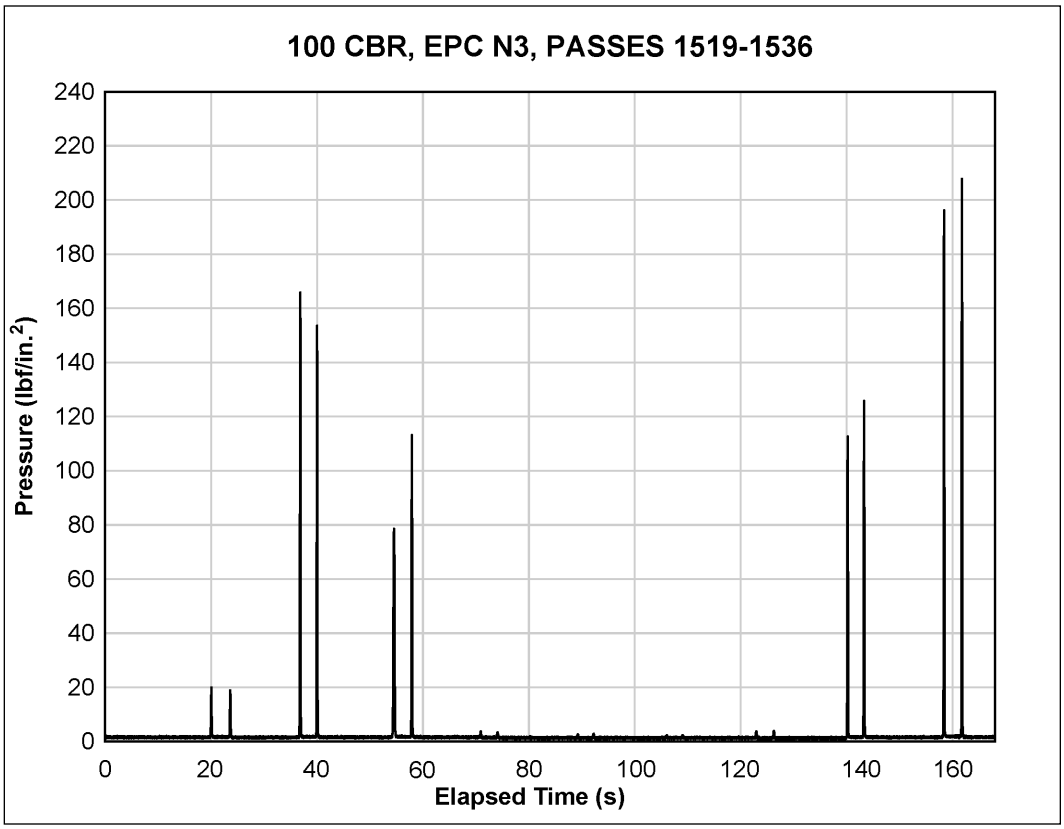
100 CBR, EPC N3, PASSES 1519-1536
Pressure (lbf/in.2)
0
20
40
60
80
100
120
140
160
180
200
220
240
0
20
40
60
80
100
120
140
160
Elapsed Time (s)

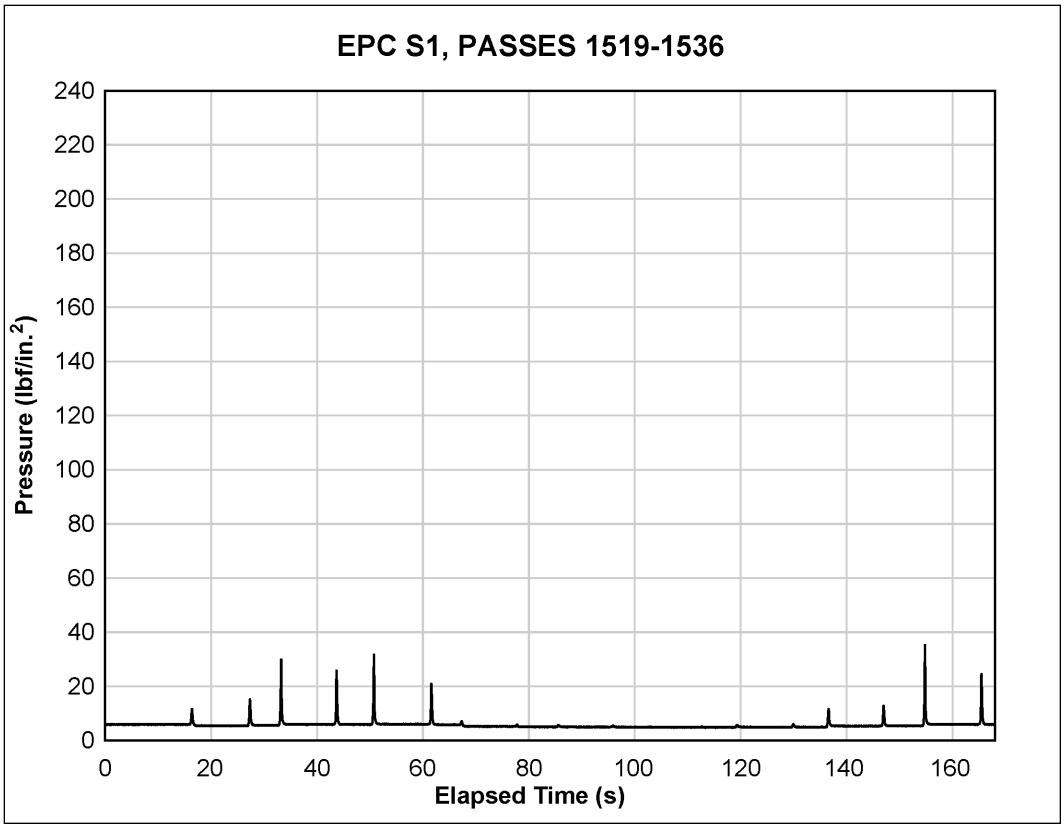
EPC S1, PASSES 1519-1536
Pressure (lbf/in.2)
0
20
40
60
80
100
120
140
160
180
200
220
240
0
20
40
60
80
100
120
140
160
Elapsed Time (s)

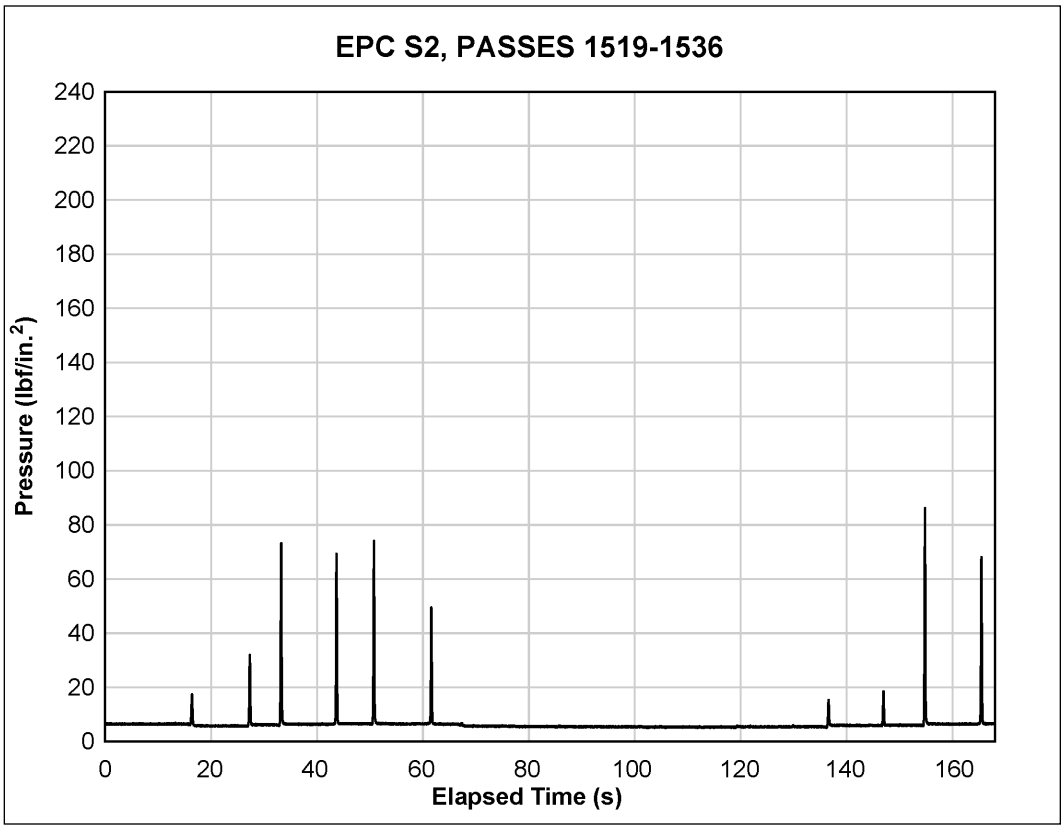
EPC S2, PASSES 1519-1536
Pressure (lbf/in.2)
0
20
40
60
80
100
120
140
160
180
200
220
240
0
20
40
60
80
100
120
140
160
Elapsed Time (s)

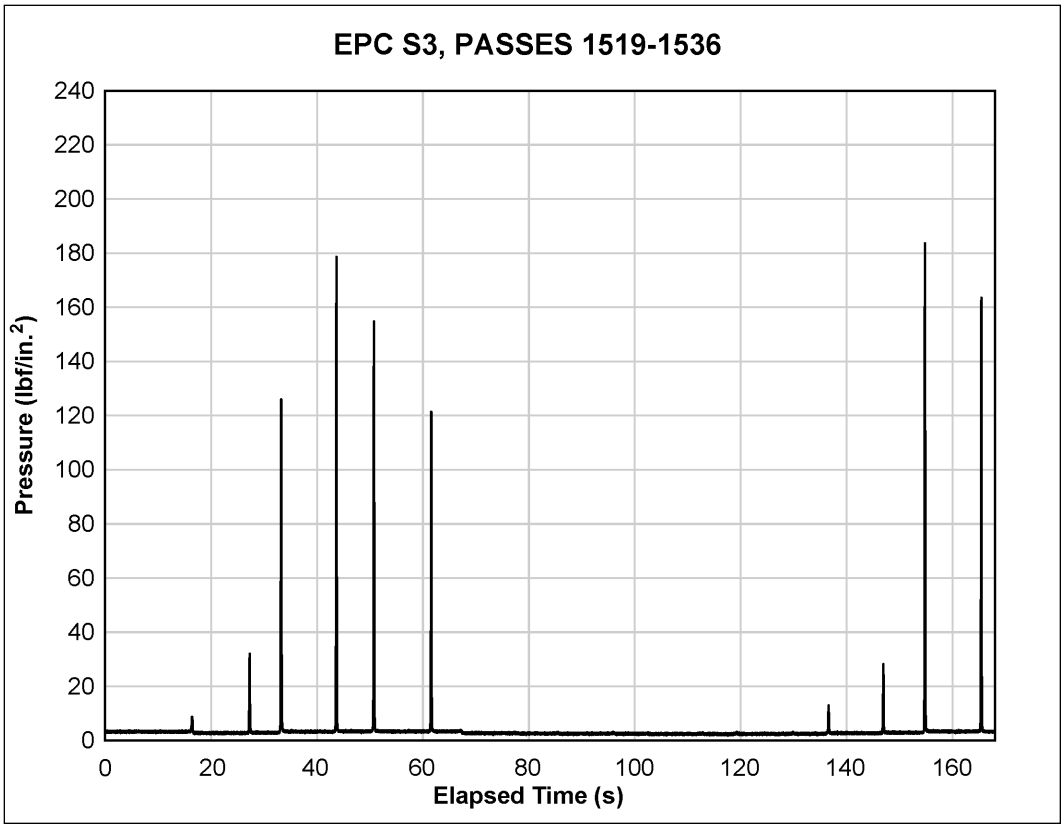
EPC S3, PASSES 1519-1536
Pressure (lbf/in.2)
240
220
200
180
160
140
120
100
80
60
40
20
0
0
20
40
60
80
100
120
140
160
Elapsed Time (s)

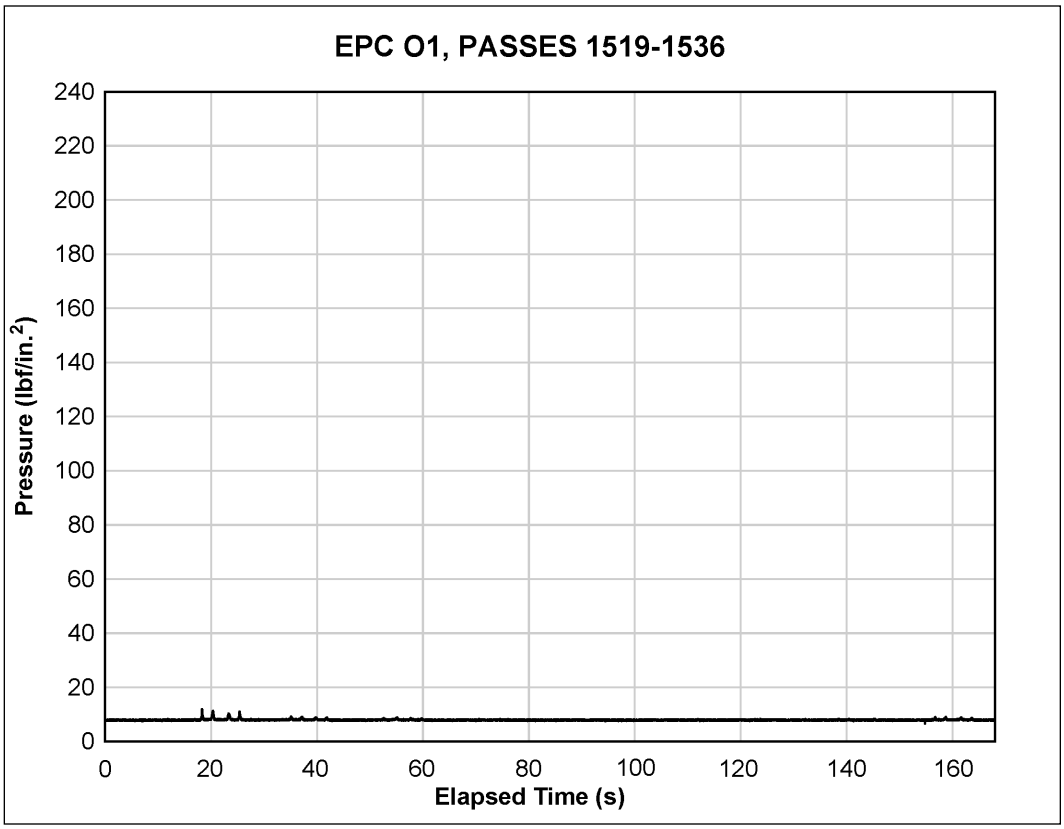
EPC O1, PASSES 1519-1536
Pressure (lbf/in.2)
240
220
200
180
160
140
120
100
80
60
40
20
0
0
20
40
60
80
100
120
140
160
Elapsed Time (s)

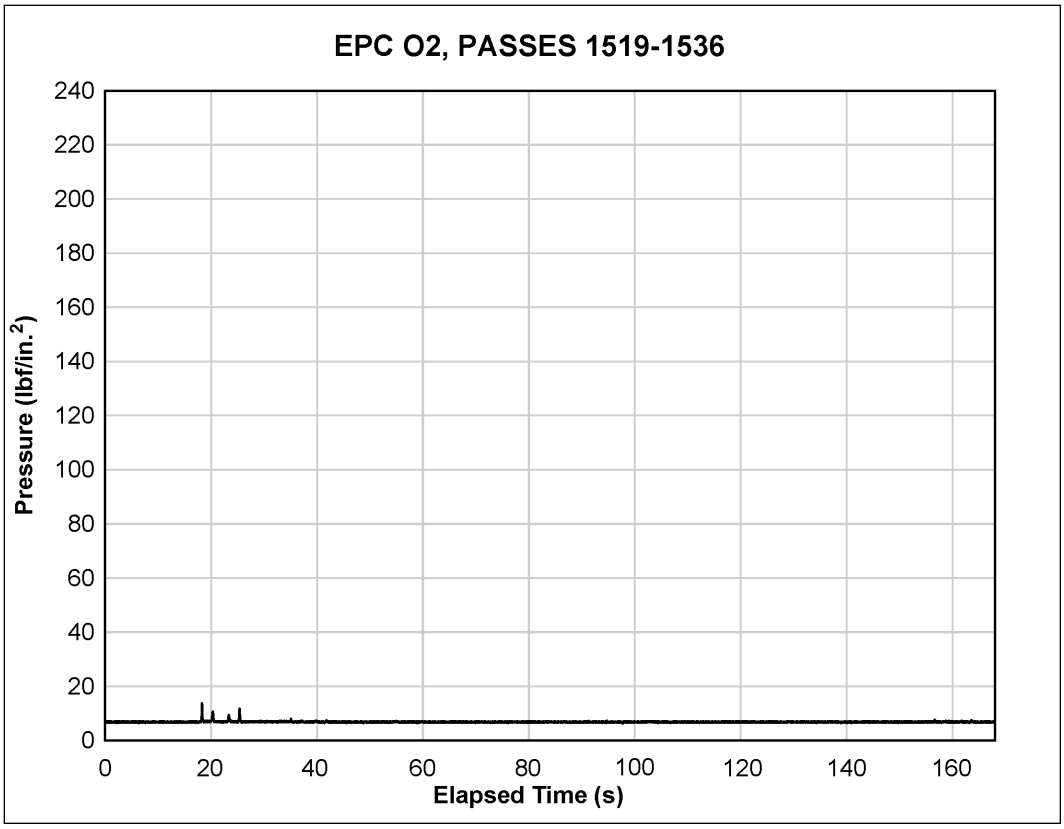
EPC O2, PASSES 1519-1536
Pressure (lbf/in.2)
240
220
200
180
160
140
120
100
80
60
40
20
0
0
20
40
60
80
100
120
140
160
Elapsed Time (s)

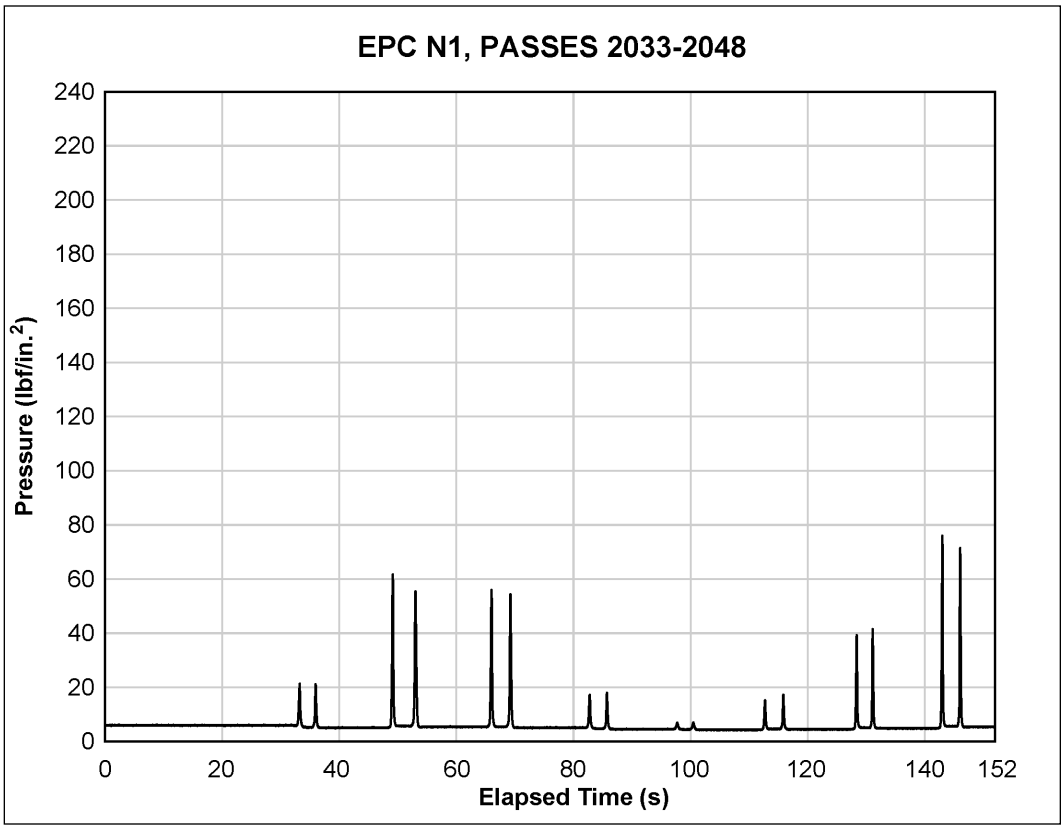
EPC N1, PASSES 2033-2048
Pressure (lbf/in.2)
240
220
200
180
160
140
120
100
80
60
40
20
0
0
20
40
60
80
100
120
140
152
Elapsed Time (s)

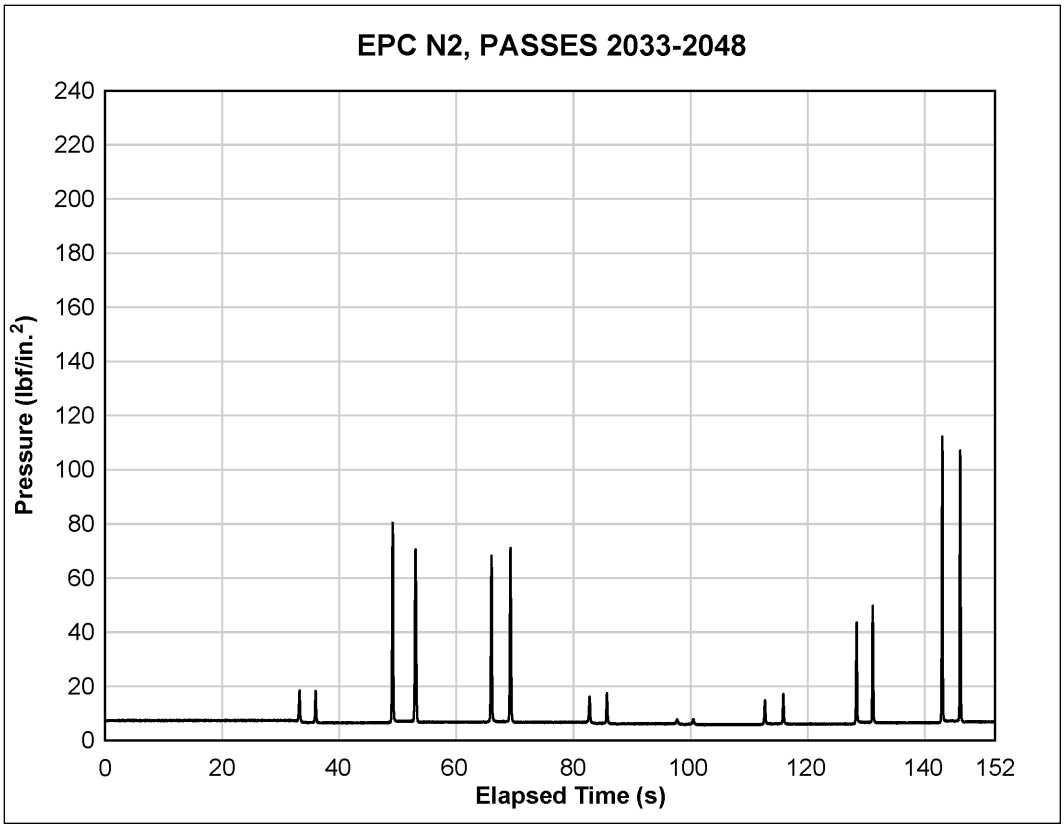
EPC N2, PASSES 2033-2048
Pressure (lbf/in.2)
0
20
40
60
80
100
120
140
160
180
200
220
240
0
20
40
60
80
100
120
140
152
Elapsed Time (s)

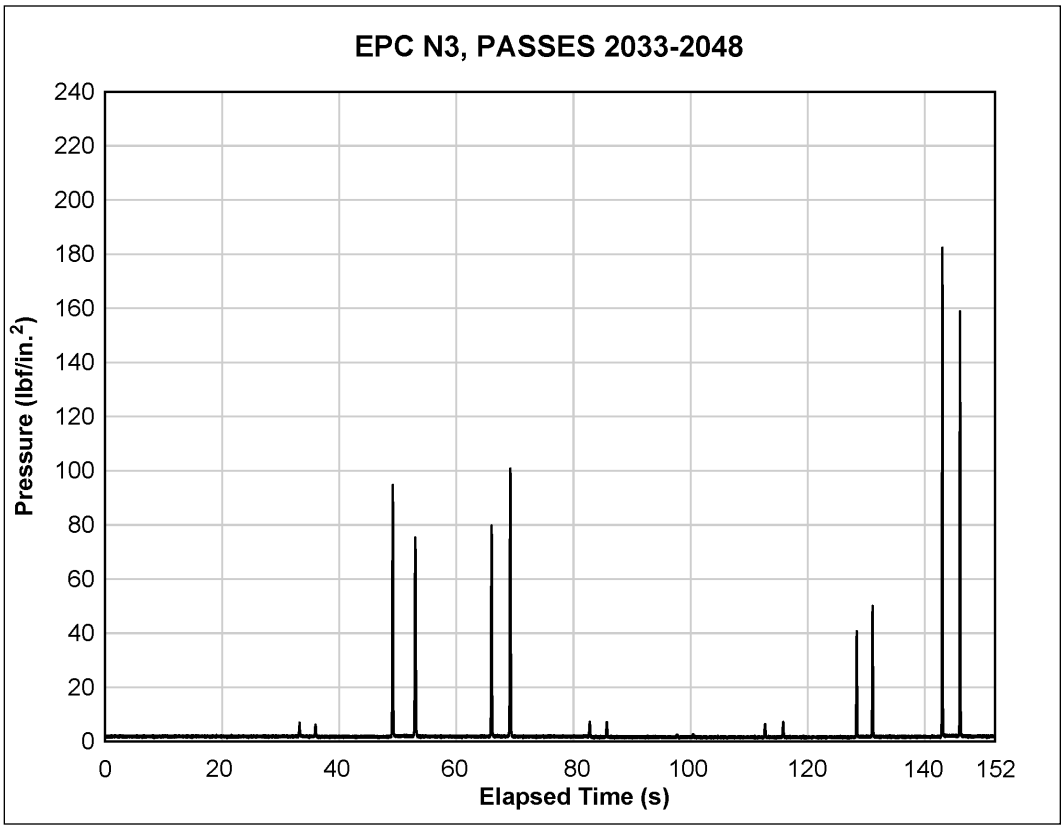
EPC N3, PASSES 2033-2048
Pressure (lbf/in.2)
0
20
40
60
80
100
120
140
160
180
200
220
240
0
20
40
60
80
100
120
140
152
Elapsed Time (s)

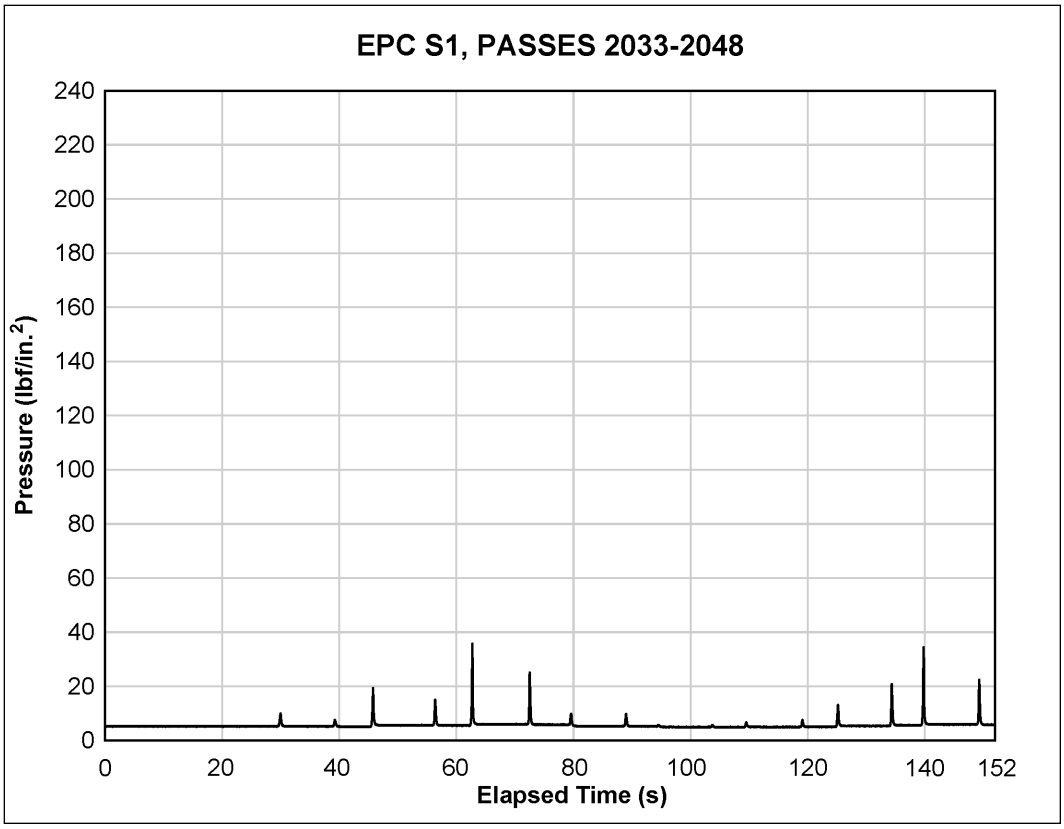
EPC S1, PASSES 2033-2048
Pressure (lbf/in.2)
240
220
200
180
160
140
120
100
80
60
40
20
0
0
20
40
60
80
100
120
140
152
Elapsed Time (s)

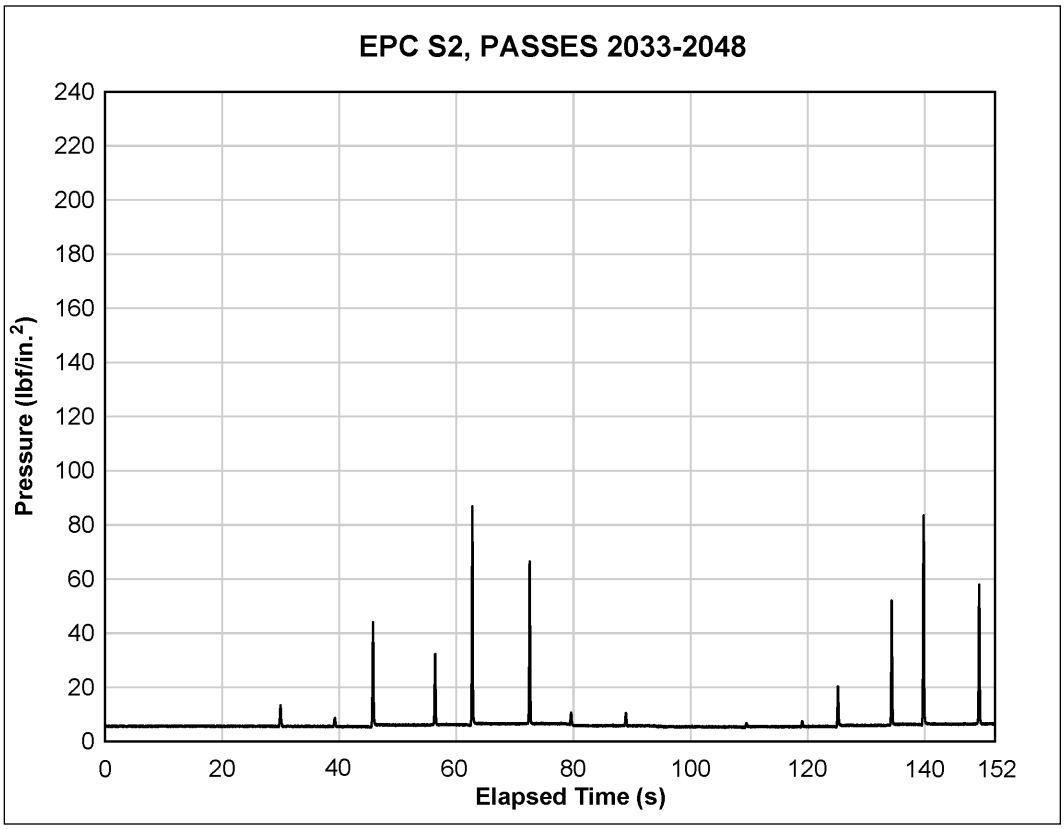
EPC S2, PASSES 2033-2048
Pressure (lbf/in.2)
240
220
200
180
160
140
120
100
80
60
40
20
0
0
20
40
60
80
100
120
140
152
Elapsed Time (s)

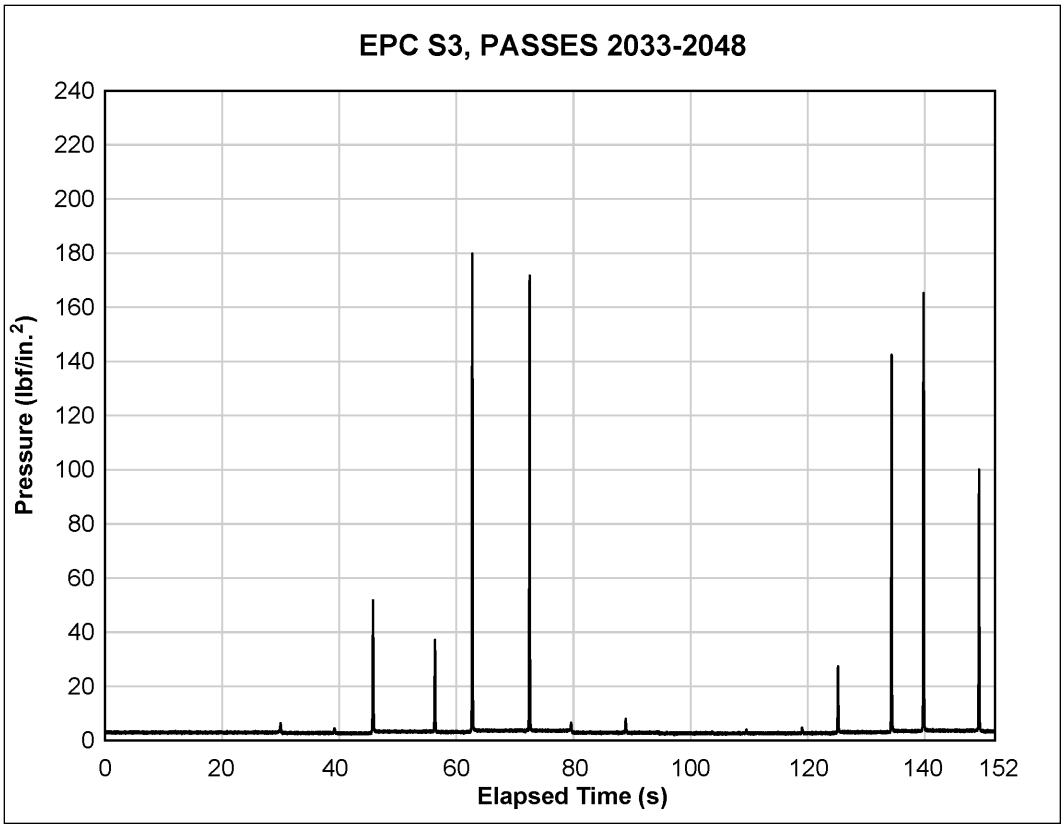
EPC S3, PASSES 2033-2048
Pressure (lbf/in.2)
0
20
40
60
80
100
120
140
160
180
200
220
240
0
20
40
60
80
100
120
140
152
Elapsed Time (s)

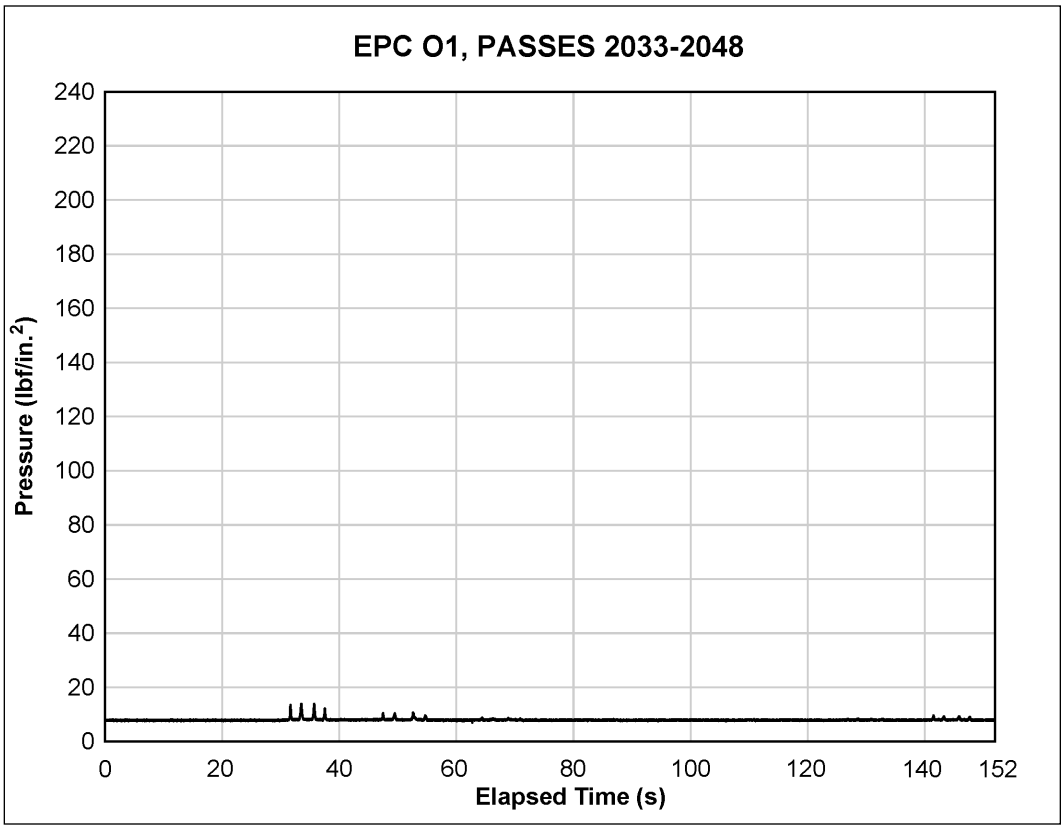
EPC O1, PASSES 2033-2048
Pressure (lbf/in.2)
0
20
40
60
80
100
120
140
160
180
200
220
240
0
20
40
60
80
100
120
140
152
Elapsed Time (s)

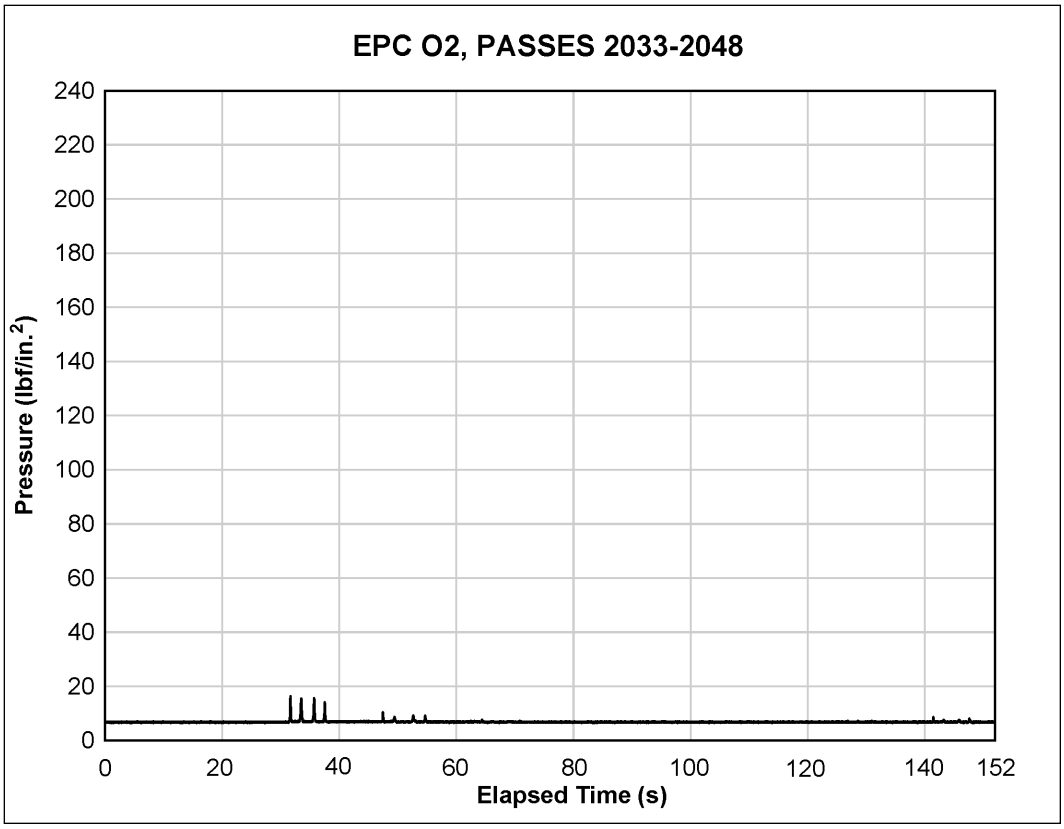
EPC O2, PASSES 2033-2048
Pressure (lbf/in.2)
240
220
200
180
160
140
120
100
80
60
40
20
0
0
20
40
60
80
100
120
140
152
Elapsed Time (s)

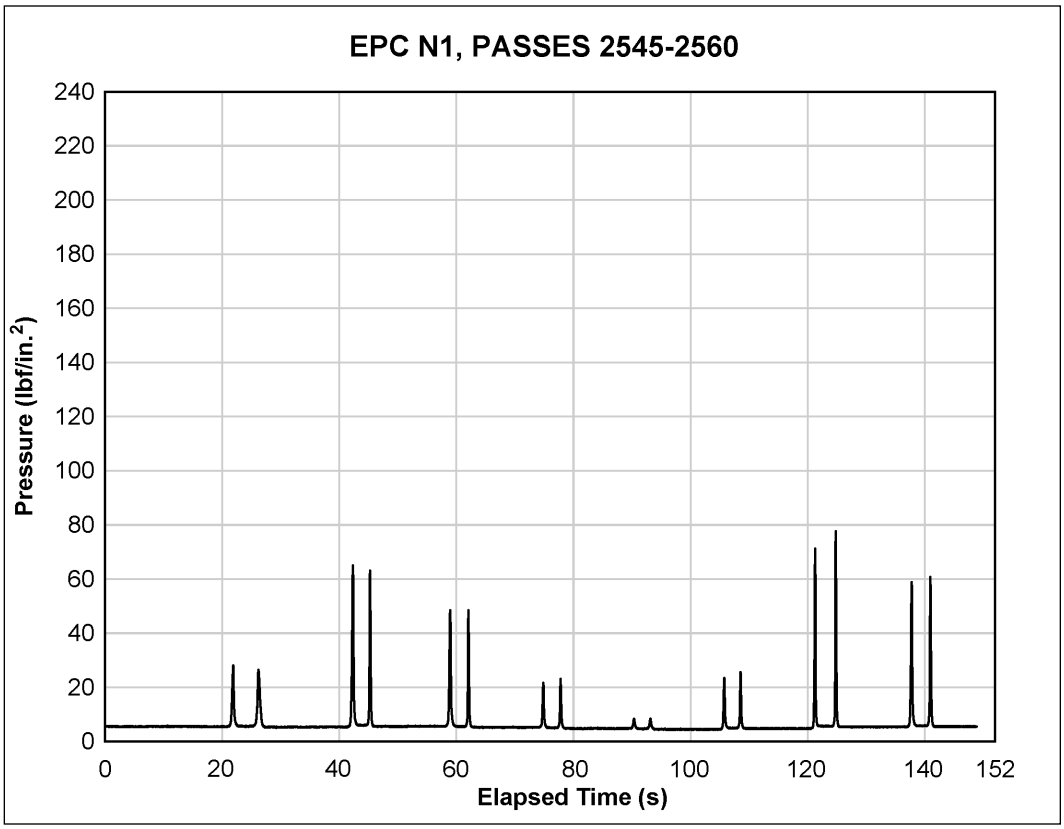
EPC N1, PASSES 2545-2560
Pressure (lbf/in.2)
240
220
200
180
160
140
120
100
80
60
40
20
0
0
20
40
60
80
100
120
140
152
Elapsed Time (s)

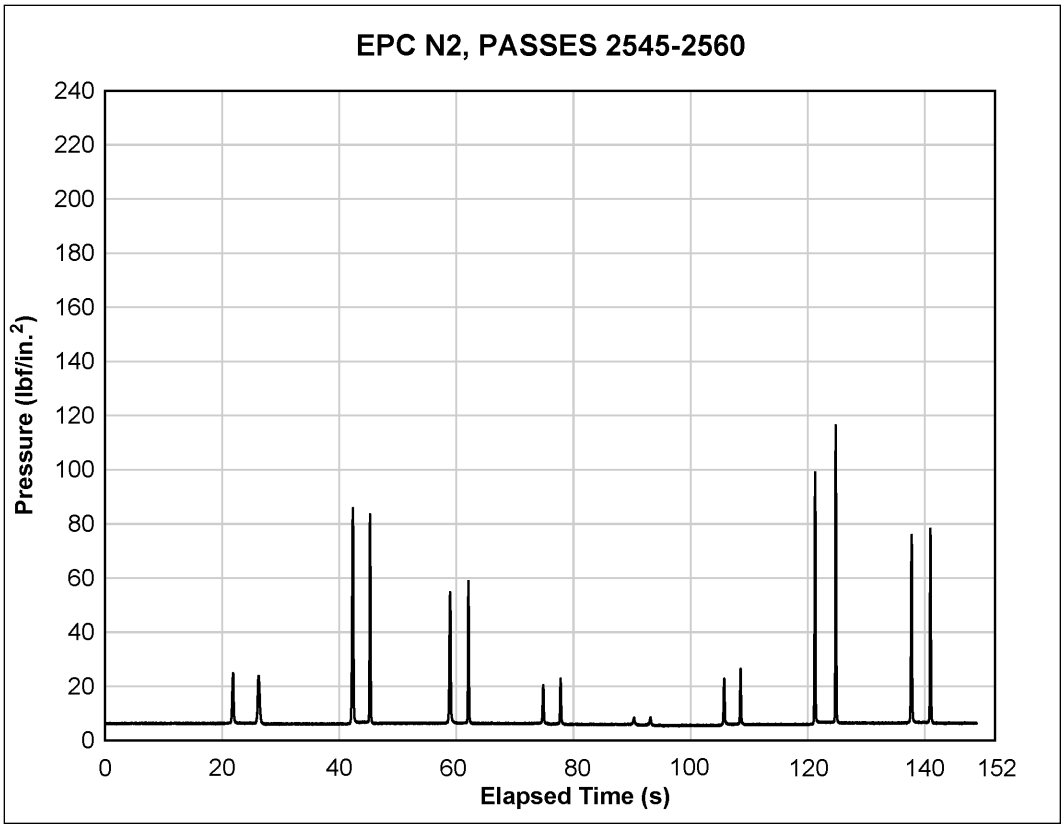
EPC N2, PASSES 2545-2560
Pressure (lbf/in.2)
0
20
40
60
80
100
120
140
160
180
200
220
240
0
20
40
60
80
100
120
140
152
Elapsed Time (s)

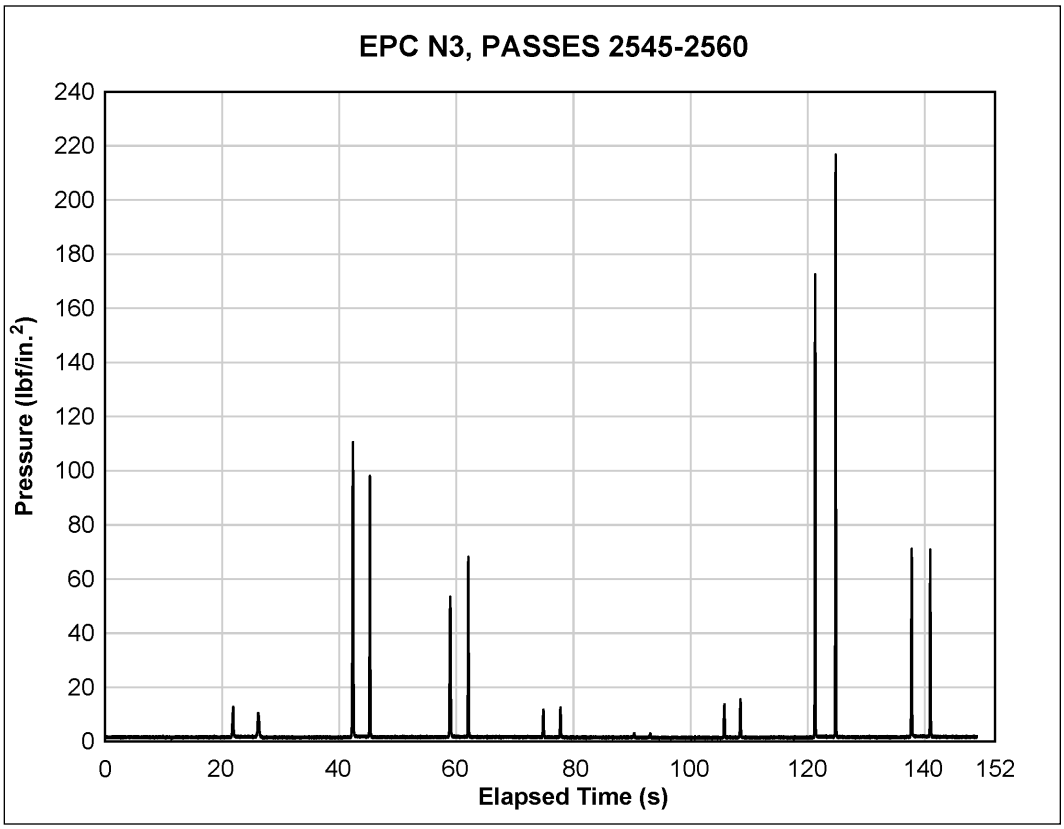
EPC N3, PASSES 2545-2560
Pressure (lbf/in.2)
0
20
40
60
80
100
120
140
160
180
200
220
240
0
20
40
60
80
100
120
140
152
Elapsed Time (s)

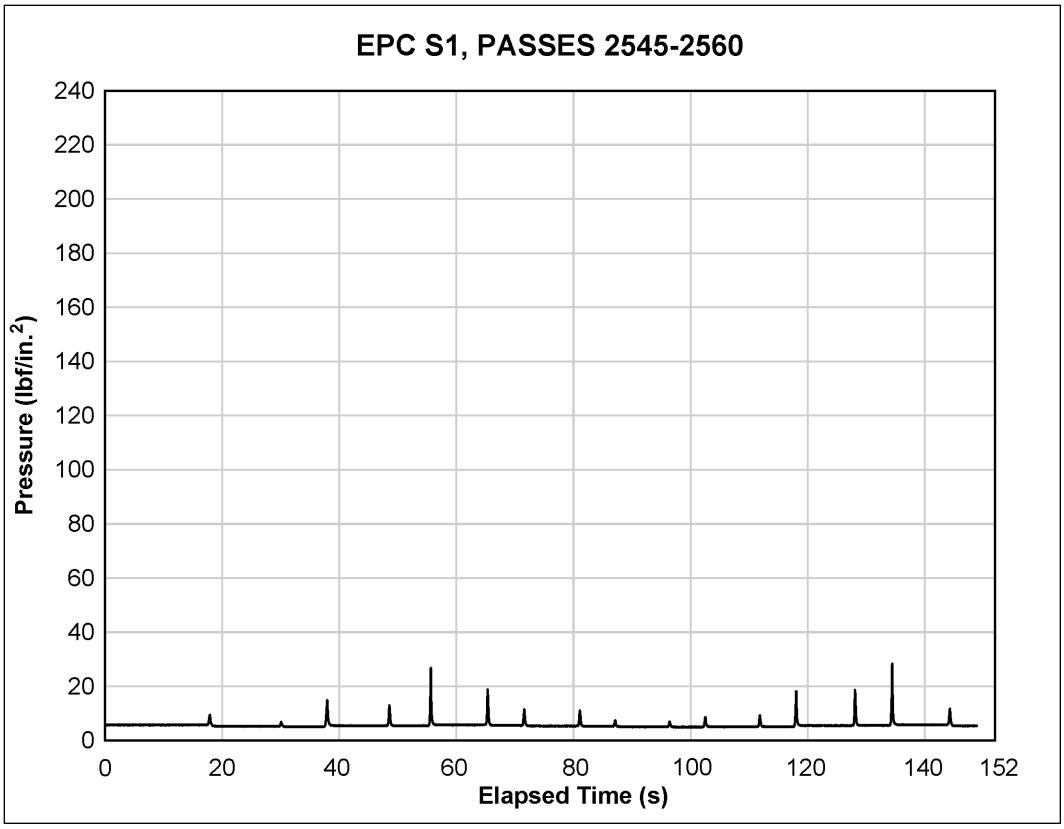
EPC S1, PASSES 2545-2560
Pressure (lbf/in.2)
240
220
200
180
160
140
120
100
80
60
40
20
0
0
20
40
60
80
100
120
140
152
Elapsed Time (s)

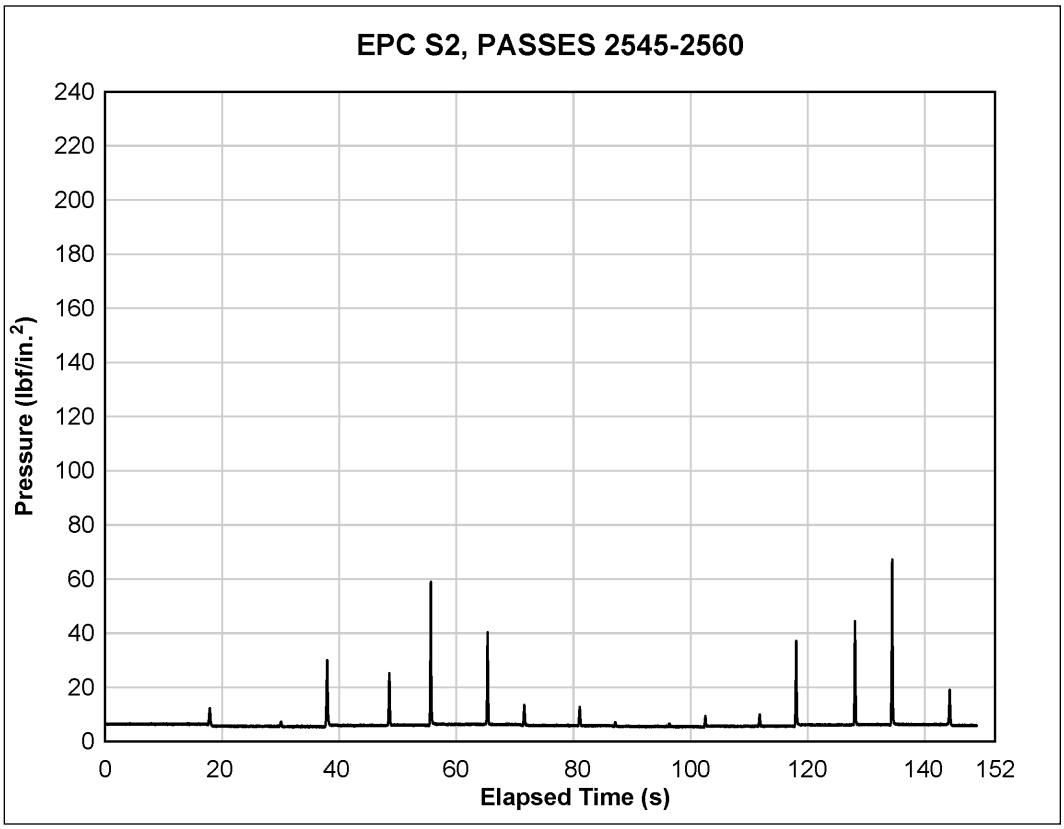
EPC S2, PASSES 2545-2560
Pressure (lbf/in.2)
240
220
200
180
160
140
120
100
80
60
40
20
0
0
20
40
60
80
100
120
140
152
Elapsed Time (s)

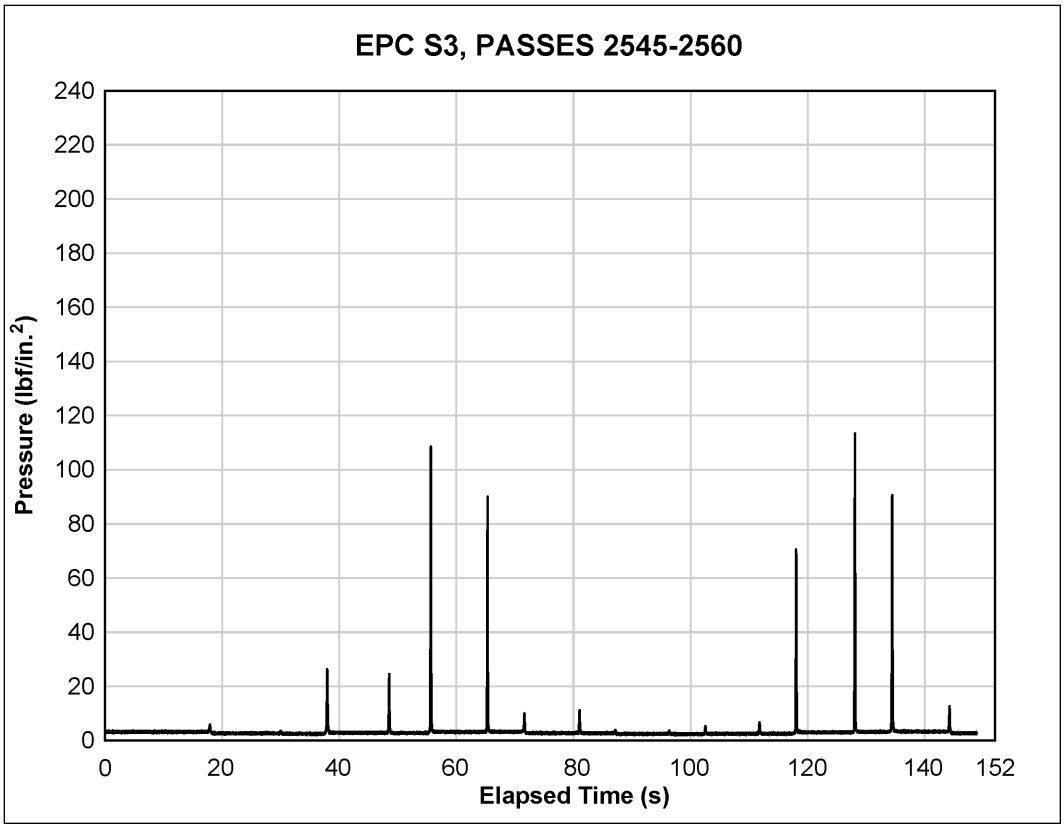
EPC S3, PASSES 2545-2560
Pressure (lbf/in.2)
0
20
40
60
80
100
120
140
160
180
200
220
240
0
20
40
60
80
100
120
140
152
Elapsed Time (s)

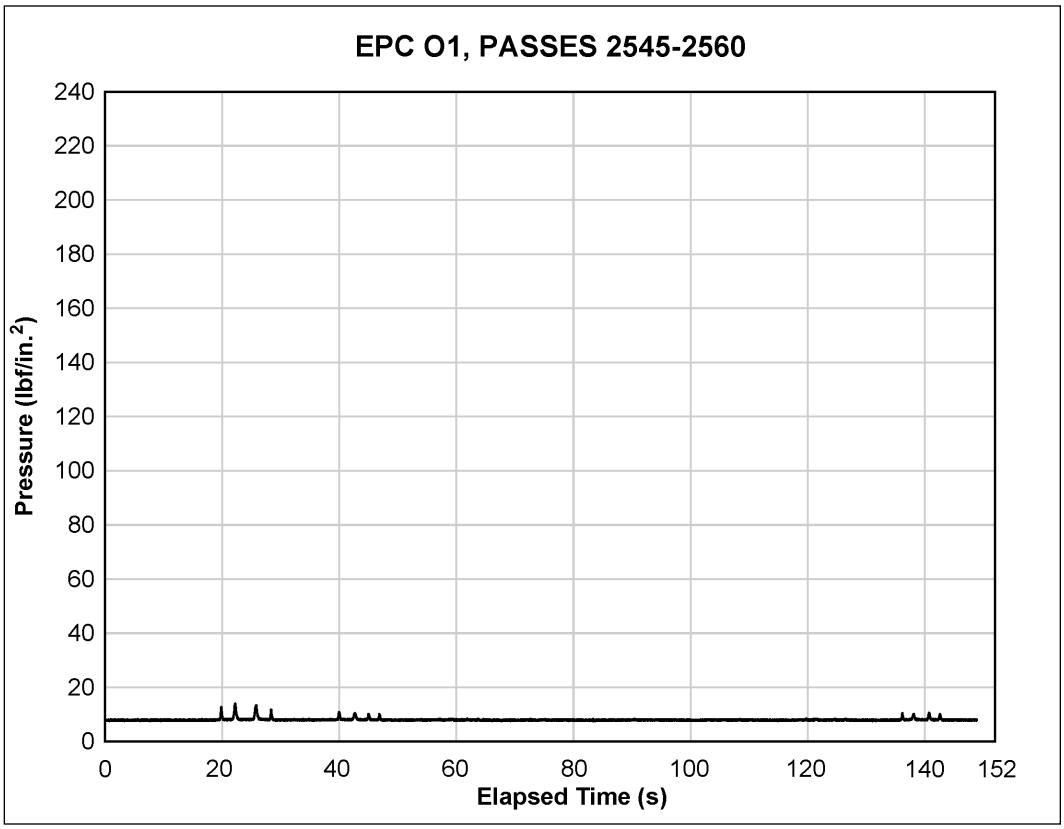
EPC O1, PASSES 2545-2560
Pressure (lbf/in.2)
0
20
40
60
80
100
120
140
160
180
200
220
240
0
20
40
60
80
100
120
140
152
Elapsed Time (s)

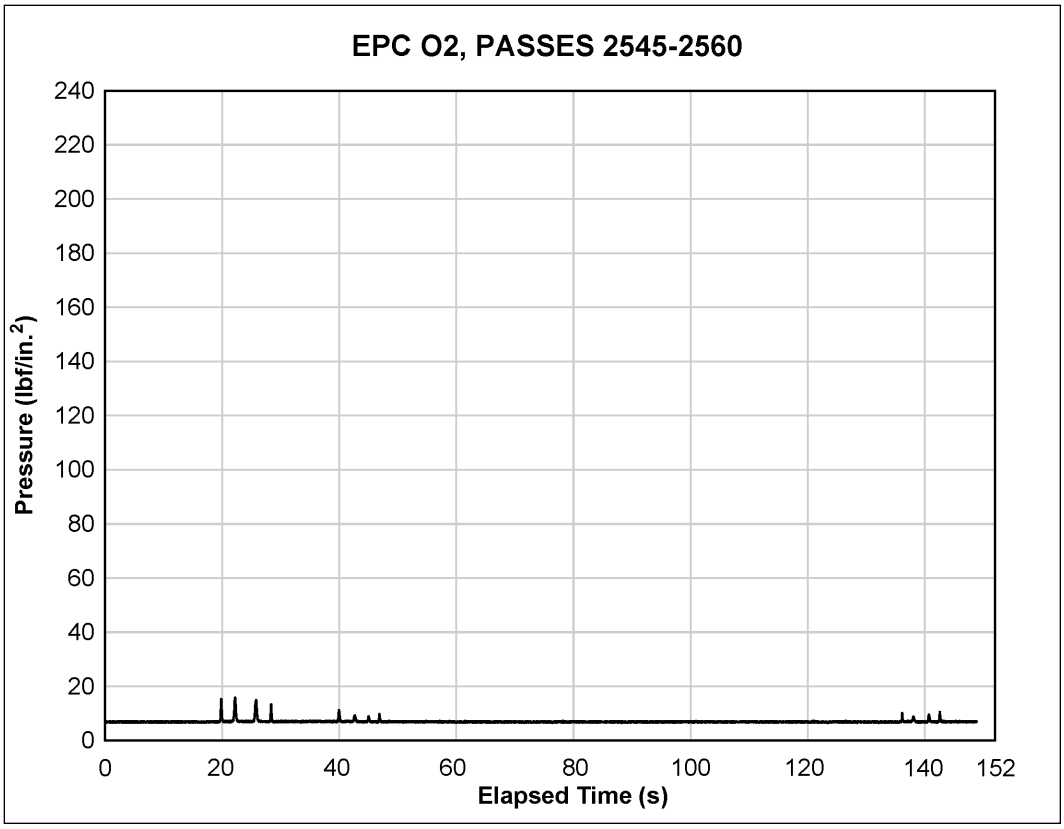
EPC O2, PASSES 2545-2560
Pressure (lbf/in.2)
240
220
200
180
160
140
120
100
80
60
40
20
0
0
20
40
60
80
100
120
140
152
Elapsed Time (s)

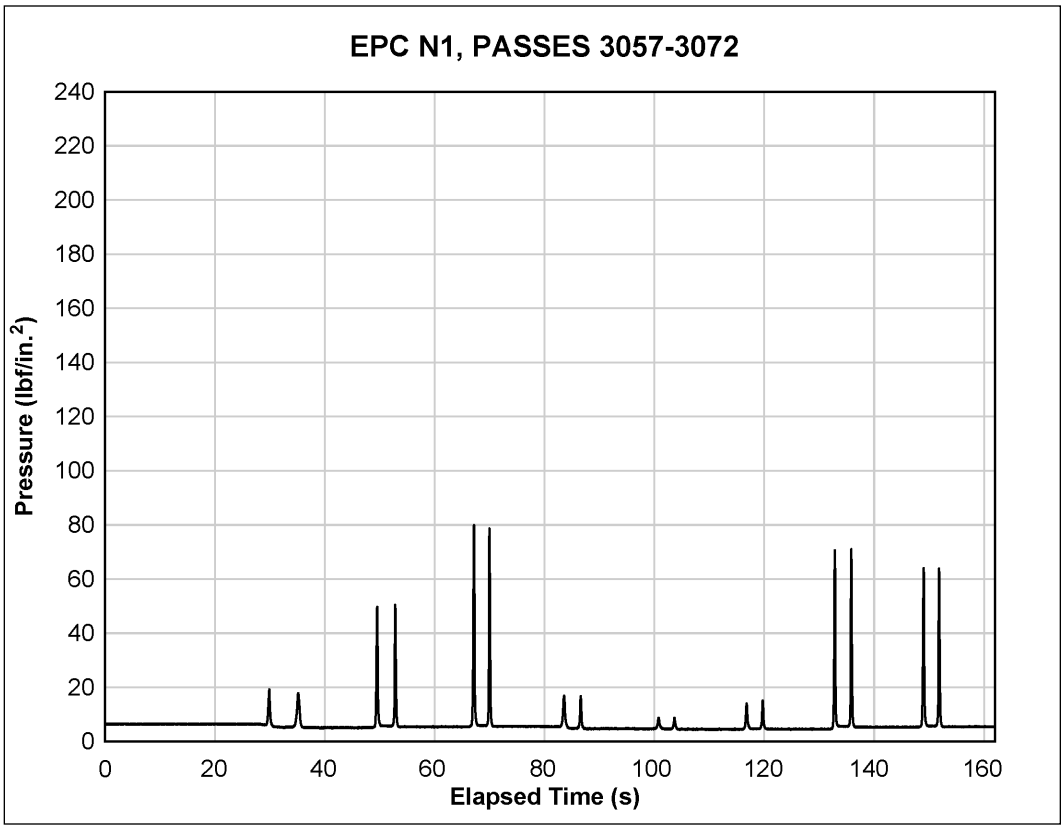
EPC N1, PASSES 3057-3072
Pressure (lbf/in.2)
240
220
200
180
160
140
120
100
80
60
40
20
0
0
20
40
60
80
100
120
140
160
Elapsed Time (s)

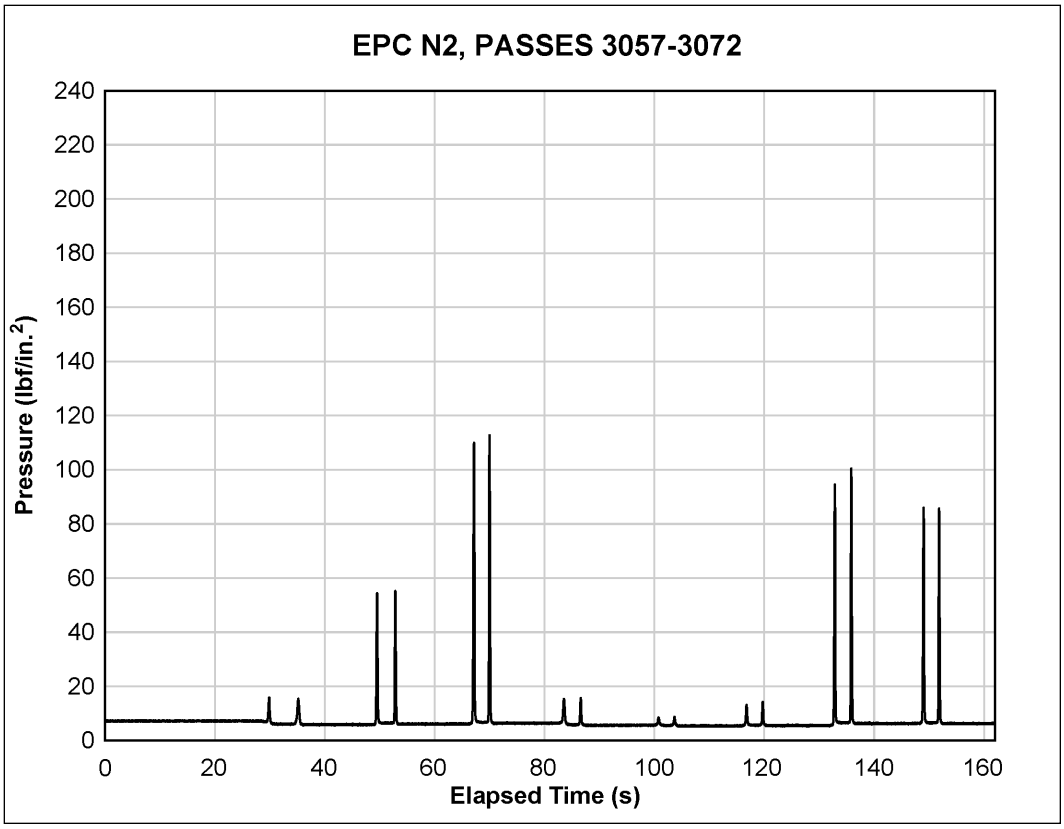
EPC N2, PASSES 3057-3072
Pressure (lbf/in.2)
Elapsed Time (s)
0
20
40
60
80
100
120
140
160
180
200
220
240

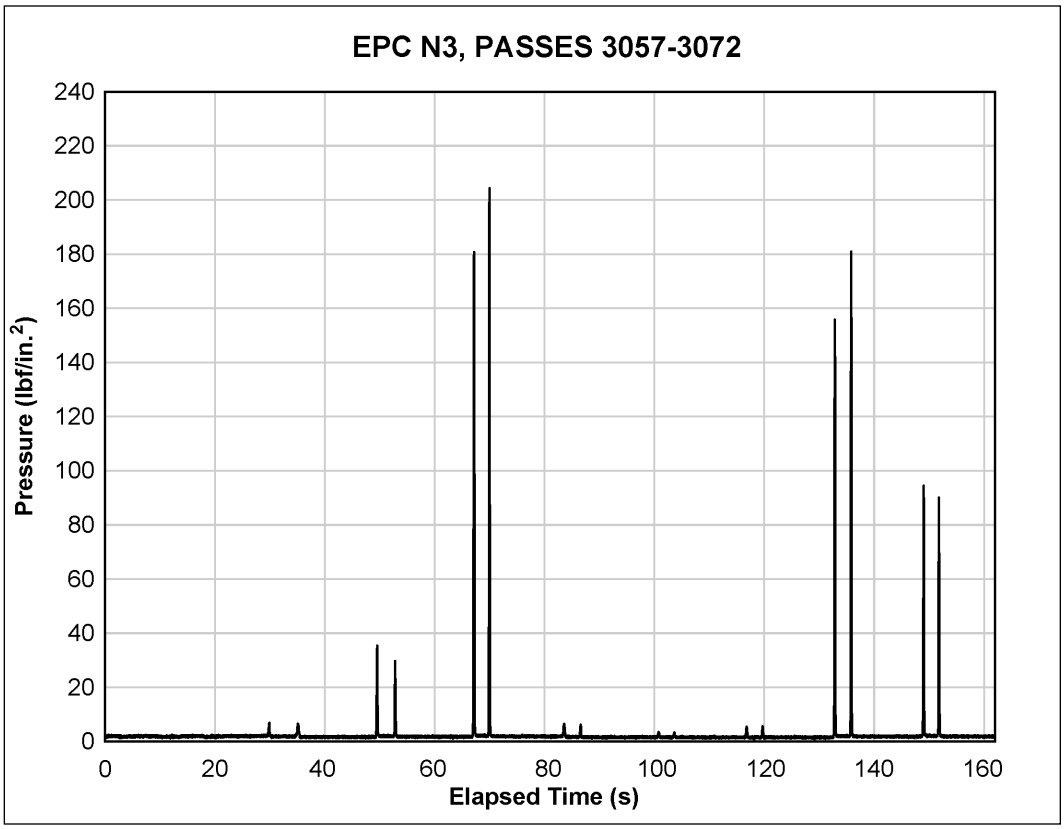
EPC N3, PASSES 3057-3072
Pressure (lbf/in.2)
Elapsed Time (s)
0
20
40
60
80
100
120
140
160
180
200
220
240

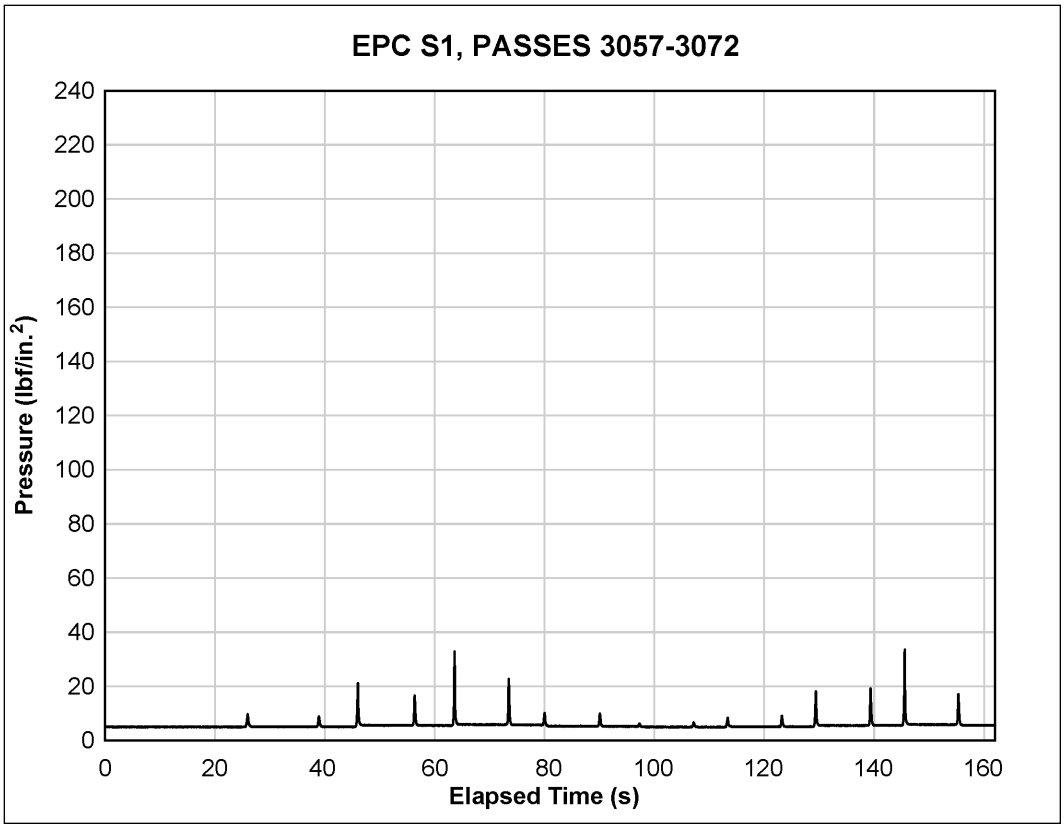
EPC S1, PASSES 3057-3072
Pressure (lbf/in.2)
0
20
40
60
80
100
120
140
160
180
200
220
240
0
20
40
60
80
100
120
140
160
Elapsed Time (s)

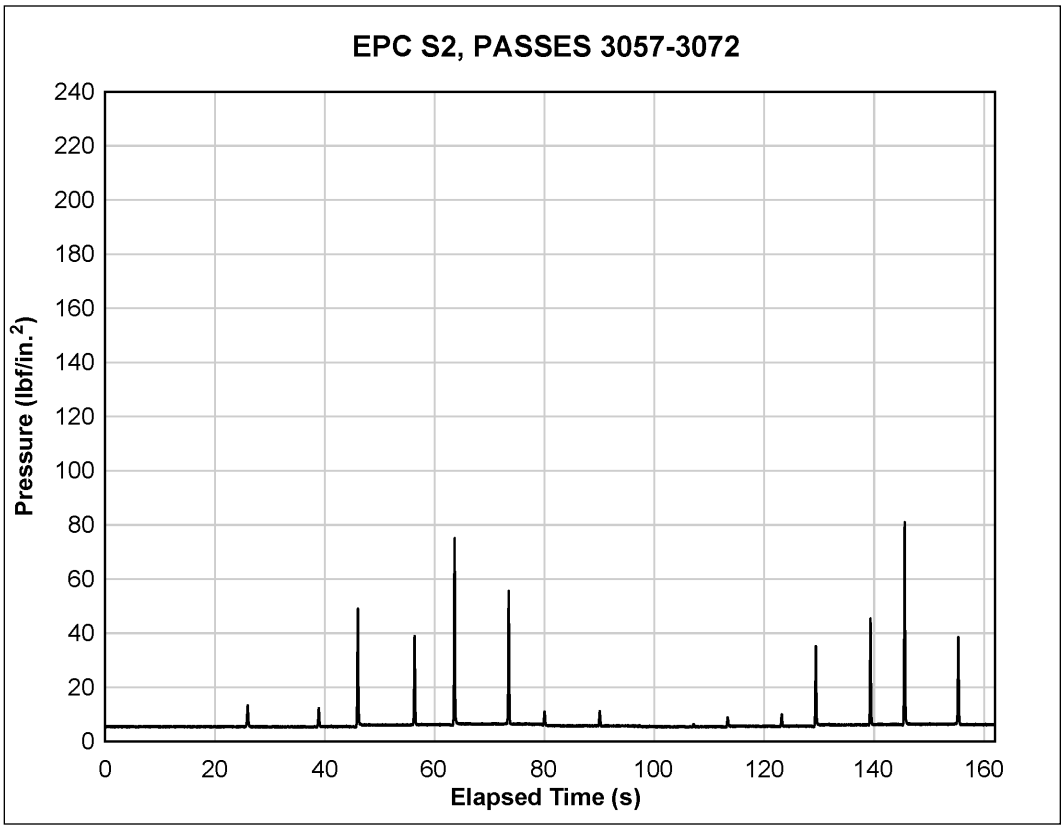
EPC S2, PASSES 3057-3072
Pressure (lbf/in.2)
0
20
40
60
80
100
120
140
160
180
200
220
240
0
20
40
60
80
100
120
140
160
Elapsed Time (s)

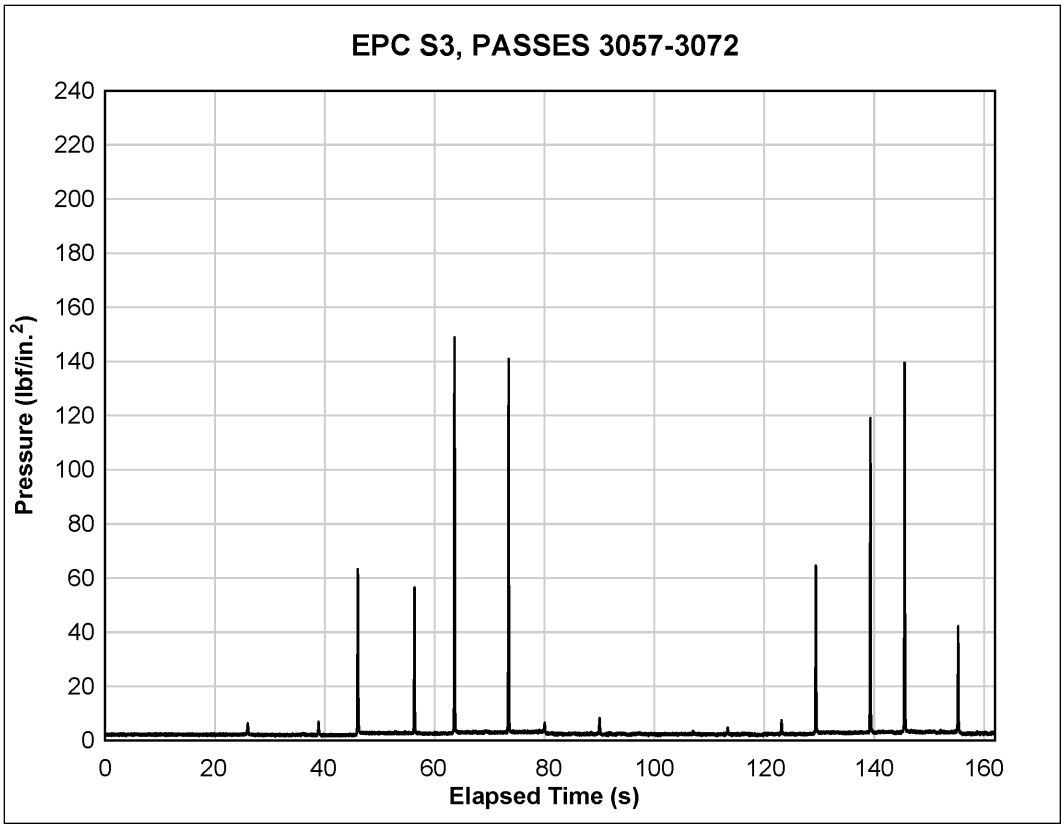
EPC S3, PASSES 3057-3072
Pressure (lbf/in.2)
0
20
40
60
80
100
120
140
160
180
200
220
240
0
20
40
60
80
100
120
140
160
Elapsed Time (s)

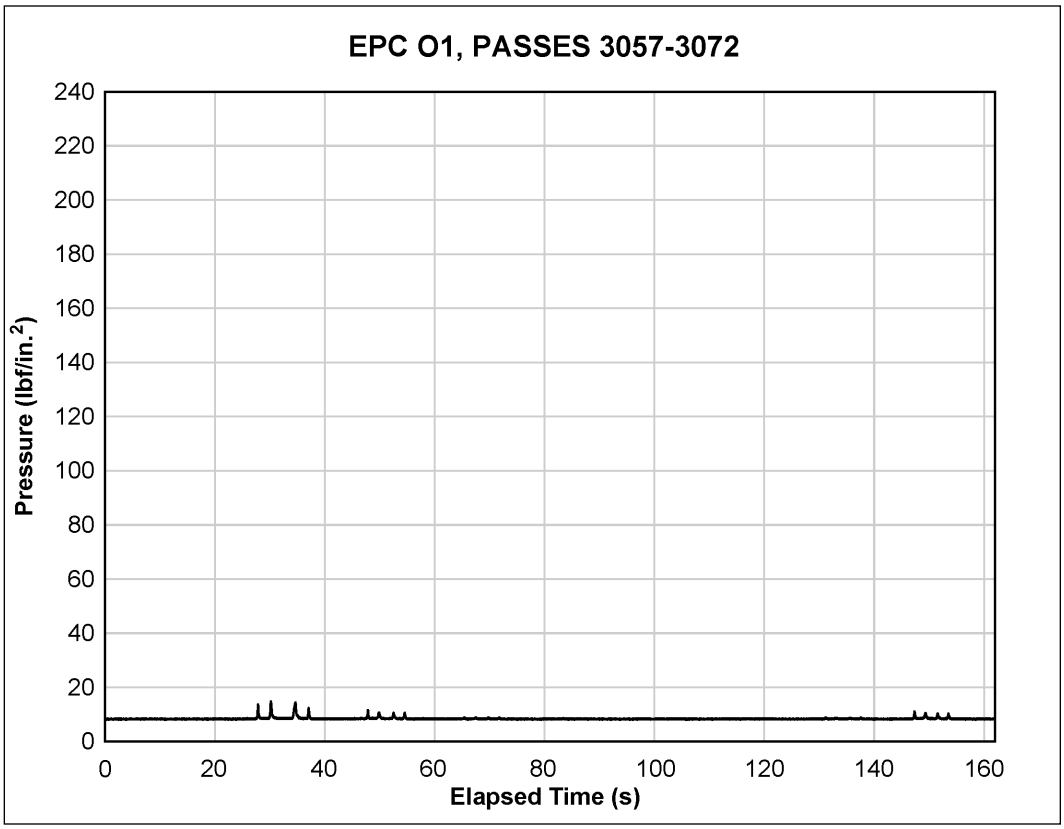
EPC O1, PASSES 3057-3072
Pressure (lbf/in.2)
0
20
40
60
80
100
120
140
160
180
200
220
240
0
20
40
60
80
100
120
140
160
Elapsed Time (s)

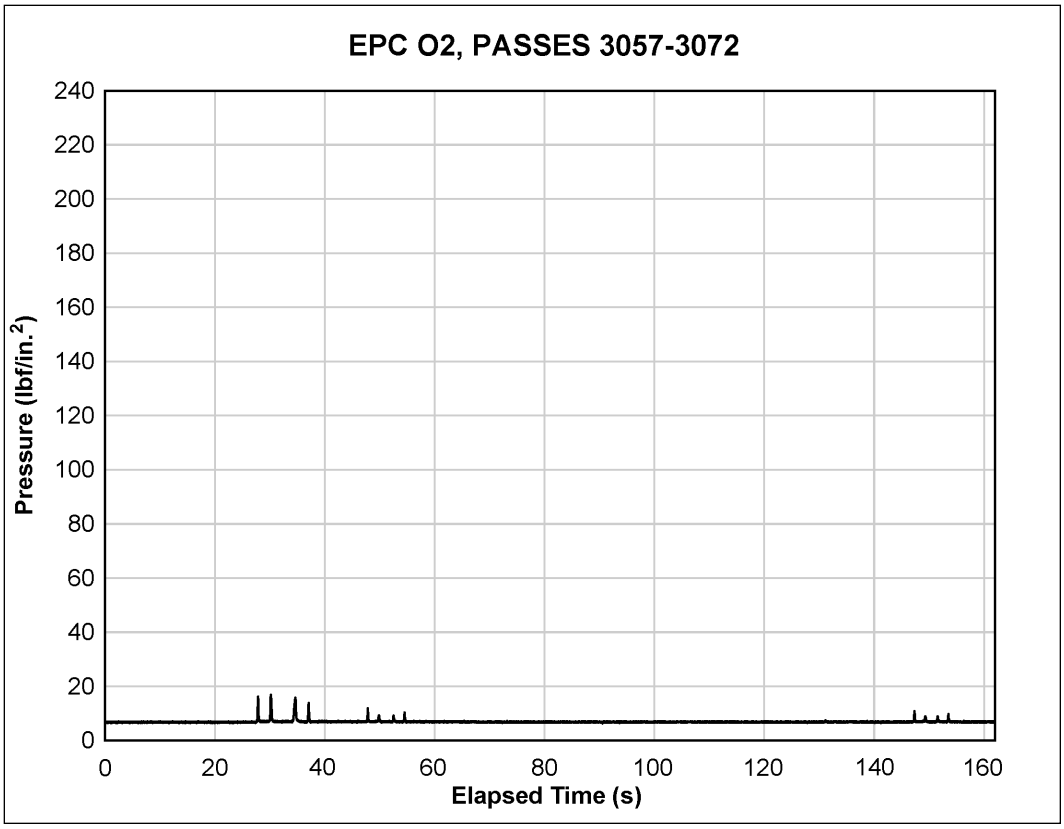
EPC O2, PASSES 3057-3072
Pressure (lbf/in.2)
240
220
200
180
160
140
120
100
80
60
40
20
0
0
20
40
60
80
100
120
140
160
Elapsed Time (s)

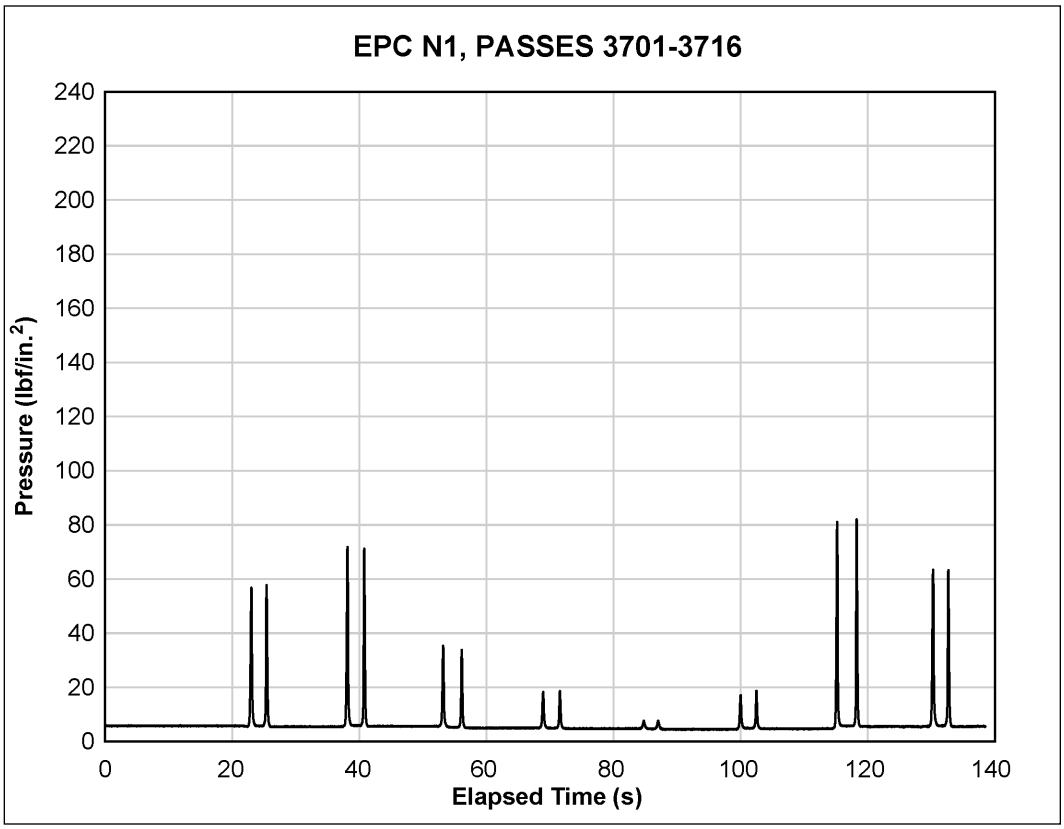
EPC N1, PASSES 3701-3716
Pressure (lbf/in.2)
240
220
200
180
160
140
120
100
80
60
40
20
0
0
20
40
60
80
100
120
140
Elapsed Time (s)

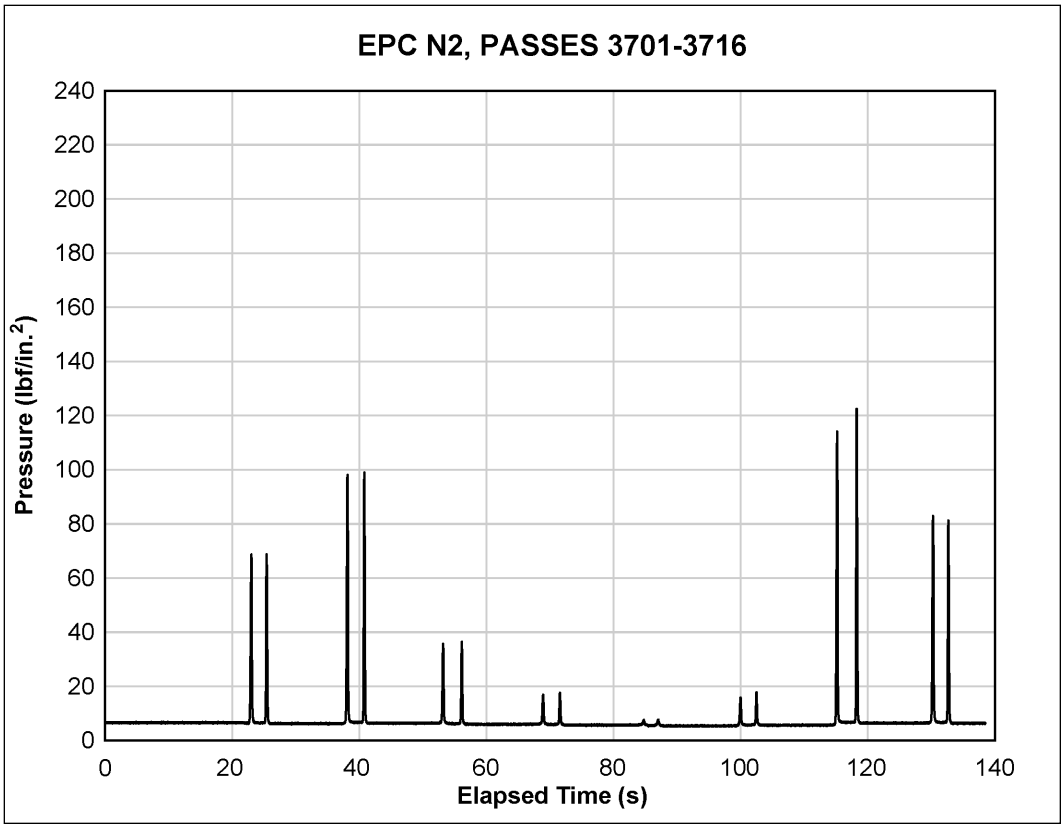
EPC N2, PASSES 3701-3716
Pressure (lbf/in.2)
0
20
40
60
80
100
120
140
160
180
200
220
240
0
20
40
60
80
100
120
140
Elapsed Time (s)

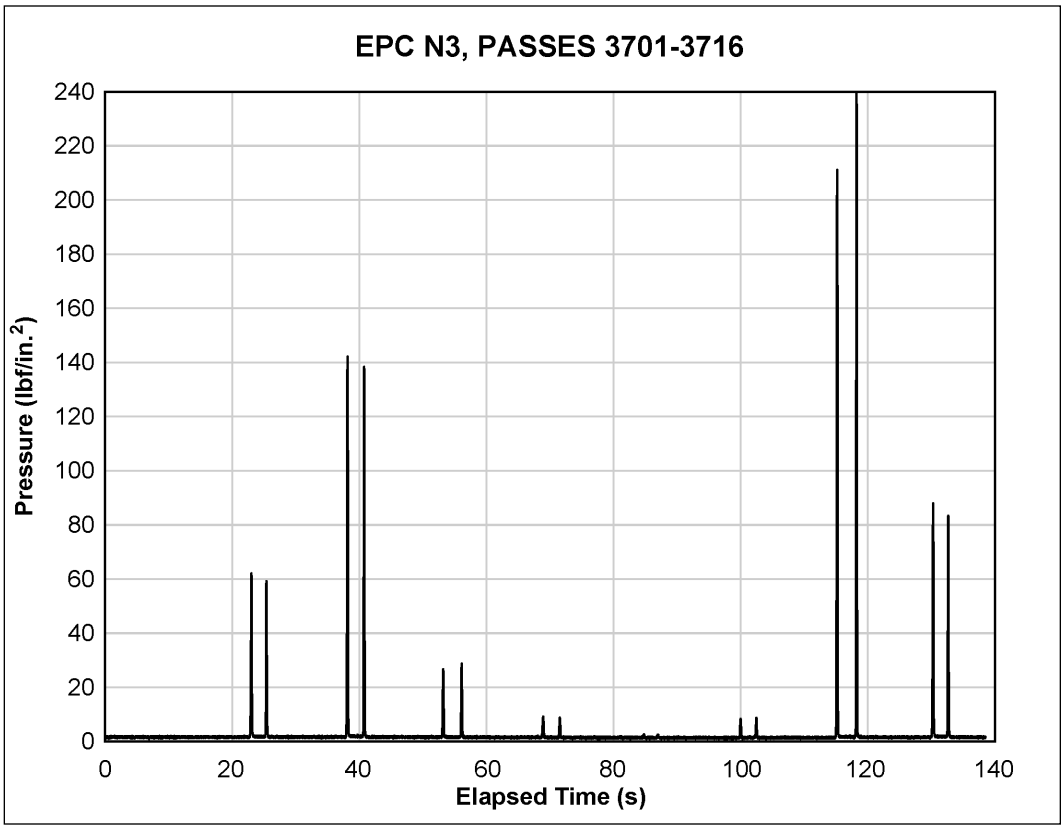
EPC N3, PASSES 3701-3716
Pressure (lbf/in.2)
0
20
40
60
80
100
120
140
160
180
200
220
240
0
20
40
60
80
100
120
140
Elapsed Time (s)

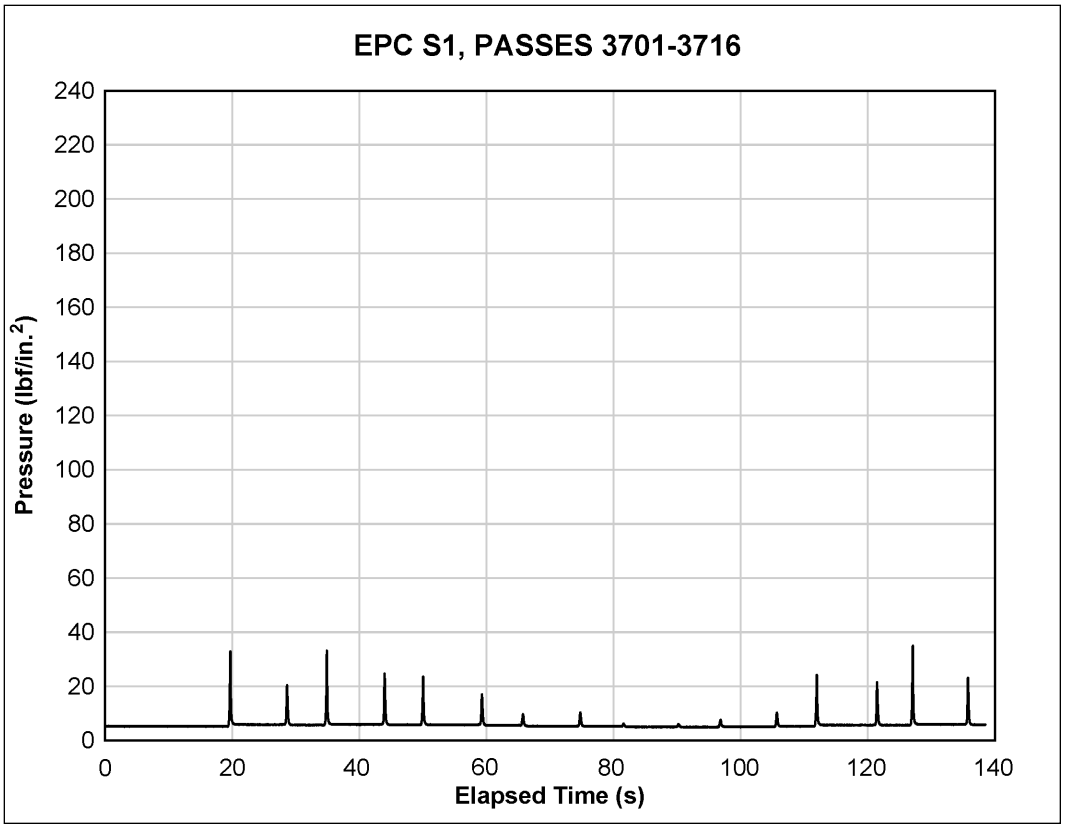
EPC S1, PASSES 3701-3716
Pressure (lbf/in.2)
0
20
40
60
80
100
120
140
160
180
200
220
240
0
20
40
60
80
100
120
140
Elapsed Time (s)

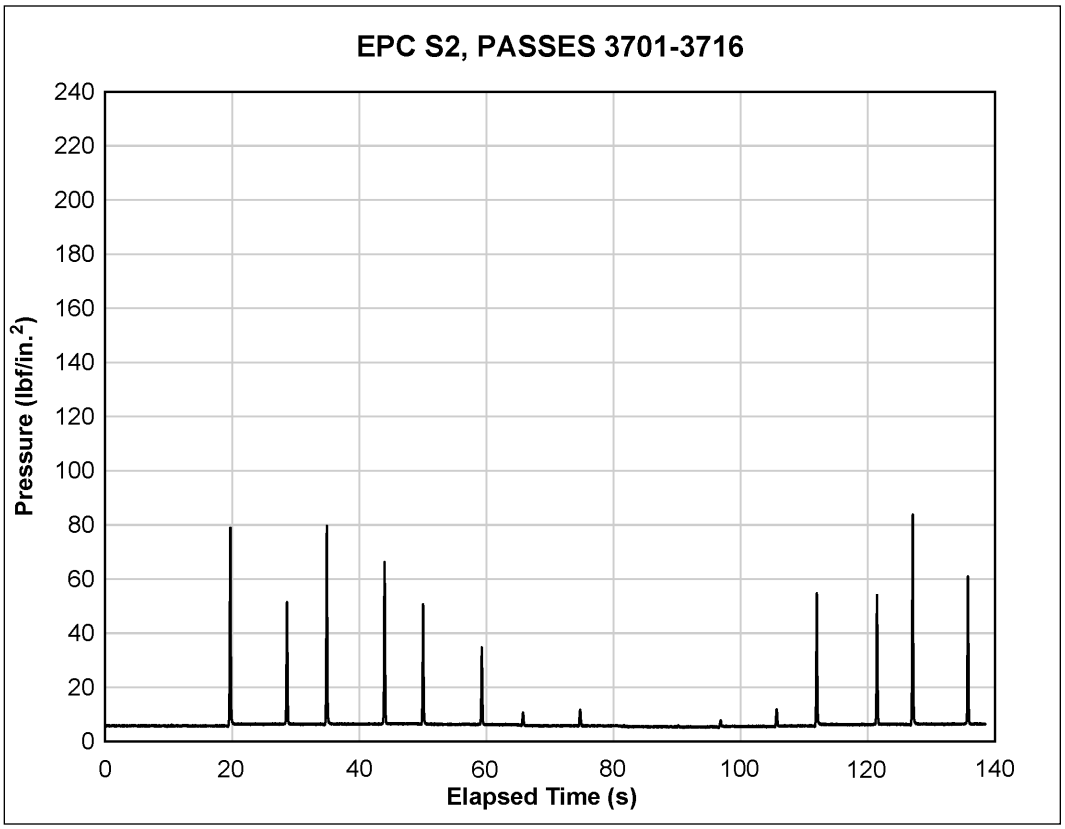
EPC S2, PASSES 3701-3716
Pressure (lbf/in.2)
0
20
40
60
80
100
120
140
160
180
200
220
240
0
20
40
60
80
100
120
140
Elapsed Time (s)

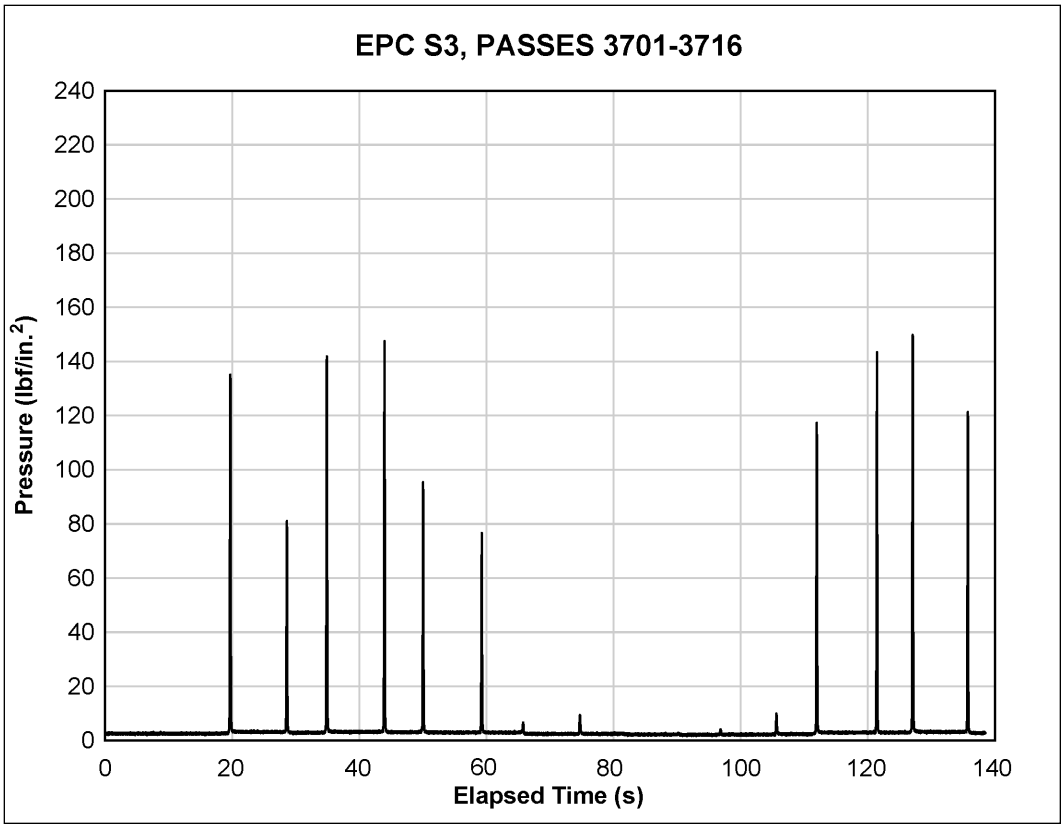
EPC S3, PASSES 3701-3716
Pressure (lbf/in.2)
240
220
200
180
160
140
120
100
80
60
40
20
0
0
20
40
60
80
100
120
140
Elapsed Time (s)

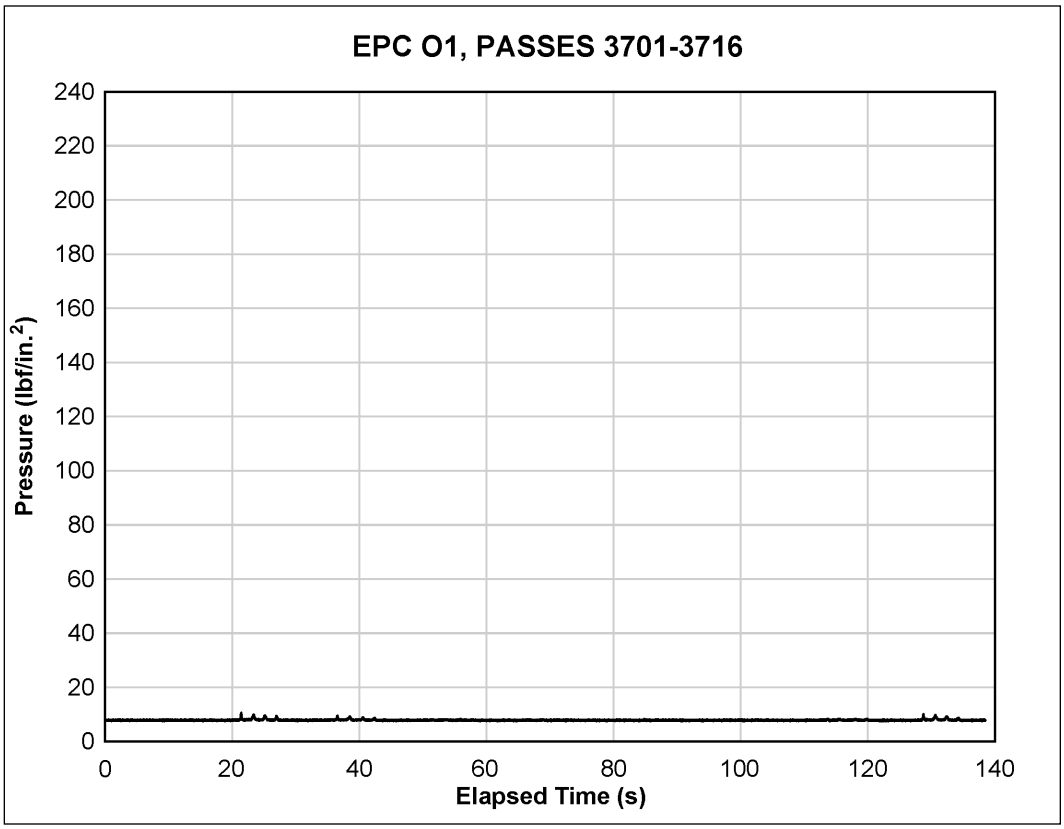
EPC O1, PASSES 3701-3716
Pressure (lbf/in.2)
240
220
200
180
160
140
120
100
80
60
40
20
0
0
20
40
60
80
100
120
140
Elapsed Time (s)

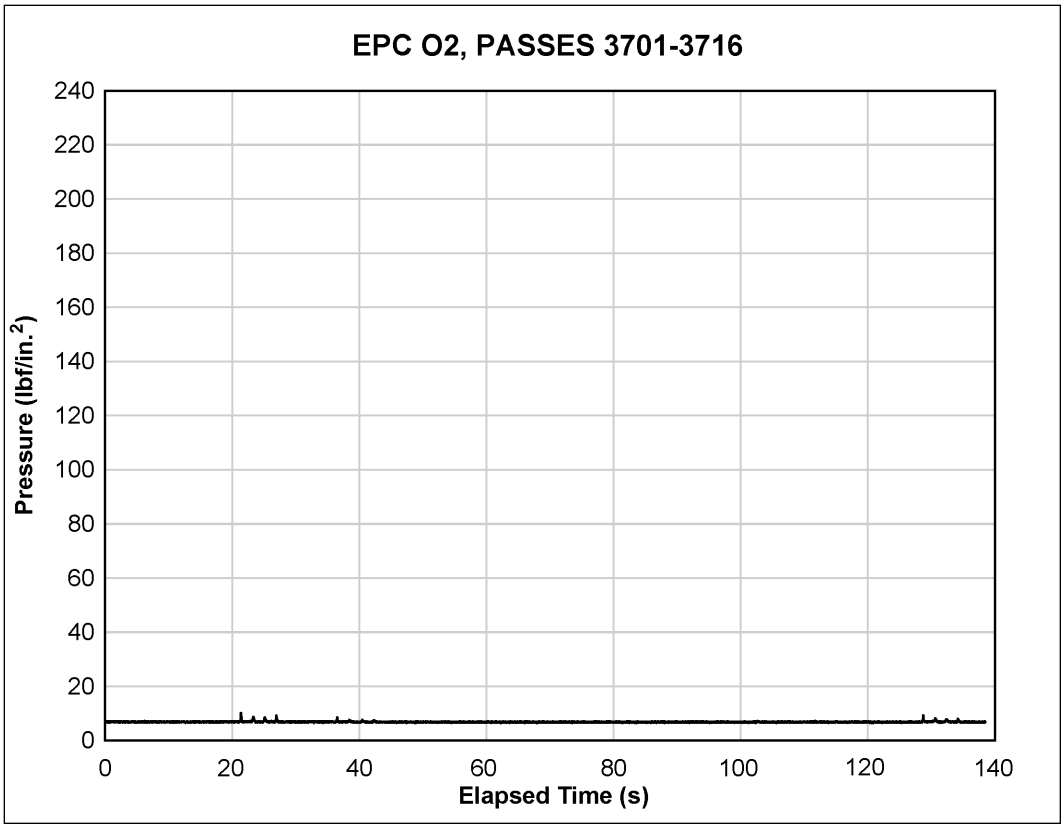
EPC O2, PASSES 3701-3716
Pressure (lbf/in.2)
240
220
200
180
160
140
120
100
80
60
40
20
0
0
20
40
60
80
100
120
140
Elapsed Time (s)

REPORT DOCUMENTATION PAGE

Form Approved
OMB No. 0704-0188

1. REPORT DATE *(DD-MM-YYYY)*	2. REPORT TYPE	3. DATES COVERED *(From - To)*
May 2014	Final	

4. TITLE AND SUBTITLE

Evaluation of Faun MLC-70 Trackway Mat System Under Simulated F-15 Traffic

5a. CONTRACT NUMBER

5b. GRANT NUMBER

5c. PROGRAM ELEMENT NUMBER

6. AUTHOR(S)

Timothy W. Rushing, Lyan Garcia, and Quint S. Mason

5d. PROJECT NUMBER

5e. TASK NUMBER

5f. WORK UNIT NUMBER

7. PERFORMING ORGANIZATION NAME(S) AND ADDRESS(ES)

Geotechnical and Structures Laboratory
US Army Engineer Research and Development Center
3909 Halls Ferry Road
Vicksburg, MS 39180-6199

8. PERFORMING ORGANIZATION REPORT NUMBER

ERDC/GSL TR-14-13

9. SPONSORING / MONITORING AGENCY NAME(S) AND ADDRESS(ES)

Headquarters, Air Force Civil Engineer Support Agency
Tyndall Air Force Base, FL 32403-5319

10. SPONSOR/MONITOR'S ACRONYM(S)

AFCEC

11. SPONSOR/MONITOR'S REPORT NUMBER(S)

12. DISTRIBUTION / AVAILABILITY STATEMENT

Approved for public release; distribution is unlimited.

13. SUPPLEMENTARY NOTES

14. ABSTRACT

Faun Trackway's airfield matting products have been encountered by US military personnel during joint operations with coalition partners. The MLC-70 Trackway matting system was previously evaluated under F-15E and C-17 simulated traffic over a subgrade with a California Bearing Ratio (CBR) of 6 and was found to be inadequate. However, substantially stronger materials are often found around existing airfields. Therefore, the US Air Force Civil Engineer Center tasked the US Army Engineer Research and Development Center to evaluate the MLC-70 system under simulated F-15E aircraft traffic to determine the number of allowable aircraft passes the system can sustain over stronger soils. Results of traffic tests presented herein include individual mat panel properties, pretest and posttest subgrade soil conditions, subgrade earth pressure cell instrumentation results, physical damage descriptions of the mat system, and system passes-to-failure under simulated F-15E aircraft traffic for specified failure criteria. Results from these evaluations showed that the MLC-70 Trackway system was capable of supporting more than 1,000 F-15E operations when placed over a subgrade with a CBR of 25 or greater. Operations over weaker soils should be limited to emergency or expedient operations for heavy fighter aircraft.

15. SUBJECT TERMS

Airfield Mat	Trackway	MLC-70
Landing Mat	Aluminum Mat	Airfield Damage Repair
	British Mat	

16. SECURITY CLASSIFICATION OF:			17. LIMITATION OF ABSTRACT	18. NUMBER OF PAGES	19a. NAME OF RESPONSIBLE PERSON Timothy Rushing
a. REPORT	b. ABSTRACT	c. THIS PAGE			19b. TELEPHONE NUMBER *(include area code)*
Unclassified	Unclassified	Unclassified		121	601-634-2858